DEPARTMENT OF TRANSPORTATION

Haul Road and Detour Maintenance

Mihai Marasteanu, Principal Investigator
Civil, Environmental, and Geo- Engineering University of Minnesota

January 2026

Research Report
Final Report 2026-06

To get this document in an alternative format or language, please call 651-366-4720 (711 or 1-800-627-3529 for MN Relay). You can also email your request to ADArequest.dot@state.mn.us. Please make your request at least two weeks before you need the document.

Technical Report Documentation Page

1. Report No.	2.	3. Recipients Accession No.
MN 2026-06		

4. Title and Subtitle	5. Report Date
Haul Road and Detour Maintenance	January 2026
	6.

7. Author(s)	8. Performing Organization Report No.
Mihai Marasteanu, Michael Levin, Zifeng Zhao, Shaghayegh Nouhi, Mugurel Turos	

9. Performing Organization Name and Address	10. Project/Task/Work Unit No.
Department of Civil, Environmental, and Geo- Engineering University of Minnesota 500 Pillsbury Drive S.E. Minneapolis, Minnesota 55455	#2024005
	11. Contract (C) or Grant (G) No. (c) 1036342 (wo)52

12. Sponsoring Organization Name and Address	13. Type of Report and Period Covered
Minnesota Department of Transportation Office of Research & Innovation 395 John Ireland Boulevard, MS 330 St. Paul, Minnesota 55155-1899	Final Report
	14. Sponsoring Agency Code

15. Supplementary Notes

http://mdl.mndot.gov/

16. Abstract (Limit: 250 words)

Highway construction projects frequently require detours and haul roads that divert traffic, including heavy trucks, onto local roads not originally designed for such loads. These temporary routes can accelerate pavement deterioration, reduce service life, and impose significant maintenance costs on local agencies. Current compensation practices, such as Minnesota's Gas Tax Method and Equivalent Overlay Method, offer partial solutions but do not fully capture the variability of damage across different pavements and traffic conditions. This study investigates the structural and economic impacts of detours and haul roads on Minnesota's roadway network and develops a framework for improved evaluation and planning. A comprehensive literature review of empirical and engineering-based approaches to estimating pavement damage is first conducted, along with a survey of compensation practices across U.S. states. Field data are next collected from five detour routes and two haul roads using Falling Weight Deflectometer (FWD), and Ground Penetrating Radar (GPR). The results are then used to estimate Remaining Service Life (RSL). Due to significant variability in FWD testing, MnDOT's calibrated pavement performance curves are applied to estimate damage, with a case study demonstrating that a three-month detour could reduce service life by more than two years. Additionally, a multiclass traffic assignment model is implemented to predict vehicle-type-specific flows under closures, and optimization techniques using genetic algorithms are developed to identify detour routes that minimize truck-related pavement damage while maintaining network efficiency. While the findings provide some practical tools and recommendations for more equitable compensation and improved detour planning, more research is needed to validate the results obtained in this study.

17. Document Analysis/Descriptors	18. Availability Statement
Detours, Haul roads, Pavement performance, Deterioration, Service life, Traffic assignment, Optimization	No restrictions. Document available from: National Technical Information Services, Alexandria, Virginia 22312

19. Security Class (this report)	20. Security Class (this page)	21. No. of Pages	22. Price
Unclassified	Unclassified	96	

Haul Road and Detour Maintenance

Final Report

Prepared by:

Mihai Marasteanu
Michael Levin
Zifeng Zhao
Shaghayegh Nouhi
Mugurel Turos
Department of Civil, Environmental, and Geo- Engineering
University of Minnesota

January 2026

Published by:

Minnesota Department of Transportation
Office of Research & Innovation
395 John Ireland Boulevard, MS 330
St. Paul, Minnesota 55155-1899

Acknowledgements

The authors gratefully acknowledge the financial support provided by the Minnesota Department of Transportation.

Special acknowledgements go to the project champion, Timothy Andersen, whose guidance and technical support, provided over the entire duration of the research investigation, were instrumental in successfully completing this project.

Technical Advisory Panel members Charles Kremer, Christine Dulian, James Roberts, Paul Johns, and Scott Zeidler are acknowledged for providing feedback and helping with the detour projects selection process.

We also acknowledge the continuous logistical support provided by the project coordinator, Marcus Bekele.

Table of Contents

List of Figures

List of Tables

Executive Summary

The use of local roads as detours and haul routes during highway construction projects is common practice. However, these temporary designations often accelerate pavement deterioration, particularly when heavy truck traffic is rerouted onto roads not originally designed for such loads. Current practices for compensating local agencies, such as Minnesota's Gas Tax Method and Equivalent Overlay Method, provide partial solutions but have limitations in accurately reflecting the true extent of pavement damage. This research effort builds on prior studies on pavement damage assessment and compensation policies, with the main thrust being the development of improved methods for quantifying detour-related damage and identifying strategies to minimize long-term impacts on Minnesota's road network.

In Chapter 2, a comprehensive literature review is presented, summarizing both empirical and engineering-based approaches to estimating pavement damage costs. National and state policies for compensating local governments are discussed, with emphasis on MnDOT's current reimbursement methods and the survey of practices in other states.

In Chapter 3, pavement structural damage is evaluated using non-destructive testing methods, including Falling Weight Deflectometer (FWD), Traffic Speed Deflectometer (TSD), and Ground Penetrating Radar (GPR). Remaining Service Life (RSL) calculations are performed for multiple detour and haul road sites across Minnesota. While reductions in service life are observed in some cases, inconsistencies due to testing variability highlight the challenges of relying solely on None Destructive Testing (NDT)-based evaluations.

In Chapter 4, a multiclass traffic assignment model, integrated with MnDOT's CUBE framework, is developed to predict changes in vehicle flows caused by construction-related closures. Cube-based modeling is a dataset-oriented approach to data modeling. The model incorporates user equilibrium conditions for cars and heavy trucks, providing insights into congestion, rerouting behavior, and increased truck flows on vulnerable local roads.

In Chapter 5, pavement performance curves calibrated by MnDOT are applied to estimate detour-related damage more consistently. Two methods—reduction in RSL and loss of effective service area—are used to quantify the impact of detours. A case study on Goodhue County CSAH 5 demonstrates that a three-month detour can reduce service life by more than two years and decrease effective service area by more than 25%. The chapter also introduces an optimization framework based on genetic algorithms to identify detour configurations that reduce truck Vehicle Miles Traveled (VMT) or minimize truck use of restricted links. Simulation results show that optimization can achieve meaningful reductions in truck flows on vulnerable roads while maintaining network efficiency.

Chapter 6 synthesizes the findings and proposes a framework for quantifying pavement damage and optimizing detour planning. The framework integrates pavement condition data, non-destructive testing, performance curves, and traffic assignment with optimization tools. Practical recommendations

are provided, including the adoption of performance curve–based evaluations, standardized NDT protocols, and the integration of traffic modeling into detour planning.

Chapter 1: Introduction

1.1 Background

Highway construction and maintenance projects often require temporary detours and haul roads to divert traffic or move construction materials. While these measures are necessary to ensure work zone safety and maintain mobility, they impose additional stresses on local roadways that were not originally designed to accommodate high volumes of traffic, particularly heavy trucks. The increased load can accelerate pavement deterioration, shorten service life, and generate unanticipated repair costs for local agencies.

In Minnesota, current policies provide mechanisms for reimbursing local governments when their roads are used as official detours or haul routes. The Gas Tax Method estimates compensation based on fuel tax revenue generated by detoured traffic, while the Equivalent Overlay Method estimates the cost of restoring capacity through additional overlays. However, both methods have limitations, as they may not capture actual damage or the variability of pavement conditions across different routes. Nationally, compensation practices vary, with some states providing direct repair or repaving, while others lack formal reimbursement procedures.

Accurately quantifying detour-related pavement damage remains a challenge due to variability in traffic behavior, pavement structure, and environmental factors. Recent advances in non-destructive testing, performance modeling, and traffic assignment analysis offer opportunities to address these challenges. By integrating Falling Weight Deflectometer (FWD), Traffic Speed Deflectometer (TSD), and Ground Penetrating Radar (GPR) data with traffic modeling and optimization techniques, this study aims to provide a framework for evaluating detour impacts and developing strategies that reduce costs, improve equity, and preserve infrastructure longevity.

1.2 Objectives

The overarching objective of this study is to evaluate the structural and economic impacts of detours and haul roads on Minnesota's pavement infrastructure and to identify approaches that minimize long-term damage. The specific objectives of this study are to: 1) review existing national and state practices for estimating pavement damage and compensating local agencies, with emphasis on MnDOT policies; 2) apply non-destructive testing methods (FWD, TSD, GPR) and performance curve modeling to quantify structural deterioration and service-life reduction caused by detours and hauling; 3) develop and implement a traffic assignment model that captures vehicle-type-specific detour flows, with particular attention to heavy trucks; 4) formulate optimization strategies, including genetic algorithm–based approaches, to identify detour routes that minimize truck-related pavement damage while maintaining network efficiency; 5) propose a practical framework to guide MnDOT and local agencies in evaluating detour-related damage, estimating costs, and designing equitable compensation and mitigation policies.

Together, these objectives aim to improve the accuracy of pavement damage assessment, enhance decision-making for detour planning, and ensure fair treatment of local agencies affected by construction-related traffic diversions.

Chapter 2: Literature Review

This chapter presents a comprehensive literature review on the methods used to assess the damage cost of detours on local roads, including the methods for estimating pavement damage cost and the policies for reimbursing local road damage. In addition, the results of a recent survey will be discussed.

2.1 Estimation of Pavement Damage Cost

As part of construction project activities, local roads are typically used for detours and hauling, which can cause significant damage to them. Many studies have investigated the estimation of additional pavement damage due to detours and hauling; however, there is no consensus on what method is best.

As classified by Ahmed et al. (2012), there are mainly two approaches for pavement damage costs estimation: the empirical approach, which establishes the relationship between the damage cost and pavement usage based on data, and the engineering approach, which is based on theoretical relationships between damage cost or damage, and pavement usage (load).

2.1.1 Empirical Approach

The empirical approach is top-down, starting with actual knowledge of the cost and the usage of pavements and then establishing a relationship between them. The form of this model is typically a data-based regression.

Gibby et al. (1990) studied the factors affecting pavement maintenance costs and evaluated the impact of heavy traffic on maintenance costs. A database containing information on traffic, weather, geometric conditions, and pavement maintenance cost for the sample sections was used to formulate a model for pavement maintenance costs. It was found that the impact of one heavy truck on the pavement is about 70 times that of a light truck. The authors estimated that the average annual maintenance cost per heavy truck and passenger car was approximately $7.60 and $0.08 per mile, respectively.

Martin (1994) estimated load-related pavement maintenance and construction costs for the Australian Road Research Board (ARRB). Separate regression models were developed for annual average total maintenance expenditure, annual average routine maintenance expenditures, and annual average periodic maintenance expenditure. The study estimated that, on average, 50% of pavement maintenance expenditures were load-related and can be attributed to heavy vehicles. Also, approximately 45% of pavement construction/replacement costs were found to be load-related.

Hajek et al. (1998) quantified the pavement damage cost of proposed changes in regulations governing truck weights and dimensions in Ontario. The marginal pavement cost of truck damage was defined as a unit cost of providing pavement structure for one additional passage of a unit truckload (expressed as equivalent single axle load). A regression model was developed to characterize the pavement damage cost. The results indicate that the highway type (or truck volumes associated with the highway type) has a major influence on marginal costs. For example, the annualized pavement life-cycle cost of the

passage of one additional typical truck on 1 km of a highway in southern Ontario can range from about $0.004 for a freeway to $0.46 for a local road (Canadian dollars in 1998).

Li and Sinha (2000) estimated the load and non-load shares of pavement maintenance and rehabilitation expenditures using Indiana DOT data. The pavement maintenance and rehabilitation expenditure were estimated separately for flexible, rigid, and composite pavements. Regression models were developed to establish the relationship between pavement rehabilitation expenditures and pavement deterioration factors. The study estimated the marginal pavement rehabilitation expenditure using the average thickness for different types of pavements. The marginal pavement rehabilitation expenditure was estimated at $0.023 and $0.038 per ESAL-mile (2000 constant $) for flexible and rigid pavements, respectively.

Herry and Sedlacek (2002) estimated marginal maintenance and renewal (rehabilitation) costs using data from Austria. Cost and traffic data (volume, gross tons, and axle loads) for 46 motorway sections from 1987 to 2004 were used to estimate regression models. Based on the developed model, the estimated marginal pavement damage cost (in 2002 constant dollars) was found to be $0.0007 per vehicle-kilometers (V-Km) for vehicles up to 3.5 tons (gross vehicle weight (GVW)) and $0.023 (2002 Constant $) per V-Km for vehicles weighing more than 3.5 tons. An issue with this study was that the independent variables in the model were found to be statistically insignificant at a 95% significance level, which raised concerns about the statistical validity of the regression model.

Schreyer et al. (2002), using 1985–1998 data from 127 sections on the Swiss road network, estimated marginal maintenance and rehabilitation costs for different vehicle classes based on regression models. The developed model showed that the marginal pavement damage cost (in 2002 constant dollars) was found to be $0.0005 per V-Km for passenger cars and $0.0472 (2002 constant $) per V-Km for trucks.

Ahmed et al. (2012) developed data-based regression models for pavement damage cost. First, the data for maintenance and rehabilitation (M&R) schedules and the cost of each M&R activity were collected from the transportation agency. A linear equation that input equivalent single axle load (ESAL) and pavement type and output equivalent annual cost (EUAC) was fit to the collected data. The derivative of this equation was taken to compute the marginal EUAC with respect to ESAL. The developed model includes the establishment of asset families, realistic types and timings of reconstruction, rehabilitation, and maintenance, traffic volumes, and growth projections. This study showed that the damage cost of highway assets due to overweight trucks is influenced significantly by the asset type and age. For pavement assets, the pavement damage cost estimates were found to range from $0.006 per ESAL-mile on Interstates to $0.218 per ESAL-mile on non-national highways. The study also showed that non-consideration of reconstruction or maintenance costs can result in an underestimation of the actual pavement damage cost by 79% and 83%, respectively. The analysis also showed that the unrealistic approach of considering only rehabilitation treatments applied at fixed intervals can lead to as much as 86% underestimation of the actual pavement damage cost. The results also suggest that pavement damage cost is highly sensitive to the pavement life-cycle length, interest rate, rest period, and the costs and service lives of rehabilitation treatments.

Gungor et al. (2019) evaluated the impact of overweight vehicles on pavements in Illinois. A data-driven regression model was prosed to estimate the pavement damage cost based on the most recent databases on the infrastructure condition. The model was used to quantify the impact of overweight trucks on highway safety and to develop a geographical information system (GIS) based online permit issues tool to compute the overweight permit fee based on the extraction of the information of each route (such as pavement type, bridge load carrying capacity) that is traveled by the overweight vehicle.

2.1.2 Engineering Approach

The engineering approach for pavement damage estimation is bottom-up, which uses pavement performance models and/or non-destructive testing measurements to estimate pavement damage and cost.

2.1.2.1 Mechanistic-Empirical Pavement Performance Models

Prozzi et al. (2012) evaluated the damage that oversize/overweight vehicles cause to pavements and bridges in Texas. The project developed methodologies to quantify pavement consumption rates per mile based on the Mechanistic-Empirical (ME) Pavement Design Principles, which correlate the pavement mechanical responses (characteristic stress or strain in structural layers) to pavement service life. The consumption rates were calculated for multiple axle loads based on the axle configurations. A new fee structure for oversize/overweight vehicle permits was suggested to TxDOT.

Chowdhury et al. (2013) investigated the impact of heavy vehicle traffic on pavements and bridges in South Carolina and developed policy recommendations. The analysis was conducted on two pavement models: (1) based on equivalent single-axle loads (ESALs) in accordance with the SCDOT Pavement Design Guidelines and (2) based on the ME model. The pavement models revealed that overweight trucks reduce pavement service life significantly. Recovering the damage will require a flat fee of $65 per trip. Several alternative fee structures are proposed, such as an axle-based system in which permits costs between $24 and $175 per trip according to load, vehicle configuration, and trip distance.

Ghosn et al. (2015) developed models for assessing the effect of overweight vehicles on New York State (NYS) highway pavements and the associated costs. The MEPDG method is used to estimate the pavement damage cost due to overweight trucks. The cost allocation study performed on the entire NYS pavement network consisting of over 16,000 miles showed that the overall cost to NYS pavements due to overweight trucks is on the order of $145M/yr divided into $78M/yr for divisible permit trucks, $7M/y for special hauling trucks and $60M/yr for illegally overweight trucks.

Banerjee and Prozzi (2015) proposed a practical method for determining permit fees for overweight (OW) trucks, based on the consumption of service life of highways. A Mechanistic-Empirical design philosophy is used to estimate the deterioration of the pavement structure. The methodology uses permanent deformation, load-related fatigue damage, and roughness scores as descriptors to estimate service life consumption. Consumption of service life was estimated by the additional pavement structure required to accommodate OW traffic. The cost of the additional structure is used for

estimating the OW permit fee. Permit fees of 3.7¢/mi per equivalent single-axle load for flexible pavements and 2.9¢/mi per equivalent single-axle load for rigid pavements were suggested.

Laxdal (2016) estimated the cost of industrial bulk hauling on the Yukon (Canada) highway network. Pavement damage and rehabilitation with and without the bulk-haul traffic are estimated based on: 1) the American Association of State Highway and Transportation Officials (AASHTO) Guide for Design of Pavement Structures (1993); 2) Minnesota Seal Coat Handbook (Janisch & Gaillard, 1998); 3) the Shell Method for Bituminous Surface Treatment (BST); 4) United States Department of the Army Technical Manual (TM 5-626), unsurfaced Road Maintenance Management for gravel surface road segments. The result showed that the damage cost is a function of many factors, including weather and climate change, surface type (asphalt concrete, BST, or gravel), pavement structure thickness, subsurface conditions (soil, groundwater, and permafrost), and timing of preventative measures and rehabilitation.

Batioja-Alvarez et al. (2018) presented a probabilistic approach for estimating asphalt pavement damage costs attributed to overweight (OW) vehicles. The approach is based on mechanistic-empirical analyses considering statistical distributions of critical factors influencing pavement damage. Monte Carlo simulation was used to generate OW vehicle cases for a wide range of conditions observed in Nevada. The pavement damage cost was found to be sensitive to environmental conditions and AC layer thickness. The probabilistic nature of the proposed approach allows the pavement damage cost to be evaluated over a variety of OW vehicle configurations and environmental conditions.

2.1.2.2 Non-Destructive Testing

With the advance in non-destructive testing technologies, they have been increasingly used for estimating pavement damage and associated cost. Typical methods include the Failing Weight Deflectometer (FWD), Traffic Speed Deflectometer (TSD), etc., which characterize the structural damage of pavements.

FWD represents the most widely used non-destructive testing method for estimating the loading-bearing capacity of asphalt pavements. It measures the deflection of the pavement surface resulting from load applications. Methods have been developed to back-calculate the modulus of pavement structural layers (Ali and Khosla, 1987; Meier, 1995; Gopalakrishnan and Papadopoulos 2011; Kheradmandi and Modarres, 2018; Kim et al., 2021; Zhao et al., 2022; Mehta and Roque, 2003; Stubstad et al., 2006). Since the asphalt material is temperature sensitive, the FWD results depend closely on the test temperature. Methods have been developed to convert FWD results measured at arbitrary temperatures to that of a reference temperature so that a fair comparison can be made between FWD test results obtained at different temperatures (Lukanen et al., 2000; Nasimifar et al., 2020).

FWD has been used as a tool to estimate pavement deterioration. For example, Park and Kim (2003) developed a framework that uses FWD to estimate pavement remaining service life (RSL). The FWD results were first used to predict the pavement responses, i.e., the tensile and compressive strain in pavement layers. Then the critical pavement responses were used to predict the pavement performance, e.g., the fatigue cracking and rutting depth, which is then converted to an RSL of the pavement. The Long-Term Pavement Performance (LTPP) data were used to verify the proposed RSL

prediction methods. Methods have also been developed combining FWD and GPR data (providing the layer thickness information) to improve the accuracy of pavement condition estimation (Domitrović and Rukavina, 2013; Kheradmandi and Modarres, 2018).

FWD is relatively time-consuming and not efficient in terms of data collection, due to the stop-and-go process required by the measurements, and the need for traffic control. To improve efficiency, the Traffic Speed Deflectometer (TSD) has been developed (Flintsch et al. 2012; Zofka et al., 2014, Xiao et al., 2021; Huynh et al., 2021). Canestrari et al. (2022) developed a method to assess the RSL of pavements at the network level using the TSD measurements. In this approach, the curvature index SCI300 measured from TSD was used to estimate the residual fatigue resistance (considering bottom-up cracking as the critical distress) which is then used to predict the RSL of the pavements. The obtained RSL predictions can be used for network-level pavement management.

In addition to FWD and TSD, which characterize the structural damage of the pavement, pavement condition surveys that characterize the surface condition of pavements also provide necessary information for characterizing pavement damage. The Pavement Condition Index (PCI) which characterizes pavement surface distresses has been used to characterize pavement damage and RSL (Setyawan et al., 2015). Huynh et al. (2021) investigated the correlation between structural capacity data (TSD results) and surface condition data (Pavement Quality Index (PQI)). The results showed that PQI does not necessarily correlate with the pavement's underlying structural condition, which indicates that a more comprehensive approach to estimate pavement damage and RSL is to consider both the underlying structural damage and also the surface distresses.

2.2 Polices for Compensating Pavement Damage

2.2.1 MnDOT Policies

Minnesota Statutes §161.25, Temporary Trunk Highway Detour and Haul Road, requires that: "prior to revoking the designation [of detour or haul road] the commissioner shall restore such streets or highways to as good condition as they were prior to the designation."

To provide uniformity and consistency in reimbursing local agencies for use of their roads as detours by MnDOT, a task force of MnDOT staff and County Engineers recommended a gas tax method formula to compute payments for the use of local roadways as trunk highway detours (MnDOT, 1991). The formula is as follows:

Gas Tax Income Generated by the Detour = Average Daily Traffic (ADT) of traffic diverted x Length of detour (miles) x Duration (days) x 0.00513

This formula is included in the current MnDOT Cost Participation and Maintenance Responsibilities with Local Units of Government Manual (MnDOT, 2021). In addition, this manual also included the procedure for reimbursing the damage of unofficial detours. First, the increased costs of maintenance on the local roadway are documented by the local road authority and submitted to the MnDOT district for payment consideration. If the district concurs with the additional costs, an unofficial detour agreement is written

to provide payment to the local road authority. If MnDOT and the local road authority cannot agree upon the amount of additional maintenance costs that should be paid, the "Gas Tax Method," used for determining payment for a detour placed on paved roadways, may be used.

As documented in the Technical Memorandum (No. 13-19-MAT-01) Detour Restoration Road Life Analysis (MnDOT, 2013), an alternative to the "Gas Tax Method" is the "Equivalent Overlay Method". This method analyzes Falling Weight Deflectometer (FWD) data collected on the detour route. Based on the deflections, this method calculates the traffic capacity of the existing pavement structure. If the existing traffic capacity is less than twice the normal traffic plus the detour traffic, then an overlay thickness that will provide the required traffic capacity is calculated. A final cost is calculated from the cost of applying the calculated overlay thickness. This procedure is only applicable to bituminous on aggregate base pavements and full-depth bituminous pavements. The equivalent overlay method analysis is typically performed when the local agency feels that the road is in poor condition and will be significantly impacted by the detour (Smadi & Hans, 2005).

Payments to local agencies for haul roads are covered under MnDOT Specification 2051 of Minnesota Standard Specifications for Construction (MnDOT, 2020). For invisible damage, local agencies are reimbursed for haul road use on bituminous roadways with a spring load capacity of less than 9 tons. This is paid at a rate of $0.01 per ton per mile of material hauled. No reimbursement is made for gravel and concrete roadways. For visible damage, local agencies are reimbursed based on predetermined unit prices as listed in MnDOT's Special Provisions 2051 to be paid as extra work with the contractor and MnDOT sharing equally in the costs.

2.2.2 MnDOT Survey on Compensating Local Roads for Detour and Hauling

CTC & Associates LLC and MnDOT Office of Materials and Road Research (2017) have performed a survey on how state departments of transportation (DOTs) in the U.S. are compensating local governments for damage to local roads during highway detours that route traffic onto local roads or use local roads as haul roads during construction. An online survey was distributed to members of the American Association of State Highway and Transportation Officials (AASHTO) Subcommittee on Construction, which covered the following topics: 1) does DOT compensate local agencies for damage caused by detours or hauling, 2) what methods are used for calculating compensation, 3) are there written policy or statute for the compensation method, 4) Are there complaints about inadequate compensation 5) Are there plans to change the current compensation practice?

Twenty-one state DOTs responded to the survey. The findings are summarized in the next paragraphs. With the exception of Iowa and Arizona, DOTs do not seem to use a method (based on gas taxes or other factors) to compensate local governments monetarily. Instead, DOTs will repair or repave (or have contractors repair or repave) roads, as necessary.

2.2.2.1 Compensation for Damage or Use of Local Roads

Eight state DOTs (Arizona, Connecticut, Indiana, Iowa, Michigan, Nebraska, South Dakota, and Wyoming) compensate local governments for damage to local roads due to detours or hauling. The other (thirteen)

state DOTs reported that they don't compensate local governments. However, eight of them (Alabama, Arkansas, Missouri, New Hampshire, Oklahoma, Oregon, South Carolina, and Utah) mentioned they have informal policies for compensating local governments at least on some occasions, usually by repairing or repaving roads, or by having contractors repair or repave roads. Virginia and West Virginia do not compensate because they own and maintain their secondary road system.

2.2.2.2 Method for Calculating Compensation

Among the eight state DOTs that compensate local governments, seven shared a method, which is summarized in Table 2.1.

Table 2.1 Methods for compensate local agencies for detours and hauling.

State	Method
Arizona	Negotiate with local governments on a case-by-case basis in advance to compensate for damage to the road—either by hiring a contractor to repair the road, providing funds to allow localities to repair the road, or improving the road before the detour
Connecticut	Assess the existing road condition and, if the road needs improvements, project staff may negotiate with the town or city for in-kind replacement after construction. If the road is in good condition, construction personnel will evaluate the roadway and may direct improvements as extra work.
Iowa	Compensate for detours based on gas tax income earned by the detoured traffic during the detour. However, the county or city may request compensation based on an alternate method that requires the county or city to prepare a cost estimate for restoring the detour route to its pre-detour condition.
Michigan	Repair or repave the road as part of the project.
Nebraska	Responsible for fixing the road used as a detour for damage caused during use.
South Dakota	Inspect the road after the detour and make repairs at no cost to the local government
Wyoming	Overlay the road after the detour, if needed

2.2.2.3 Written Policy or Statute for the Compensation Method

Three of the eight states that said they compensated local governments (Connecticut, Iowa, and Nebraska) provided a written policy for their method. Their policies are summarized in Table 2.2.

Table 2.2 Policies for compensate local agencies for detours and hauling.

State	Policy
Connecticut	Section 2-922A: Detour of a State Highway to a Town Road, Volume 2, Construction Manual, Version 3.0, Connecticut Department of Transportation, January 2017. Assess the existing road condition and if the road needs improvements, project staff may negotiate with the town or city for in-kind replacement after construction. If the road is in good condition, construction personnel will evaluate the roadway and may direct improvements as extra work.
Iowa	Policy 600.05: Temporary Closure of Primary Highways and Establishment and Revocation of Detours, Policies and Procedures Manual, Iowa Department of Transportation, February 2006. Compensate for detours based on gas tax income earned by the detoured traffic during the detour. However, the county or city may request compensation based on an alternate method that requires the county or city to prepare a cost estimate for restoring the detour route to its pre-detour condition.
Nebraska	Nebraska Revised Statute 39-1347: County Roads; City and Village Streets; Authority to Use for Detour; Duties of Department, Nebraska Legislature, undated. Responsible for fixing the road used as a detour for damage caused during use.

2.2.2.4 Complaints about Inadequate Compensation

Only two states, South Dakota and Wyoming, said they have received complaints about inadequate compensation from local governments. In South Dakota, sometimes local governments request a thicker overlay, and sometimes contractors want to do less (or something different). In some rare cases, Wyoming has agreed to additional road user costs requested by cities.

2.2.2.5 Plans to Change the Current Method or Policy

Of the 13 states that said they do not compensate local governments, two—Virginia and West Virginia—do not compensate because they own and maintain their secondary road system. Three of the 13 states (Missouri, Oregon and Utah) said they had considered implementing a policy. Five additional states (Alabama, Arkansas, New Hampshire, Oklahoma, and South Carolina) answered “no” to this survey question but indicated that they actually already have informal policies for compensating local governments, typically by repaving roads. Comments from these eight state DOT survey respondents are summarized in Table 2.3.

Table 2.3 Comments for compensate local agencies for detours and hauling.

State	Comments
Alabama	The contractor is required to limit loads on roads or must patch or resurface roads as necessary.
Arkansas	Arkansas State Highway and Transportation Department doesn't use local roads for detours. Contractors are responsible for repairing public road damage caused by hauling.
Missouri	Missouri DOT detours only on state routes. In special situations, the agency enters a formal agreement during the design phase of the contract to compensate cities and counties.
New Hampshire	New Hampshire DOT sometimes repaves a section of a local road if the agency needs to use the road for a detour.
Oklahoma	Oklahoma DOT has on occasion paved or improved a local road designated as a detour.
Oregon	Oregon DOT may include repaving of a local road as part of a project if the road is designated in the project as a detour route for truck traffic.
South Carolina	South Carolina DOT fixes local roads that it damages.
Utah	Utah DOT leaves it up to the contractor to trade road repairs on a local road for permission to use the road as a haul route.

2.3 Conclusion

In this Chapter, a literature review was performed on pavement damage cost estimation and methods for compensating for the damage to local roads caused by detours and hauling. The following conclusions were drawn from this review.

- The research efforts for estimating pavement damage can be classified as empirical approach and engineering approach. The empirical approach is typically based on data-driven regression and the engineering approach is (partially) based on theoretical models of pavement response. Though practically useful, the empirical approach lacks a fundamental understanding of pavement damage. The engineering approach is theoretically sound, but the difficulty lies in the complexity of characterizing pavement damage and the evolution of damage with time.
- In the engineering approach, the Mechanistic-Empirical (ME) Pavement Performance Models have been used to estimate pavement damage. ME models are developed for the pavements under regular use. Local roads can be subjected to loads over their capacity when they are used for detours or hauling. The validity of the ME models for this scenario is not clear.
- Non-destructive testing methods like FWD, TSD, and GPR are promising methods for estimating the interior structural damage of pavement structures. A more comprehensive approach is a combination of these methods with the pavement surface condition survey (roughness, surface cracking, etc.) to estimate pavement damage considering both structural damage and surface distresses.

- MnDOT has two methods for compensating local agencies for using the local roads for detours. One is the “Gas Tax Method”, which uses the gas tax income earned by the detoured traffic for compensation. The Gas Tax Method does not consider the actual damage happened to pavements and has been complained of being insufficient. The other method is the “Equivalent Overlay Method", which estimates the pavement damage cost as the cost of constructing an overlay to prevent the pavement from being damaged by the extra traffic due to detours. This method does not consider the scenario where the pavements are already damaged, and therefore, it might not be able to provide an accurate estimation of the cost of restoring a damaged pavement.
- A survey was distributed to 21 different states in the U.S. on how they compensate local agencies for using the local roads for detours or hauling. The results showed that eight of them have formal methods to do the compensation; two do not compensate because they own and maintain their secondary road system; three said that their DOT had considered implementing a policy on compensating local agencies; five states indicated that they have informal policies for compensating local governments, typically by repaving roads.

Chapter 3: Evaluating Pavement Damage

This chapter quantitively estimates pavement damage using the remaining service life (RSL) approach. This method relies on non-destructive testing techniques, including the falling weight deflectometer (FWD), traffic speed deflectometer (TSD), and ground penetration radar (GPR). To begin with, a comprehensive literature review on structural evaluation using the FWD was conducted, covering back-calculation method, limitations, and deflection basin-related indices. Next, the theoretical basis for RSL estimation, derived from the deflection data obtained by TSD, was presented. Then, methods for converting FWD data to TSD data were studied, compared, and selected. Five detour routes and two haul roads in Minnesota were chosen for pavement damage assessment using FWD. After the detour and hauling operations were completed, RSLs were calculated and quantitively analyzed using the aforementioned methods.

3.1 FWD Structure Evaluation

The Falling Weight Deflectometer (FWD) is a non-destructive testing method used in pavement engineering to assess the structural integrity and load-bearing capacity of pavement sections. FWD applies a dynamic load to the pavement surface and measures the resulting deflections. During the FWD back-calculation process, these measured deflections are used to estimate the stiffness and thickness of the pavement layers. This information is then employed to determine the structural capacity of the pavement and to identify any potential distresses or failures in the pavement layers.

3.1.1 FWD Back-Calculation

The back-calculation of layer parameters is performed by matching the FWD load and deflection data to those generated by a mechanical model. These mechanical models simulate the pavement responses during an FWD test, or more broadly, the mechanical behavior of a layered half-space under an impact load on the surface.

Mechanical models can be broadly classified into two categories—static and dynamic—depending on whether inertia forces and wave propagation are considered. Static mechanical models assume that the pavement structure is in static equilibrium under the applied load, ignoring inertia forces and wave propagation. As a result, back-calculation is carried out by fitting the deflection basin (the measured deflection at different geophone locations). The analytical solution for an elastic multilayered system is the most widely used mechanical model in this category (Burmister 1945; Ullidtz 1998). Several software programs based on this model have been developed and are commonly used in practice, including MODULUS (Uzan et al. 1988) and TONN2010 (Khazanovich et al. 2011). To account for the viscoelastic properties of asphalt materials, the viscoelastic multilayered system model has also been applied to FWD back-calculations (Hopman 1996; Kim 2011). While the finite element method (FEM) can be used to solve multilayered systems, it is less computationally efficient compared to analytical solutions.

Static models are widely used in practice due to their simplicity and efficiency. However, the FWD test is inherently a dynamic test, where a large weight is dropped from a specified height, creating a 20 to 60

ms impulse load. This impulse generates waves in the pavement and underlying subgrade soil. These waves propagate and reflect at the interfaces between successive layers, continuing through the pavement structure. A key question is whether the inertial forces generated by this dynamic loading are significant enough to warrant consideration. Research has shown that the dynamic effects of the FWD test are significant and should not be ignored in back-calculation when aiming to accurately estimate layer properties such as modulus, Poisson's ratio, thickness, and unit weight (Ketcham 1993; Foinquinos et al. 1995). However, if the goal of the back-calculation is to obtain parameters to characterize pavement structural integrity—rather than material properties—static models are acceptable due to their simplicity and computational efficiency.

Theoretically, dynamic models, which simulate wave propagation in pavements, are more rational for FWD tests than static models. Numerical methods have been developed to solve dynamic models, including the finite layer method (Ketcham 1993; Foinquinos et al. 1995; Lee 2014; Lee et al. 2019; Quan et al. 2022), the spectral element method (Al-Khoury et al. 2001; Grenier et al. 2009; Gu et al. 2014), and the time-domain finite element method (Xu et al. 2015). Furthermore, dynamic back-calculation uses time histories, which contain more information than peak load and deflection values used in static methods. As a result, dynamic back-calculation can estimate a greater number of parameters than static methods (Lee et al. 2019). Despite these advantages, dynamic approaches are more complex and computationally expensive (Chatti et al. 2017). A summary of the methods is shown in Table 3.1.

3.1.2 Limitations of FWD Back-Calculation

There are some limitations to FWD back-calculation. The first is its limited spatial coverage. FWD back-calculation involves measuring deflections at specific points along a pavement section, which may not represent the entire pavement. To assess a pavement section comprehensively, FWD tests must be performed at multiple locations, making the process time-consuming and costly, especially for large pavement sections. Currently, the Traffic Speed Deflectometer (TSD), which assesses pavement structure at regular traffic speeds, is being developed to address these limitations (Zofka and Sudyka 2015; Zhang et al. 2022).

Another limitation is the inability to detect certain types of distress. FWD back-calculation primarily evaluates the structural capacity of pavement sections, but it may not detect issues like cracking or rutting. Therefore, FWD is often used in combination with other non-destructive tests, such as Ground Penetrating Radar (GPR) and image-based surface distress identification methods, to provide a more comprehensive assessment of pavement conditions.

Additionally, studies have shown that FWD tests have high variability (Siddharthan et al. 1992, Grogan et al. 1998, Neves and Cardoso 2017). For a uniform pavement section, the back-calculated moduli can vary by up to 65% (Siddharthan et al. 1992). Thus, reducing variability in FWD back-calculation is a key area for future research. Beyond back-calculating mechanical properties, a simpler approach to assessing pavement structural condition involves using Deflection-Basin-Related Indices, which are computed from two or more measured deflections.

Table 3.1 References on mechanical models for FWD back-calculation.

References	Static /Dynamic	Material model	Back-calculated Variables	Numerical Method
Uzan et al 1988	Static	Elastic	modulus	Analytical solution Elastic multilayered system, MODULUS
Khazanovich et al 2011	Static	Elastic	modulus	Analytical solution of Elastic multilayered system, TONN2010
Hopman 1996	Static	Viscoelastic	NA	Analytical solution of viscoelastic multilayered system
Kim 2011	Static	Viscoelastic	NA	Analytical solution of viscoelastic multilayered system
Ketcham. 1993. TRR	Dynamic	Elastic with damping	Four layers, Modulus, Poisson Ratio, thickness, damping ratio	Finite layer method. PUNCH
Foinquinos, et al. 1995. TRR	Dynamic	Elastic with damping	NA	Finite layer method.
Al-Khoury et al. 2001. Int. Jour. Solid. & Struct.	Dynamic	Elastic	NA	Spectral Element Method
Grenier et al 2009. Cana. J. Civ. Eng.	Dynamic	Viscoelastic	NA	Spectral Element Method
Gu et al. 2014. KSCE J. Civ. Eng.	Dynamic	Viscoelastic	NA	Spectral Element Method
Lee 2014. Int. J. Pavement Eng. Lee et al. 2019. TRR	Dynamic	Viscoelastic	Three layers. Modulus, thickness, unit weight, damping ratio.	Finite layer method Integral Transforms, Visco-wave
Xu and Prozzi 2015. Computers and Structures	Dynamic	Viscoelastic	NA	Time-domain finite element method
Quan et al. 2022. Road Mater. Pavement Des.	Dynamic	Viscoelastic with transverse isotropy	NA	Finite Layer Method

3.1.3 Deflection-Basin-Related Indices

Compared to back-calculation, Deflection-Basin-Related Indices lack a rigorous mechanical foundation but offer a more efficient means of pavement condition assessment. One such index is the Surface Curvature Index (SCI), which quantifies the difference in deflection at a specific location compared to the loading point. A higher SCI value indicates a weaker pavement structure, suggesting potential distress or structural deficiencies. In practice, SCI has been applied using both FWD and TSD data (Nasimifar et al.

2020, Molenaar 2007) and is now standard procedure for assessing pavements at the network level (Canestrari et al. 2022, Rada et al. 2016).

Among the various SCIs, SCI300 (the difference between the deflection under the load and the deflection at an offset of 300 mm) has shown a high correlation with pavement structural capacity (Rada et al. 2016, Molenaar 2007) and is widely used in current practice (Canestrari et al. 2022, Huynh et al. 2021, Katicha et al. 2017).

In this study, an approach based on SCI300 was used to evaluate pavement Remaining Service Life (RSL), following the method proposed by Canestrari et al. (2022). The approach involves the following steps: a) Load normalization of SCI300, b) Temperature adjustment of the normalized SCI300, c) Selection of the representative SCI300, d) Estimation of residual fatigue resistance, and e) Prediction of the RSL. The details of this approach are presented in the next section.

3.2 Estimate Pavement RSL based on TSD SCI_{300}

3.2.1 Load Normalization of the SCI_{300}

The measured deflections by TSD were normalized to the reference load of 40 kN. For the normalization, the following relationship was used:

$$SCI_{300} = SCI_{300,meas} \times \frac{40}{F_{actual}} \quad (1)$$

where $SCI_{300,meas}$ is the measured SCI_{300} value and Factual (kN) is the actual load applied in FWD test.

3.2.2 Temperature Adjustment of the Normalized SCI_{300}

The temperature adjustment of the SCI_{300} is necessary because of the variability of the pavement temperature during the FWD test and the strong effect of temperature on FWD results. The method proposed by Nasimifar et al. (2020) was used for the temperature adjustment.

$$SCI_{300,r} = SCI_{300} \times \lambda \quad (2)$$

$$\lambda = \frac{10^{[-0.0521 \times T_r + 0.0322 \times T_r \times log(h_{AC})]}}{10^{[-0.0521 \times T_f + 0.0322 \times T_f \times log(h_{AC})]}} \quad (3)$$

where $SCI_{300,r}$ (μm) is the value at the reference temperature. λ is the correction factor for temperature adjustment. T_r (°C), SCI_{300} (μm) is the value normalized to the load of 50 kN (Equation (1)), h_{AC} (mm) is the thickness of the asphalt layers and T_f (°C) is the temperature at $h_{AC}/2$.

The value of T_r was chosen as equal to 20°C whereas the value of T_f was estimated through the BELLS3 model (Lukanen et al. 2000).

$$T_f = 0.95 + 0.892 \times T_p + [log(h_{AC}/2) - 1.25] \times \left[-0.448 \times T_p + 0.621 \times T_{day} + 1.83 \times F_{T1}\right] + 0.042 \times T_p \times F_{T2} \quad (4)$$

$$F_{T1} = sin(hr_{18} - 15.5) \quad (5)$$

$$F_{T2} = sin(hr_{18} - 13.5) \quad (6)$$

where T_p (°C) is the temperature of the pavement surface and T_{day} (°C) is the average air temperature on the day before the survey. The functions sin(hr_{18} − 15.5) and sin(hr_{18} − 13.5) are two 18-hour sine functions whose value is equal to −1 between 5 and 11 am and between 3 and 9 am, respectively.

3.2.3 Selection of the Representative SCI_{300}

In a pavement section to be evaluated, multiple spots will be surveyed to compute the SCI300. Therefore, it is more rational to apply a reliability-based concept. A representative SCI300 value is defined as the SCI300 value at a certain percentile. The 85th percentile SCI300 value (denoted as SCI300r,85) was recommended by Canestrari et al. (2022), as it strikes a good balance between maintaining the structural condition and asset value on one hand, and budget constraints on the other.

3.2.4 Estimation of the Residual Fatigue Resistance

For a pavement section, the residual fatigue resistance is estimated based on the classical fatigue function.

$$N_{80}^r = f_1 \times \left(\frac{1}{\varepsilon_{t,max}^r \times 10^{-6}}\right)^{f_2} \left(\frac{1}{E_r \times 10^3}\right)^{f_3} \quad (7)$$

where N^r_{80} is the residual number of 80 kN ESALs, $\varepsilon^r_{t,max}$ (µm/m) is the maximum tensile strain at the bottom of the asphalt layers (at the reference temperature) and E_r (MPa) is the stiffness of the asphalt layers (at the reference temperature). In the present study, the values 0.414, 3.291 and 0.854 were assigned to f_1, f_2 and f_3, respectively. These are the values proposed by Finn et al. (1986) and adopted by the Asphalt Institute (Asphalt Institute 1981).

$$\varepsilon_{t,max}^r = a \times \left(SCI_{300r,85}\right)^b \quad (8)$$

$$E_r = c\left(\varepsilon_{t,max}^{r}\right)^{d} \quad (9)$$

where a, b, c, d are coefficients that depend on the thickness of the asphalt layers. The relationships in Equation (8) and (9) are obtained based on numerical simulation of pavement response under tire loading (Rada et al. 2016). The recommended values suggested by Nasimifar et al. are shown in Table 3.2. Please note the overlap of thickness values in column one, which translates into difference coefficient values for the same thickness, a drawback of this method.

Table 3.2 Model parameters for SAM* (Nasimifar et al. 2020).

AC layer thickness	SCITSD and maximum tensile train, Equation (8)			Strain and AC modulus, Equations (3) and (6)	
	a	b	R^2	c	d
76-102 mm (3-4 inches)	2.335	0.962	0.82	3.64E+06	-1.27
102-127 mm (4-5 inches)	1.875	1.02	0.9	4.52E+06	-1.36
127-152 mm (5-6 inches))	1.957	1.024	0.95	4.98E+06	-1.44
152-178 mm (6-7 inches)	2.452	0.987	0.97	4.41E+06	-1.46
176-203 mm (7-8 inches)	2.876	0.952	0.97	3.42E+06	-1.46
203-229 mm (8-9 inches)	3.381	0.912	0.97	3.39E+06	-1.51
229-254 mm (9-10 inches)	3.786	0.882	0.96	2.54E+06	-1.49
254-279 mm (10-11 inches)	4.375	0.8373	0.95	2.27E+06	-1.51
279-305 mm (11-12 inches)	4.701	0.8103	0.94	1.99E+06	-1.52
305-330 mm (12-13 inches)	4.905	0.7895	0.94	1.72E+06	-1.53
330-356 mm (13-14 inches)	5.392	0.7479	0.92	1.59E+06	-1.55
356-381 mm (14-15 inches)	5.015	0.7594	0.94	1.11E+06	-1.49
381-406 mm (15-16 inches)	5.248	0.7285	0.92	1.00E+06	-1.51
Thin: 76-152mm (3-6 inches)	2.883	0.927	0.9	9.65E+05	-1.072
Medium: 152-229 mm (6-9 inches)	3.071	0.935	0.97	1.37E+06	-1.264
Thick: 229-406 (9-16 inches)	4.115	0.8412	0.94	2.76E+05	-1.076

*SAM: Stiffness Adjustment Model

Combining the above equations, the relationship between $SCI_{300r,85}$ and N^{r}_{80} can be expressed as follows:

$$N_{80}^{r} = \alpha \times \left(SCI_{300r,85}\right)^{\beta} \quad (10)$$

$$\alpha = f_1 \times a^{-(f_2+f_3 d)} \times c^{-f_3} \times \left(\frac{1}{10^{-6}}\right)^{f_2} \left(\frac{1}{10^{3}}\right)^{f_3} \quad (11)$$

$$\beta = -b \times (f_2 + f_3 d) \quad (12)$$

3.2.5 Prediction of the RSL

The predicted RSL, in years, can be calculated by dividing the estimated residual fatigue resistance N^r_{80} by the estimated traffic (N_0) expressed in terms of 80 kN ESALs:

$$RSL = \frac{N_{80}^r}{N_0} \tag{13}$$

3.3 FWD and TSD Data Conversion

The deflection basins measured by FWD and TSD differ due to their operating conditions. The FWD is a stationary device, whereas the TSD measures deflection under a continuously moving load. The FWD applies a stationary impact load to the pavement surface, while the TSD applies a moving load at speeds of up to 60 mph via its rear axle. TSD records the pavement response under maximum loading for all sensors at a fixed time, whereas FWD measures maximum deflection, which occurs at different times for different sensors, as shown in Figure 3.1. Despite these differences in loading, recent studies in the U.S. and Australia have demonstrated a strong correlation between FWD and TSD deflection measurements.

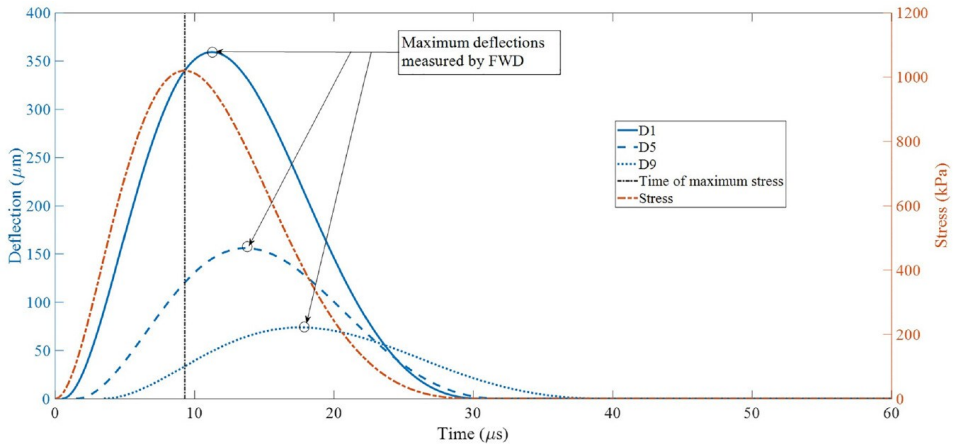

Figure 3.1 Deflection measurement from FWD and TSD (S. Katicha, Flintsch, and Diefenderfer 2022).

Flintsch et al. (2012) conducted section-level comparisons between Rolling Weight Deflectometer (RWD) and FWD maximum deflections. Results suggest that the average RWD measurements, normalized to a standard temperature, correlated relatively well with the average maximum FWD deflection when aggregated by homogenous sections.

S. W. Katicha et al. (2014) used the limits of agreement (LOA) method to compare FWD and TSD data. While the TSD measures deflection slope and FWD measures deflection, both were converted to the Surface Curvature Index (SCI) and Base Damage Index (BDI), respectively. Results revealed that although the relationship between the SCI and BDI calculated from both devices is reasonably close to the line of equality, there is significant variation and bias in this relationship.

Chai et al. (2016) employed the Simplified Deflection Model (SDM) to study deflection basins generated by TSD. Based on six test sections in Queensland, they collected 400 TSD and FWD deflection data points. A consistent trend in the pattern of maximum D0 deflections was discovered, establishing a correlation between the two datasets, as expressed in Equation 14, with an R^2 value of 0.88.

$$D_{0(TSD)} = 1.116 \times D_{0(FWD)} - 123.49 \quad (14)$$

A report by the New Zealand Transport Agency (NZTA) in 2016 made efforts to transform TSD data into FWD-equivalent deflections. The transformation was based on nationwide TSD and FWD tests conducted in 2015 and 2016. A simple transfer function was developed to compare the distribution of FWD deflections (dx) at any given offset position (ranging from 0 to 1500 mm) from the load center (x) with corresponding TSD deflections. The transfer function is expressed in Equation 15. However, the comparison between the 2015 and 2016 TSD datasets showed a significant year-to-year shift (Figure 2). This may be due to the 2016 raw TSD deflections being, on average, about 15% smaller than the previous year's values, coupled with an 8% increase in the applied load from 2015 to 2016, which compounded the standardized deflection error to a 25% drop between the years. NZTA concluded that a transfer function generated from one year's data for a specific Route Station (RS) cannot be confidently applied to historical or future data, although relative consistency between chainages remains likely.

$$FWD(TSD\ d_x) = A \times TSDd_x^2 + B \times TSD\ d_x \quad (15)$$

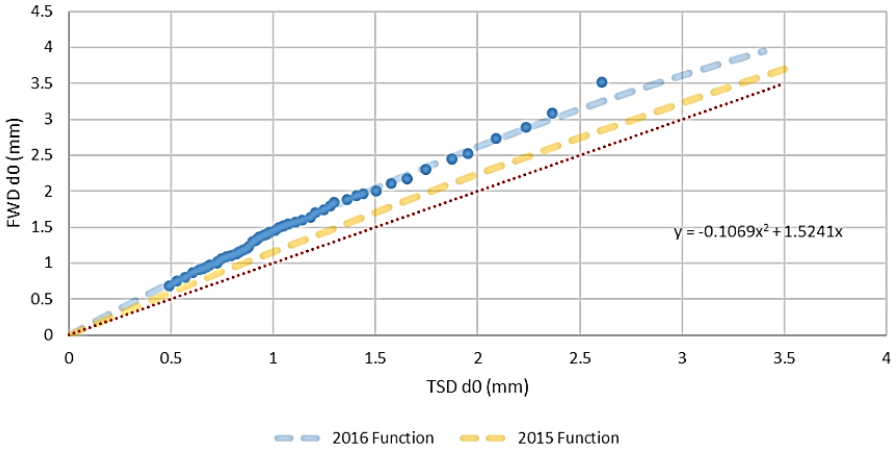

Figure 3.2 Example case plot of FWD d_0 vs 2016 TSD d_0 comparison and showing 2015 transfer function.

Levenberg et al. (2018) based on 80 FWD test section points, used TSD at operation speeds of 20, 50, 60, and 70 km/h to investigate the dissimilarity between the two methods. A Taylor diagram was employed to visualize the dissimilarity between FWD and TSD datasets. In addition to Pearson correlation analysis, a modern metric (λ) was proposed to quantify the closeness of the two datasets, rank-calculating agreement levels across different test sections. It was found that the running speed of TSD greatly

impacts the dissimilarity between TSD and FWD, with the highest agreement levels occurring at TSD speeds of 60 or 70 km/h.

Rabe (2018), in a German Federal Highway Research Institute pilot project, compared SCI_{300} data obtained from FWD and TSD across nine sections. The TSD data was calculated as the mean value of up to three repeated measurements along each test section, considering only positive SCI_{300} values while excluding unreasonable negative ones. As shown in Figure 3.3, the TSD SCI_{300} mean values are generally higher than the FWD SCI_{300} values for all sections. Most notably, the TSD SCI_{300} values indicated a different structural strength ranking than FWD SCI_{300}, with only the weakest section being consistent between the two, while the strongest section differed.

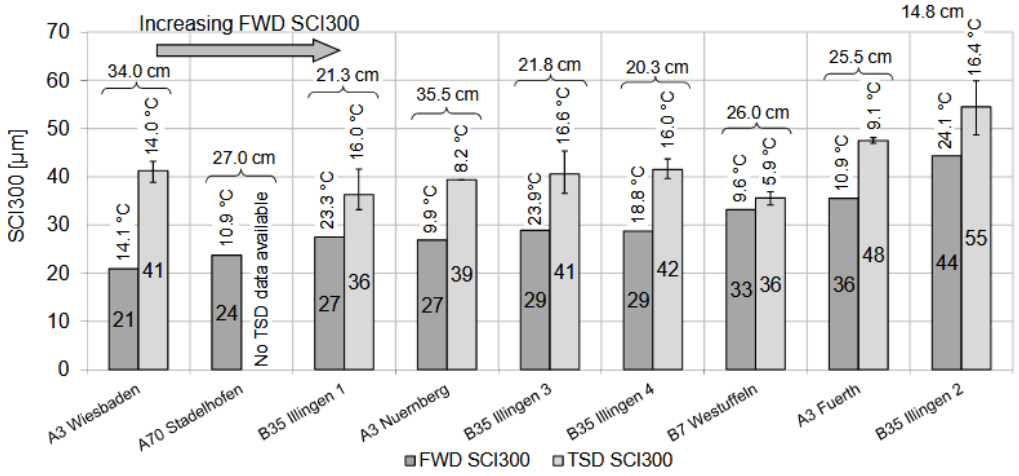

Figure 3.3 FWD SCI_{300} and TSD SCI_{300} values, average surface temperatures and total asphalt thickness per section (Rabe 2018).

In a recent report by the Idaho Transportation Department, Kassem et al. (2023) developed empirical regression models between FWD and TSD based on more than 100 tests. Correlations between deflection, theoretical maximum deflection (D0), and surface curvature index (SCI) are expressed in Equations 16-18, with R^2 values of 0.88, 0.80, and 0.84, respectively. However, after correcting both FWD and TSD data for temperature, Kassem et al. (2023) observed that temperature correction tended to increase deflections in TSD data, while decreasing deflections in FWD data.

$$D_{(TSD)} = 1.151 \times D_{(FWD)} + 0.664 \quad (16)$$

$$D_{0(TSD)} = 0.945 \times D_{0(FWD)} + 3.866 \quad (17)$$

$$SCI_{(TSD)} = 0.809 \times SCI_{(FWD)} + 1.573 \quad (18)$$

Zhang et al. (2022) created six 3D-Move models to explore the influence of different testing factors on pavement response with FWD and TSD. Their simulation results showed that under the same load magnitude, peak deflections and strains caused by TSD were greater than those caused by FWD, likely

due to TSD's lower equivalent load frequency. Compared to peak deflection, the deflection basin shape of TSD was found to be more sensitive to dynamic effects and the viscoelasticity of the asphalt concrete layer.

In general, previous studies have proven that deflections obtained by FWD and TSD are correlated and can be converted. According to findings from Chai et al. (2016), Rabe (2018), Kassem et al. (2023), deflections obtained from TSD tend to be larger than those from FWD. On the contrary, NZTA found that FWD deflections were larger than TSD deflections. In this study, Equation 16 was adopted to convert FWD-obtained deflections to TSD-equivalent values. After completing the conversions, the method introduced in Section 3.2 was used to calculate the Remaining Service Life (RSL).

3.4 Monitored Detour Routes and Haul Roads with FWD Testing

3.4.1 Basic Information

In total, five detour routes and two haul roads across seven counties (Brown, Renville, Jackson, St. Louis, Goodhue, Watonwan, and Faribault) were selected for FWD testing. The haul roads are located in Watonwan County and Faribault County, while all the detour routes are in the other five counties. Only data for the detour section in Goodhue County was available in this study. As a consequence, the research team used the data provided by Michigan State University for the other six test sections.

In Brown County, construction was performed on TH 14 between Highway 71 and CASH 4, with vehicles originally using this section of TH 14 being detoured onto CSAH 4, CSAH 3, CSAH 23, CSAH 2, CSAH 21, CSAH 11, and Highway 71 in both directions.

In Renville County, construction occurred on TH 71 between Highway 212 and CSAH 4. Vehicles that initially used this section of TH 71 to access or leave Olivia were detoured onto CSAH 4 and CSAH 1 in both directions.

In Jackson County, TH 86 was closed between Lakefield and Highway 90. Vehicles using TH 86 to access Lakefield had to use CSAH 14 from either the west or east side. Vehicles on TH 86 needing to reach Highway 60 had to use Highway 90 and CSAH 9, and vice versa.

In St. Louis County, a roundabout was constructed at the intersection of TH 194 and Midway Road (CSAH 13), closing both TH 194 and Midway Road to traffic during the construction. TH 194 traffic was detoured onto CR 889 in both directions.

In Goodhue County, the detour was located between MNTH 58 and US 61, along the river near Lake City.

In Watonwan County, trucks used CSAH 9 to haul heavy materials from the pit to Highway 60.

In Faribault County, a concrete plant was built at Interchange No. 128 on I-90. CSAH 17 was used to haul materials between the concrete plant and both the eastbound and westbound lanes of I-90.

Information on locations, test sections, detour times, test times, and data availability is presented in Table 3.3 and Figure 3.4.

Table 3.3 Test sections, detour time, test time, and data availability of studied sections.

Locations	Detour/Haul Roads	Name	Testing Date (before)	Testing Date (After)	FWD Data Availability	
					Before	After
Brown	Detour between 5/9/2022~8/5/2022 (**91 days**)	CSAH 2	6/10/2022	5/18/2023	A	NA
		CSAH 3	6/10/2022	5/18/2023	A	A
		CSAH 4	6/10/2022	5/18/2023	A	NA
		CSAH 21	6/10/2022	5/18/2023	A	NA
		CSAH 23	6/10/2022	5/18/2023	A	NA
St. Louis	Detour between 6/13/2022~9/29/2022 (**76 days**)	CR 889	8/8/2022	5/16/2023	A	A
Faribault	Haul Roads	CR 17	5/2/2023	10/26/2023	A	A
Jackson	Detour between Apr.2022~Nov.2023 (**215 days**)	CSAH 9	7/13/2022	5/2/2023	A	A
		CSAH 14	7/13/2022	5/2/2023	A	A
		CSAH 16	7/13/2022	5/2/2023	A	A
		CSAH 19	7/13/2022	5/2/2023	A	A
Renville	Detour between 8/8/2022~9/30/2022 (**54 days**)	CSAH 1	6/17/2022	4/27/2023	A	A
		CSAH 4	6/17/2022	4/27/2023	A	A
Watonwan	Haul Roads May.2023~Sep.2023	CR 9	5/2/2023	2/6/2024	A	A
Goodhue Red wing	Detour between 7/5/2023~9/5/2023 (**62 days**)	CSAH 5 AB	7/27/2023	10/25/2023	A	A

(1 A and NA represent available and not available

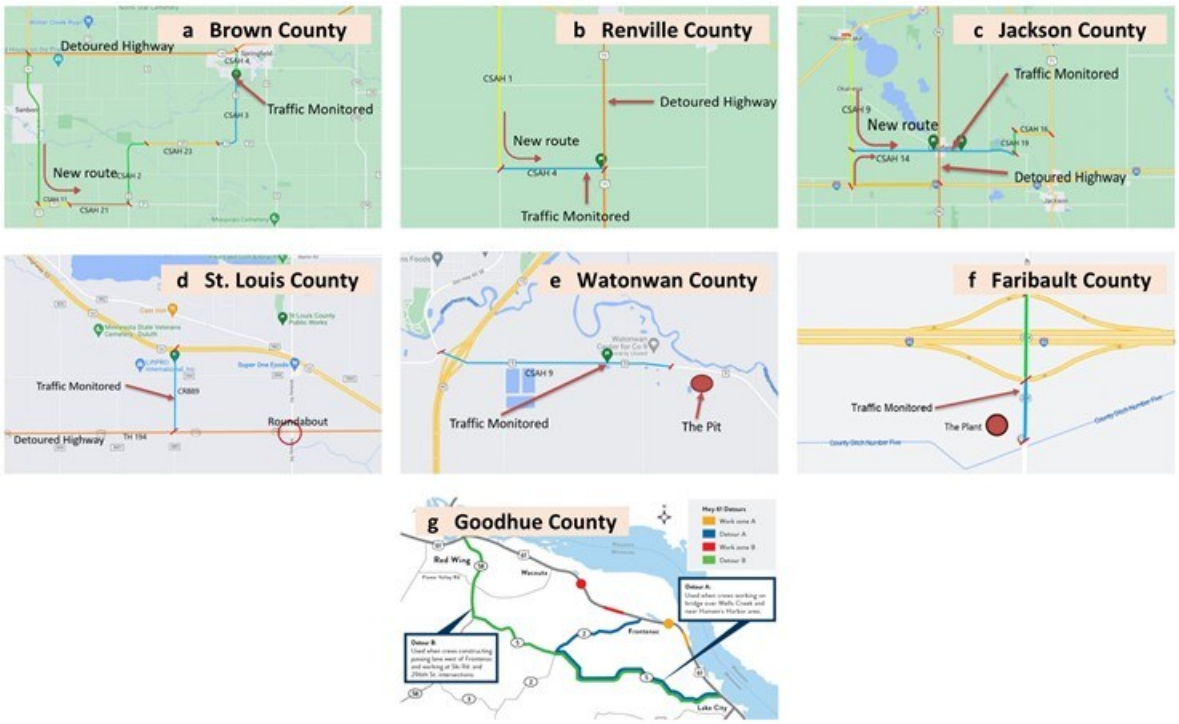

Figure 3.4 Locations of five detour routes and two haul roads.

3.4.2 Pavement Structural Characteristics

As introduced previously, determining the asphalt concrete (AC) layer thickness is essential. The pavement layer thicknesses are summarized in Table 3.4. FWD data collected in Brown County, Renville County, Jackson County, St. Louis County, Watonwan County, and Faribault County were provided by Michigan State University (Cetin et al. 2023).

For CSAH 5 in Goodhue County, Ground Penetration Radar (GPR) revealed a variation in the asphalt concrete layer thickness in the middle of the section. As shown in Figure 3.5, at mileage 4.8, the AC layer thickness decreases from 6 inches to around 5 inches, resulting in a structural difference before and after mileage 4.8. Therefore, CSAH 5 was divided into sections A and B.

3.4.3 Calculation of RSL

Based on the methods introduced previously, the Remaining Service Life (RSL) for all monitored sections was calculated and presented in Table 3.5. From Table 3.4, it is evident that some detour routes and haul roads have varying AC layer thicknesses (Brown County CSAH 2, CSAH 4, Jackson County CSAH 9), while others have no recorded thickness. In the former cases, it is impossible to calculate the RSL accurately because the specific mileages where the AC layer thickness changes are unknown. In the latter cases, the issue was addressed by assuming a typical AC layer thickness.

Table 3.4 Pavement layer thickness (inch) of roads with traffic monitoring, all pavement has semi-infinite subgrade.

County	Roadway	AC	Base	Sub-base
Brown	CSAH 2 (1)*	7.5	7	0
	CSAH 2 (2)*	6	9.5	0
	CSAH 3	9	12	0
	CSAH 4 (1)*	6	7	0
	CSAH 4 (2)*	9.5	-	0
	CSAH 21	7	9	0
	CSAH 23	7	9	0
St. Louis	CR 899	3.54	5.91	0
Renville	CSAH 1	-	-	-
	CSAH 4	6	14	0
Faribault	CSAH 17	-	-	-
Jackson	CSAH 9 (1)*	2	9	0
	CSAH 9 (2)*	3	9	0
	CSAH 9 (3)*	5.5	2.75	0
	CSAH 9 (4)*	3	9	0
	CSAH 9 (5)*	1.5	10.5	0
	CSAH 9 (6)*	1.5	11.5	0
	CSAH 14 (1)*	1.5	6	0
	CSAH 14 (2)*	1.5	3	6
	CSAH 14 (3)*	3	9	0
	CSAH 14 (4)*	1.5	9	0
	CSAH 16	1.5	8	
	CSAH 19	1.5	8	0
Watonwan	CSAH 9 (1)*	3	9.5	0
	CSAH 9 (2)*	2.25	12.5	0
Goodhue	CSAH 5	8.5	15	0

(1Brown CSAH 2(1): CSAH 21 to 1.8 miles north
(2 Brown CSAH 2(2): 1.8 miles north to CSAH 23
(3 Brown CSAH 4(1): CSAH 3 to central avenue
(4 Brown CSAH 4(2): central avenue to TH 14
(5 Jackson CSAH 9(1): CSAH 14 to south limits of Okabena
(6 Jackson CSAH 9(2): south limits of Okabena to north limits of Okabena
(7 Jackson CSAH 9(3): N limits of Okabena to CSAH 49
(8 Jackson CSAH 9(4): CSAH 49 to CSAH 43
(9 Jackson CSAH 9(5): CSAH 43 to Chapman
(10 Jackson CSAH 9(6): Chapman to TH 60
(11 Watonwan CSAH 9(1): CSAH 13 to 830th Ave
(12 Watonwan CSAH 9(2): 830th Ave to 2.82 miles east of 830th Ave

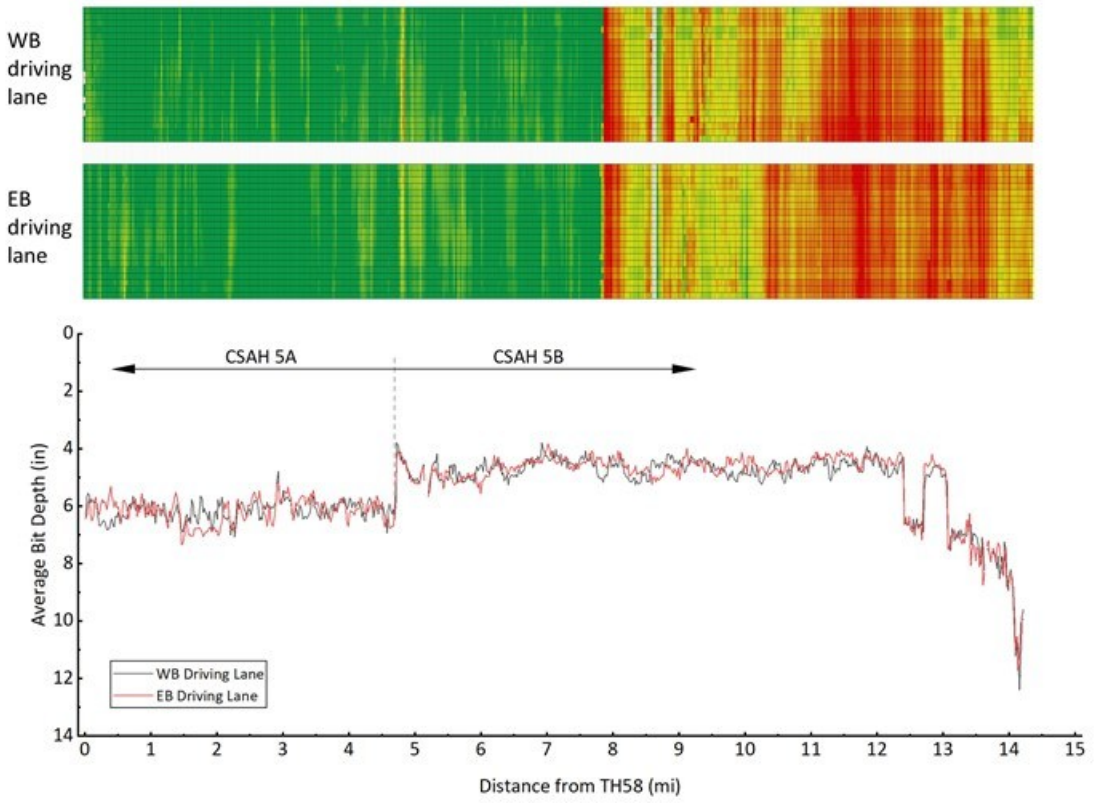

Figure 3.5 GPR result of CSAH 5 in Goodhue County.

For this calculation, the thickness of Faribault CR 17 and Renville CSAH 1 was assumed to be 6 inches. For ESAL, the same value of 69,366, provided by MnDOT, was used to calculate the RSL for all pavement sections.

Table 3.5 shows some irrational results for RSL before and after detouring/hauling. In certain cases, the RSL after the detour is higher than before, while in others, the RSL before the detour is unexpectedly low.

3.5 Monitored Detour Route with TSD Testing

3.5.1 Basic Information and Pavement Structural Characteristics

A section of US 71, located north of Bemidji in Beltrami County, was selected for TSD testing. The TSD was conducted from mile markers 322 to 336. The pavement on US 71 consists of a full-depth asphalt concrete layer approximately 14 inches thick. However, due to the unclear rehabilitation and overlay history, where milling and overlaying were repeatedly performed during pavement maintenance—the asphalt layer thickness may vary. As a result, RSL calculations were performed for different asphalt layer thicknesses.

Table 3.5 RSL of all studied test sections.

Locations	Detour/ Haul roads	Name	Description	Testing Date (before)	Testing Date (after)	RSL		
						Before	After	Diff.
Brown	Detour between 5/9/2022~8/5/2022 (91 days)	CSAH 2	AC thickness: varies from 6-7.5 in.	6/10/2022	5/18/2023	NA	NA	NA
		CSAH 3	AC thickness: 9 in.	6/10/2022	5/18/2023	28.07	33.91	-5.94
		CSAH 4	AC thickness: varies from 6-9.5 in.	6/10/2022	5/18/2023	NA	NA	NA
		CSAH 21	AC thickness: 7in.	6/10/2022	5/18/2023	27.04	NA	NA
		CSAH 23	AC thickness: 7in.	6/10/2022	5/18/2023	26.98	NA	NA
St. Louis	Detour between 6/13/2022~9/29/2022 (76 days)	CR 889	AC thickness: 3.54 in.	8/8/2022	5/16/2023	1.03	0.73	0.30
Faribault	Haul Roads	CR 17 NB	Missed AC thickness, select 6 in.	5/2/2023	10/26/2023	25.85	35.99	-10.14
						1.53	3.42	-1.89
Jackson	Detour between Apr.2022~Nov.2023 (215 days)	CSAH 9	AC thickness: varies from 2-5.5 in.	7/13/2022	5/2/2023	NA	NA	NA
		CSAH 14	AC thickness: smaller than 1.5 in.	7/13/2022	5/2/2023	NA	NA	NA
		CSAH 16	AC thickness: smaller than 1.5 in.	7/13/2022	5/2/2023	NA	NA	NA
		CSAH 19	AC thickness: smaller than 1.5 in.	7/13/2022	5/2/2023	NA	NA	NA
Renville	Detour between 8/8/2022~9/30/2022 (54 days)	CSAH 1	Missed AC thickness, select 6 in.	6/17/2022	4/27/2023	11.41	3.99	7.42
		CSAH 4	AC thickness: 6 in.	6/17/2022	4/27/2023	8.41	17.51	-9.10
Watonwan	Haul Roads May.2023~Sep.2023	CR 9 EB	AC thickness: 3 in.	5/2/2023	10/26/2023	1.26	5.92	-4.66
		CR 9 WB	AC thickness: smaller than 1.5 in.	5/2/2023	10/26/2023	NA	NA	NA
Goodhue	Detour between 7/5/2023~9/5/2023 (62 days)	CSAH 5 A	AC thickness: 6 in.	6/27/2023	10/5/2023	11.8	3.6	8.2
		CSAH 5 B	AC thickness: 5 in.	6/27/2023	10/5/2023	12.8	6.9	5.9

(1 NA represents not available

3.5.2 Calculation of RSL

The RSLs for US 71 at various asphalt layer thicknesses (7”, 8”, 9”, 10”, 11”, 12”, 13”, and 14”) were calculated. An estimated ESAL of 900,000 was used for the RSL estimation. The results are shown in Table 3.6. As expected, with an increase in the AC layer thickness, N^{r}_{80} increases while $SCI_{300,r}$ decreases. Figure 3.6 illustrates that each additional inch of AC thickness results in an increase in RSL, and this increase becomes more pronounced with greater AC thickness.

3.6 Evaluation and Discussion

In this section, the raw data were analyzed, and the nature of the Stiffness Adjustment Model (SAM) coefficients was discussed.

Table 3.6 RSL of US 71 at various AC layer thickness

AC thickness (in)	SAM model coefficients				N^r_{80}	$SCI_{300,r}$ ranges (μm)	RSL (year)
	a	*b*	*c*	*d*			
7	2.452	0.987	4.41E06	-1.46	6.33E06	18.1~97.5	7.0
8	2.876	0.952	3.42E06	-1.46	8.64E06	16.9~91.1	9.6
9	3.381	0.912	3.39E06	-1.51	1.19E07	15.9~85.5	13.3
10	3.786	0.882	2.54E06	-1.49	1.58E07	14.9~80.5	17.6
11	4.375	0.8373	2.27E06	-1.52	2.28E07	14.1~76.1	25.3
12	4.701	0.8103	1.99E06	-1.52	2.95E07	13.4~72.1	32.8
13	4.905	0.7895	1.72E06	-1.53	4.03E07	12.7~68.6	44.8
14	5.392	0.7479	1.59E06	-1.55	5.60E07	12.1~65.4	62.2

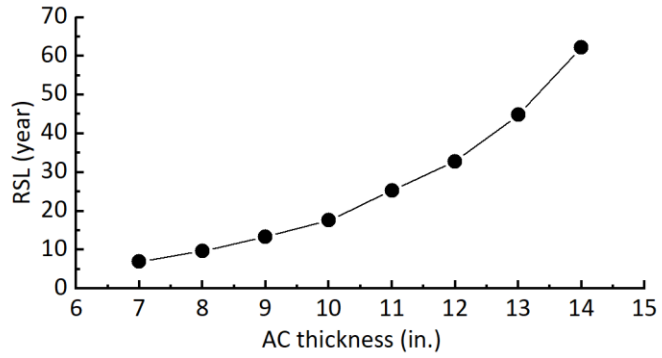

Figure 3.6 RSL variation with various AC thicknesses.

3.6.1 Variable Nature of FWD Testing

From Table 3.5, CR 17 in Faribault County, CSAH 4 in Renville County, and CR 9 EB in Watonwan County all show higher RSL after detouring/hauling. As shown in Table 3.7 to Table 3.10, deflections exhibit significant variability in all cases. For Faribault CSAH 17 SB, D305 varies from 151 to 442 microns after hauling, and for Watonwan CSAH 9 EB, D305 varies from 88 to 290 microns. This variability could be due to changes in critical factors affecting FWD testing, such as subgrade moisture content, test location, pavement discontinuities, and temperature. These factors may have contributed to an overall increase in D305 and $SCI_{300,r}$, leading to an increase in RSL after detouring/hauling.

3.6.2 Discontinuities of SAM model coefficients

From Table 3.2, discontinuities in SAM model coefficients are apparent, as two sets of coefficients can be selected when the AC layer thickness is 5 inches. Table 3.11 shows the results of RSL for the same AC thickness when different SAM model coefficients are applied. According to the GPR results, the AC layer thickness in CSAH 5 A varies from 5.5 to 7 inches, while in CSAH 5 B, it varies from 4.5 to 5.5 inches. When different SAM model coefficients are selected, the RSL can vary by more than 13 years.

Table 3.7 Deflection data at Faribault CSAH 17 NB before and after hauling.

	Before (5/2/2023)			After (10/26/2023)		
	D0	D305	$SCI_{300,r}$	D0	D305	$SCI_{300,r}$
1	266	264	0.9	206	173	37.6
2	346	263	90.0	247	205	49.5
3	586	294	337.7	259	218	48.7
4	197	175	24.9	222	176	52.5
5	226	207	21.4	301	224	88.2
6	269	240	33.9	325	215	133.5
7	221	192	32.8	229	210	21.0
8	255	204	60.1	343	296	54.4
9	163	152	11.5	238	179	67.0
10	312	258	61.5	226	192	39.

Table 3.8 Deflection data at Faribault CSAH 17 SB before and after hauling.

	Before (5/2/2023)			After (10/26/2023)		
	D0	D305	$SCI_{300,r}$	D0	D305	$SCI_{300,r}$
1	655	423	269.4	779	442	395.6
2	522	372	173.2	285	253	37.4
3	403	320	93.8	180	151	33.5
4	320	279	46.7	219	187	37.9
5	437	322	131.7	244	217	31.4
6	470	391	91.7	422	305	138.4
7	483	335	170.7	292	255	43.6
8	391	304	99.4	516	336	213.3
9	395	370	28.6	578	359	274.2
10	569	405	189.9	548	332	266.5

Table 3.9 Deflection data at Renville CSAH 4 before and after detour.

	Before (6/17/2022)			After (4/23/2023)		
	D0	D305	$SCI_{300,r}$	D0	D305	$SCI_{300,r}$
1	341	224	131.3	380	310	80.8
2	562	389	195.2	391	315	88.5
3	520	356	188.5	415	330	99.9
4	606	402	233.7	250	205	51.3
5	418	283	152.7	410	323	102.0
6	595	366	260.3	304	244	70.2
7	681	427	293.1	467	382	100.0
8	439	293	165.7	468	385	95.4
9	619	432	214.6	402	326	86.9
10	664	456	238.3	376	309	75.7

Table 3.10 Deflection data at Watonwan CSAH 9 EB before and after hauling.

	Before (6/17/2022)			After (4/23/2023)		
	D0	D305	$SCI_{300,r}$	D0	D305	$SCI_{300,r}$
1	332	187	167.1	151	128	25.9
2	358	234	141.8	178	151	29.9
3	450	268	211.0	137	118	20.9
4	588	286	356.0	114	96	20.3
5	447	228	256.8	102	88	15.2
6	521	269	296.4	189	160	32.2
7	508	286	258.5	182	155	30.4
8	513	302	244.7	220	183	41.0
9	428	267	189.6	368	290	89.2
10	640	316	378.8	268	230	43.0

Table 3.11 RSL results at various SAM model coefficients.

	CSAH 5 A			CSAH 5 B		
Description	h_{AC}=6” 8-9”MC*	h_{AC}=6” 7-8” MC	h_{AC}=6” 6-7” MC	h_{AC}=5” 8-9” MC	h_{AC}=5” 5-6” MC	h_{AC}=5” 4-5” MC
N^r_{80}	1.119E+6	7.842E+5	6.031E+5	1.767E+6	8.908E+5	7.473E+5
$SCI_{300,r}$ ranges (μm)	47.6~237.0	47.6~237.0	47.6~237.0	54.4~197.2	54.4~197.2	54.4~197.2
RSL (year)	16.1	11.8	8.7	25.5	12.8	10.8

*MC: Model Coefficients

3.7 Conclusion

In this Chapter, non-destructive testing methods, FWD, TSD, and GPR, were used to estimate pavement structural damage caused by detour and hauling activities. Based on the deflection data collected from five detour routes and two hauling roads, the impact of excessive traffic on pavement RSLs was quantitatively analyzed. After a thorough analysis of the results and reflection on the theoretical basis of

RSL calculations, the pros and cons of this approach were discussed. The following conclusions were drawn:

- Due to differences in operational conditions, deflections obtained from FWD and TSD differ and should be converted cautiously. Linear regression models have been introduced by research teams in Australia and the United States to convert FWD deflections into TSD deflections, while the New Zealand Transportation Agency developed a quadratic regression model for deflection conversion.
- Using empirical stiffness adjustment models, tensile strain and pavement layer modulus can be effectively represented by the surface deflection curve index (SCI300). With the help of the BELLS3 temperature prediction model, the remaining service life (RSL) of pavement can be estimated using only pavement deflection response data. This study successfully established an approach to calculate the RSL of asphalt pavements based on FWD and TSD deflection data.
- Five detour routes, two haul roads, and a total of 17 sections were monitored and tested for deflections. Except for sections with unknown asphalt concrete layer thicknesses, RSLs were calculated for 12 sections. The damage caused by detour and hauling was quantitatively analyzed for 7 of these sections. However, 4 sections showed a higher RSL after detour/hauling, while only 3 sections presented a decrease in RSL: CR 889 in St. Louis County, CR 17 NB in Faribault County, and CSAH 1 in Renville County.
- Through the analysis of raw deflection data and the calculation method, it was found that the increase in RSL after detour and hauling was due to the variability in the deflection data obtained from FWD tests. In some cases, the deflection data collected after detour and hauling were smaller than those collected before. This may be attributed to changes in critical factors that affect FWD testing, such as subgrade moisture content, test location, pavement discontinuities, and testing temperature. These factors may not only influence the magnitude of the deflections but also aggravate the variability of the data, making the RSL calculations less reliable and more variable.

Using non-destructive methods like FWD and TSD to evaluate pavement damage is highly sensitive to numerous environmental factors (e.g., moisture content, temperature) and pavement characteristics (e.g., thickness discontinuities, subgrade conditions). In the study conducted by Canestrari, the TSD data was obtained on interstate type pavements, with uniform thicknesses and very strong foundations with bearing capacity not affected by variations in moisture content.

The difficulty in controlling these factors and accurately taking them into account, makes it challenging to obtain reasonable and consistent deflection data. In applying this approach to determine pavement damage, there are additional concerns, such as discontinuous stiffness adjustment model coefficients, reduced traffic impact during short detour and hauling periods, and inaccuracies in pavement temperature predictions using the BELLS3 model.

Chapter 4: Traffic Assignment to Estimate Detour Route Flows

The route choice prediction will be integrated into the software application developed in Chapter 4. This application leverages data from MnDOT's CUBE model, specifically for the Minneapolis network, to forecast link flows and congestion levels for different vehicle types. A novel approach is implemented to track traffic volumes by vehicle class. The project includes a before-and-after analysis by solving traffic assignments with and without the construction project. Variations in heavy truck volumes across links will help identify roads at higher risk of damage. Post-processing will focus on analyzing the effects of detours and road closures on traffic patterns, with a particular emphasis on how changes in route choice impact traffic congestion and pavement infrastructure.

4.1 Traffic Assignment

The assessment of pavement damage caused by detours and haul roads associated with construction projects presents significant and complex challenges. Construction activities often require rerouting drivers to alternative roads, resulting in increased vehicle flows—particularly heavy trucks—on routes that were not originally designed to support such volumes or loads. This study specifically focuses on predicting the increased flow of truck traffic on surrounding roads due to road closures, to further analyze its effects on pavement infrastructure.

The challenge with predicting increased truck flow lies in the complexity and unpredictability of driver behavior. While detour signs are designed to guide traffic to specific alternative routes, not all drivers follow the designated paths. Factors such as individual route preferences, GPS routing suggestions, congestion on the detour routes, and time-sensitive deliveries can lead truck drivers to choose alternate routes that are not accounted for in the detour plan.

We have developed a traffic assignment model to estimate detour flows, drawing on established methodologies from the literature. However, slight modifications are necessary to specifically track heavy truck volumes. This task includes collecting and processing planning data from sources such as MnDOT's CUBE model, to which the project team already has access. The next step involves implementing traffic assignment within the software, which will require a novel approach to account for multiclass traffic volumes, distinguishing between different vehicle types of cars and trucks, including heavy trucks. A comparative analysis will be conducted by solving traffic assignments both with and without the construction project in place. The resulting differences in link volumes, particularly for heavy trucks, will help identify roads at higher risk of pavement damage.

This report presents our analysis of traffic volume specific to trucks and cars during detour and construction project use in relation to pavement infrastructure in Minnesota municipalities. Our work builds upon several crucial tasks completed in earlier stages of this research project:

1) Initial Memorandum: We developed an initial memorandum outlining the expected benefits of our research and potential implementation steps. This preliminary assessment helped shape our methodology and focus our efforts on outcomes most beneficial to the state of Minnesota.
2) Data Collection: Working closely with MnDOT, we gathered comprehensive travel demand data and road network information for key Minnesota municipalities, including Minneapolis and St. Paul. A crucial part of this process involved adapting and formatting this diverse data to be compatible with our analytical software.
3) Methodology Development: We developed a sophisticated methodology for predicting route choices in the context of road closures. This approach combines a logit model for tracking the flow of two classes of vehicles, cars and trucks, with a user equilibrium model for route choice, providing a robust framework for analyzing travel behavior and how the detour projects will change vehicles' behavior and the corresponding demand of each link.
4) Software Implementation: The developed models were implemented in a custom software application, creating a powerful tool for analyzing transportation networks with vehicle types components.

Building on these completed tasks, our current focus is analyzing traffic congestion and infrastructure use. Specifically, we aim to: a) based on the collected data, use our software application to predict vehicle-type-specific origin-destination traffic flows and congestion, b) post-process the outputs to study the impacts of detours on traffic flows and congestion, c) Examine how changes in link capacity affect each vehicle type flow on other links and the whole network travel time.

This analysis aims to offer valuable insights into the effects of detours on transportation patterns, congestion levels, and pavement usage in urban areas across Minnesota. The findings from this study are expected to play an important role in guiding transportation policy and infrastructure planning, particularly in the context of changing route choices and traffic behaviors. The subsequent sections of this report will outline our methodology, present the results of our analysis, and discuss the implications of these findings for transportation planning and policy development in Minnesota.

4.2 Problem Definition

Quantifying and mitigating pavement damage resulting from detours and haul roads associated with construction projects is a significant and complex challenge. Policies have been established to ensure that roads are restored to their pre-construction condition, and in some cases, overweight trucks are permitted to use certain roads through MnDOT's permit process. However, due to the complexity of assessing pavement damage, the current permit system relies on a flat fee structure rather than an evaluation based on the actual damage inflicted on the pavement.

We propose an approach to quantifying pavement damage that incorporates both traditional and advanced technologies, enabling a more accurate assessment. Techniques such as measuring pavement deflection using Falling Weight Deflectometer (FWD) or Traffic Speed Deflectometer can provide critical insights into the structural capacity of pavement before and after detour traffic. Additionally, ground-

penetrating radar can be employed to precisely determine layer thickness, while LiDAR systems can be used to evaluate the surface condition of the pavement both pre- and post-detour.

Additionally, pavement damage can be theoretically minimized by rerouting traffic to roads in better condition. While detour routes are explicitly designated, drivers' actual route choices are not controlled. To address this issue, the proposed project aims to develop an advanced modeling approach that integrates both vehicle types and route choice factors during construction projects, with a focus on heavy trucks. The model's predicted link flows will identify which additional roads should be assessed for potential damage. Furthermore, the model will be extended to suggest optimal detour routes that minimize pavement damage. This model will provide policy planners with the necessary tools to design appropriate infrastructure for alternative routes during construction detours, particularly for trucks. The model is designed to offer actionable insights into changes in travel behavior, traffic patterns, and flows across each link of the network for different vehicle types, specifically cars and heavy trucks.

The approach begins by estimating traffic flows on the network without any detours, tracking car and truck volumes on each link. Then, detours are implemented by modifying the network, including the removal of certain links due to the detours. The model is rerun with the updated network, again tracking car and truck flows. The results are compared with the initial scenario to analyze how detours alter traffic flows on other links and across the entire network. We utilize detour data from Minneapolis, assuming that all relevant information, such as travel costs, is fully known to users when they make their route choices. Additionally, the network operates under user equilibrium (UE) conditions, a common assumption in both static and dynamic traffic assignment models for planning. Under UE conditions, each driver selects the route between their origin and destination which minimizes their travel time.

The principle of user equilibrium dictates that all utilized routes connecting a given origin and destination must have equal and minimal travel times. While unused routes may have higher travel times, and routes connecting different origin-destination pairs may exhibit different travel times, any two routes used between the same origin and destination will have identical travel times. A stable UE condition is achieved when no traveler can reduce their travel time by unilaterally switching routes, ensuring that no further improvements are possible. This is the defining characteristic of the user equilibrium condition.

The remainder of this report focuses on detailing the methodology and user equilibrium model used to evaluate the effects of construction detours, with specific consideration given to the interactions between two vehicle types: cars and heavy trucks. We propose an iterative algorithm to address the traffic assignment problem, which enables a thorough analysis of the changes in car and truck traffic flows during detours.

4.3 Methodology

We input the origin-destination demand flows for each vehicle type into a UE traffic assignment model. The UE conditions are applicable to our network based on the following assumptions: (1) users have

perfect knowledge of the path costs; (2) travel time on any given link is solely a function of the flow on that link; and (3) travel time functions are positive and increasing.

The first assumption in a UE traffic assignment is that each driver seeks to minimize their travel time by selecting the optimal path between their origin and destination. The second assumption is that drivers have knowledge of the travel times on each link. According to the UE principle, every route in use that connects an origin and destination pair has equal and minimal travel time. Routes that are not used may have higher travel times, and routes connecting different origin-destination pairs may exhibit varying travel times. However, for any two routes connecting the same origin and destination, the travel times must be equal. A stable condition, referred to as user equilibrium, is reached when no traveler can reduce their travel time by unilaterally changing routes. This characterization of the UE condition has been extensively studied and widely applied in transportation research. By solving this problem, we can determine the vehicle-specific route flows that minimize travel times in equilibrium across the network.

4.3.1 Notation

We consider a network $G = (N, A)$, where the graph G consists of a set of nodes N and a set of links A. Each link in the network is represented by a pair (i, j), denoting a connection between two nodes. Let $Z \subseteq N$ be the set of zones. Zones represent nodes that are traveler origins or destinations. Travel time is considered as the travel cost here. The travel time for the link (i, j) is a function of traffic flow on this link for each is $t_{ij}(x_{ij})$. Let Π_{rs} be the set of simple paths between $r \in Z$ and $s \in Z$. Let $\Pi = \cup (r,s) \in Z^2, \Pi_{rs}$ be the set of all paths. While separate links are not designated for cars and trucks, their flows are tracked independently. The demand between origin r and destination s is specific to the vehicle type, which can be either a car or a truck, and is denoted by d_{rs}^{v}, where v represents the vehicle type—either car or truck. Both vehicle types, cars and trucks, originate from the same nodes, which serve as the sources of demand for each type. Consequently, the total flow on each link is calculated as the sum of the individual flows from cars and trucks.

4.3.2 User Equilibrium

The paths connecting any origin-destination pair can be classified into two categories: those that carry traffic flow, where the travel time is equal to the minimum travel time, and those that do not carry flow, where the travel time is greater than or equal to the minimum travel time. If the flow pattern adheres to these conditions, no traveler can reduce their travel time by switching routes. All other available routes either have equal or higher travel times. Consequently, the UE criteria are satisfied for every origin-destination pair. The equivalence between the UE conditions and the first-order optimality conditions implies that the UE conditions are met at any local minimum of the objective function. This ensures that the system is in a stable state where no user can improve their travel experience unilaterally.

Based on the above explanation of the user equilibrium concept and Beckmann equations, we can write the following equations for our problem. If we define:

$$V = \{car, truck\} \tag{19}$$

Then,

$$\sum_{v\epsilon V} h_{\pi}^{v} \times (T_{\pi} - \mu_{rs}) = 0 \ \ \forall (r,s)\epsilon z^2, \forall \pi \in \Pi_{rs} \tag{20}$$

$$T_{\pi} \geq \mu_{rs} \ \ \ \forall (r,s)\epsilon z^2, \forall \pi \in \Pi_{rs} \tag{21}$$

The first extended condition states that for any path π with the total flow of all vehicle types of $\sum_{v\epsilon V} h_{\pi}^{v}$, the path travel time T_{π} is equal to the minimum travel time μ_{rs} for that origin-destination pair. For paths without flow, the travel time T_{π} is greater than or equal to μ_{rs}. This ensures that travelers cannot reduce their travel time by changing modes or paths. Any path π that carries flow will have the minimum travel time, while all other paths will have equal or higher travel times.

4.3.3 Mathematical Formula

The objective of the model is to determine the vehicle-specific route flows h_{π}^{v} for each vehicle type that minimizes the total system travel time, while satisfying flow conservation and non-negativity constraints. These path flows will dictate how car and truck travelers are routed through the transportation network to move from their origin r to their destination s. The model integrates vehicle-type-specific demand for each origin-destination (O-D) pair (r, s).

The mathematical program aims to assign travelers to optimal routes by balancing two competing objectives: minimizing the total travel time across the network and ensuring that path flows reach an equilibrium state where no individual traveler can improve their travel time by switching routes. The following is the mathematical formulation used to solve this problem, based on the underlying assumptions. We can prove that any solution to the following problem satisfies user equilibrium using the Karush-Kuhn-Tucker condition:

$$\min \sum_{v\epsilon V} \sum_{(i,j)\epsilon A} \int_{0}^{x_{ij}^{v}} t_{ij}(x) d(x) \tag{22}$$

4.3.3.1 Constraints

This section describes the constraints needed to analyze the entire network. The link flows, denoted as x_{ij}^{v} for vehicle type of v, and the path flows, denoted as h_{π}^{v} for vehicle type of v, are closely related. Let $\delta_{ij,\pi}$ denote the number of times link (i, j) is used by path π, so $\delta_{ij,\pi} = 0$ if path π does not use link (i,j), and $\delta_{ij,\pi} = 1$ if it does. With this notation, we have:

$$x_{ij}^{v} = \sum_{\pi \epsilon \Pi_{rs}} h_{\pi}^{v} \delta_{ij,\pi} \quad \forall (i,j)\ \epsilon\ z^2 \tag{23}$$

By assuming that every path flow cannot be negative, we will have the following constraint:

$$\sum_{v \epsilon V} h_{\pi}^{v} \geq 0 \quad \forall \pi \in \Pi \tag{24}$$

Each trip from origin r to destination s must take one of the available paths in the network. Therefore, we will assume that the summation of path flows between r and s for vehicle type v, equals the demand of this vehicle type v between r and s, denoted as d_{rs}^{v}:

$$\sum_{\pi \epsilon \Pi_{rs}} h_{\pi}^{v} = d_{rs}^{v} \qquad \forall (r,s) \epsilon z^2,\ \forall\ v\ \epsilon\ V \tag{25}$$

4.3.3.2 Vehicle Travel Time

VTT is the vehicle travel times for traveling between r to s. We derive VTT from the Bureau of Public Roads (BPR) function, which takes the form:

$$t_{ij}\left(x_{ij}^{v}\right) = t_{ij}^{0} \times \left(1 + \alpha\left(\frac{\sum_{v \epsilon V} x_{ij}^{v}}{u_{ij}}\right)^{\beta}\right) \tag{26}$$

α and β are shape parameters that can be calibrated to data. It is common to use α = 0.15 and β = 4. t_{ij}^{0} is the free-flow travel time on link (i, j), and u_{ij} is the capacity of link (i, j). This equation is used to derive the travel time of a link (i, j). To achieve the travel time between r and s, we need to sum up all the links' travel time between r and s, which are in the user's path.

4.3.3.3 Performance Metrics

The total system travel time TSTT is the sum of all actual travel times of trips, which is calculated by:

$$TSTT = \sum_{v \epsilon V} \sum_{ij} x_{ij}^{v} \times t_{ij}(x_{ij}^{v}) \tag{27}$$

The minimum cost path travel time is the sum of all shortest travel times of trips, which is calculated by:

$$SPTT = \sum_{v \epsilon V} \sum_{(r,s)} d_{rs}^{v} \times t_{ij}(x_{ij}^{v}) \tag{28}$$

The gap is the convergence criterion used in this study. To calculate the gap in the simulation, total system travel time (TSTT) and minimum cost path travel time (SPTT) were first calculated. gap is calculated by:

$$GAP = \frac{TSTT - SPTT}{TSTT} \tag{29}$$

Another metric is Average Excess Cost (AEC), which is calculated by:

$$AEC = \frac{TSTT - SPTT}{\sum_{v \in V} \sum_{(r,s)} d_{rs}^{v}} \tag{30}$$

These performance measures will be used to check the whole algorithm's convergence and compare different scenarios.

4.4 Data

The closure data used in this study was obtained from the Minneapolis city website. Additionally, to compensate for the limited closure data, we created some fictional closures. The specific links considered closed are illustrated in Figure 4.1 and Figure 4.2. The assumed closures resulted in the closure of 120 links out of a total of 57,002 in the network.

For the network and trip demand data, the project team has access to MnDOT's CUBE model, which serves as a data source for the traffic assignment model. This methodology can be extended to the entire state, provided the necessary input data on link characteristics and demand are available.

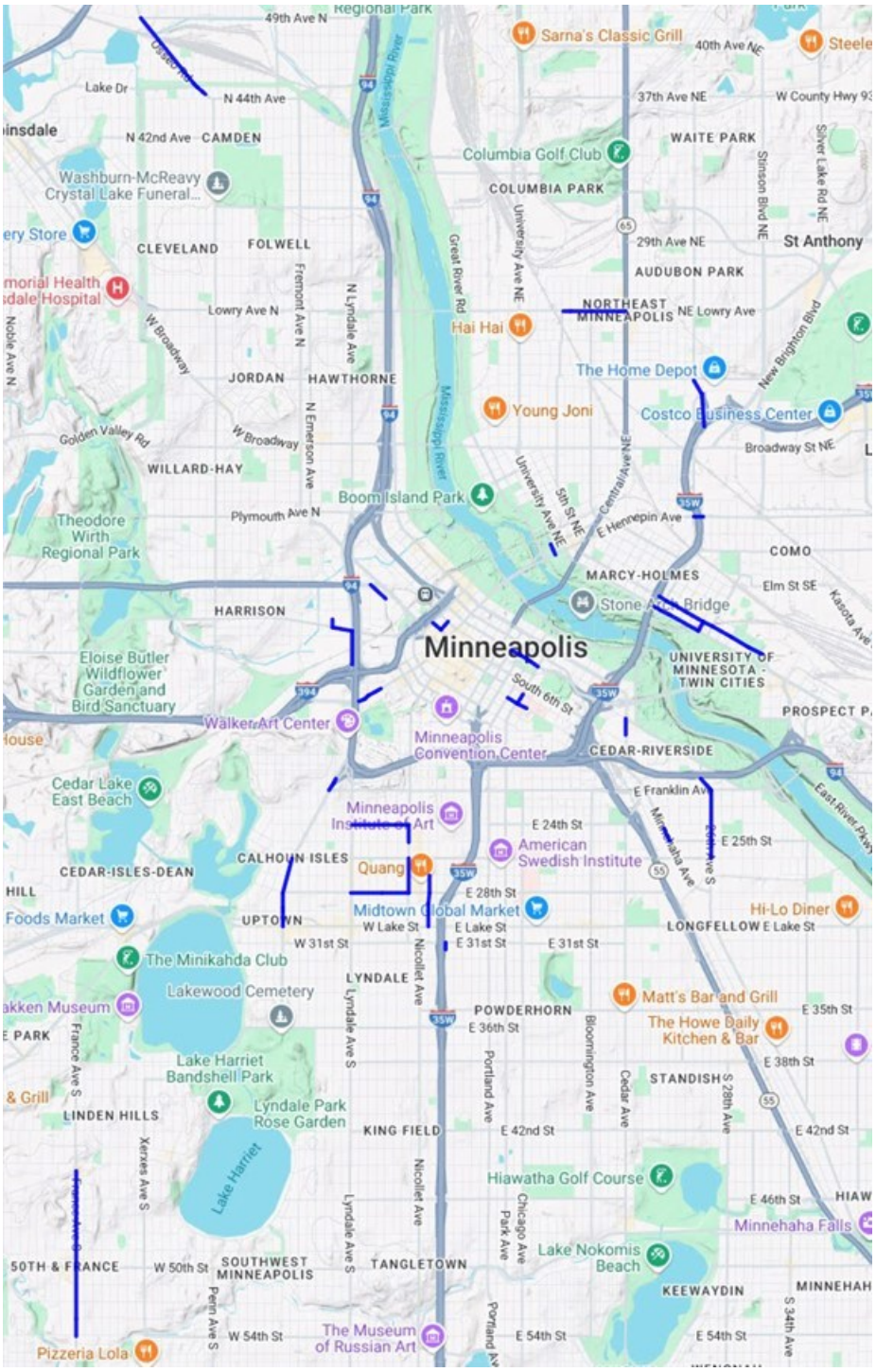

Figure 4.1 Close-up of assumed closures in Minneapolis.

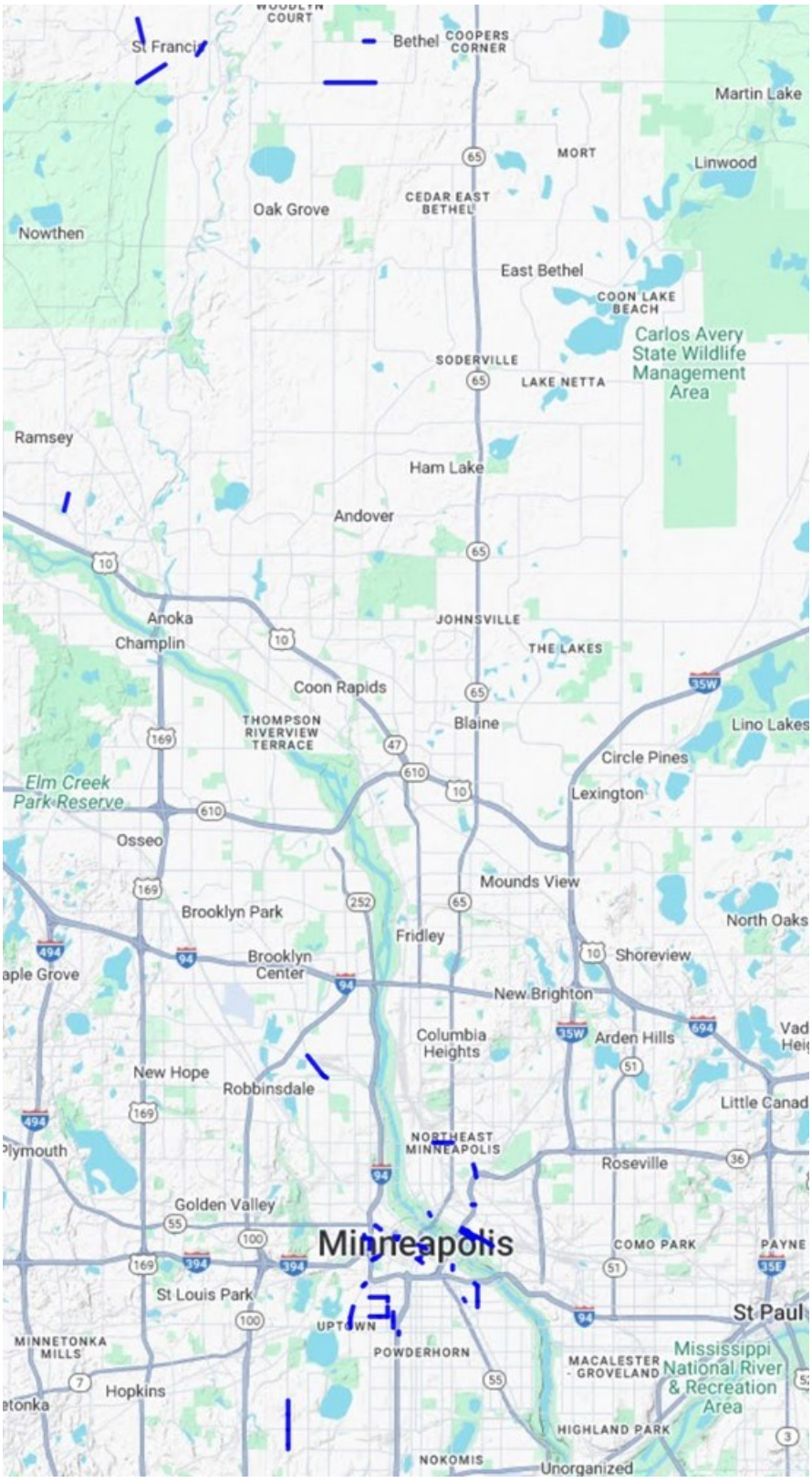

Figure 4.2 A broader view of closures across the entire network.

4.5 Solution Algorithm

To use the existing UE solution algorithm, we can write a decomposition for our optimization problem. The standard optimization traffic assignment problem will be:

$$\min \sum_{v\epsilon V} \sum_{(i,j)\epsilon A} \int_0^{x_{ij}^v} t_{ij}(x) d(x) \tag{31}$$

$$x_{ij}^v = \sum_{\pi\epsilon\Pi_{rs}} h_\pi^v \delta_{ij,\pi} \quad \forall (i,j)\ \epsilon\ z^2, \quad \forall\ v\ \epsilon\ V \tag{32}$$

$$\sum_{v\epsilon V} h_\pi^v \geq 0 \quad \forall \pi \in \Pi \tag{33}$$

$$\sum_{\pi\epsilon\Pi_{rs}} h_\pi^v = d_{rs}^v \quad \forall (r,s)\epsilon z^2,\ \forall\ v\ \epsilon\ V \tag{34}$$

$$d_{rs}^v \geq 0 \quad \forall (r,s)\ \epsilon\ z^2, \quad \forall\ v\ \epsilon\ V \tag{35}$$

To solve our problem, we have used an iterative algorithm. First, we initialize the variables and then enter into an iterative framework. In the first step, the model gets the free-flow travel time and the total demand of the network between each r and s and splits the demand into the different roads based on evaluating the highest utility.

Then the demand is an input to the user equilibrium problem. The iterative process will continue running until the difference between TSTT and SPTT from two consecutive iterations becomes smaller than the threshold 10^{-6}. This threshold ensures that the difference between TSTT and SPTT is small enough to consider the process as having converged. The algorithm in Table 1 shows the solution steps. The user equilibrium problem is being solved by the paired alternative segments (TAPAS) algorithm, introduced by Bar-Gera. TAPAS algorithm focuses on pairs of alternative segments as the key building block to the UE solution. The basic idea of the proposed algorithm is shifting flow between pairs of alternative segments for a set of stored dynamically updated pairs. The reason for using this algorithm is to obtain sufficiently precise solutions suitable for scenario comparisons as quickly as possible.

After solving this problem, we can determine the volumes of different vehicle types by disaggregating the link volumes. By comparing the link volumes of heavy trucks before and after the construction project, we can determine which roads should be examined for damage.

4.6 Numerical Results

The Minneapolis network, used as our case study, consists of 55,559 nodes, 3,061 zones, and 9,369,721 origin-destination (O-D) pairs. We applied the demand data collected to test the algorithm on this network. The results, evaluated using the TSTT, SPTT, AEC, and Gap, are shown over several iterations. The TAPAS method iterates until the Gap approaches zero, indicating that TSTT and SPTT are nearly equal by the end of the process. The table below presents these results over 10 iterations, without considering any closures.

Solving the Minneapolis network resulted in a total scaled demand of 332,123 for cars and 11,413 for trucks. Table 4.1 and 3 present the model's output over 10 iterations, both before and after the road closures, respectively.

Table 4.1 Network results before closures over 10 iterations.

	TSTT	SPTT	gap	AEC
Iteration 1	82690.0825	82662.0757	0.0003	8.1524e-05
Iteration 2	82613.6520	82608.3828	6.3780e-05	1.5337e-05
Iteration 3	82606.3529	82603.8302	3.0538e-05	7.3433e-06
Iteration 4	82601.1661	82599.5337	1.9762e-05	4.7517e-06
Iteration 5	82599.5981	82598.2567	1.6240e-05	3.9047e-06
Iteration 6	82599.6302	82598.3072	1.6016e-05	3.8510e-06
Iteration 7	82599.6352	82598.3158	1.5974e-05	3.8408e-06
Iteration 8	82599.7259	82598.4366	1.5609e-05	3.7532e-06
Iteration 9	82599.7277	82598.4394	1.5597e-05	3.7501e-06
Iteration 10	82599.7165	82598.4323	1.5547e-05	3.7381-06

Table 4.2 Network results before closures over 10 iterations.

	TSTT	SPTT	gap	AEC
Iteration 1	82846.0614	82816.8796	0.00035	8.4945
Iteration 2	82764.5240	82760.0390	5.4189	1.3055
Iteration 3	82756.5345	82754.6309	2.3002	5.5411
Iteration 4	82754.0433	82752.5527	1.8011	4.3388
Iteration 5	82754.1073	82752.7131	1.6847	4.0584
Iteration 6	82753.8815	82752.5120	1.6548	3.9862
Iteration 7	82753.8223	82752.4710	1.6328	3.9333
Iteration 8	82753.8145	82752.4652	1.6303	3.9274
Iteration 9	82753.8294	82752.5127	1.5912	3.8330
Iteration 10	82753.8261	82752.5124	1.5875	3.8242

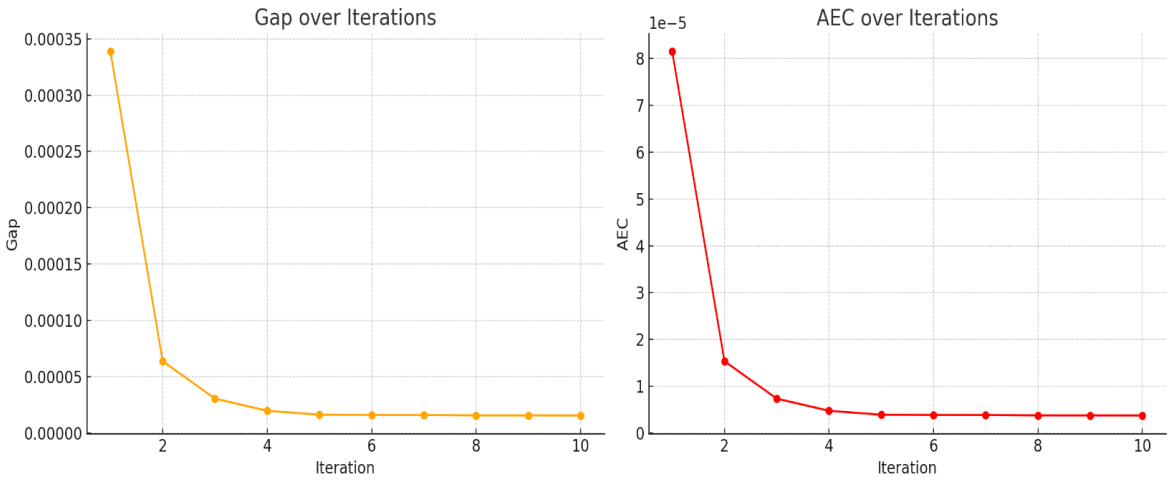

Figure 4.3 GAP and AEC value over iterations before closures.

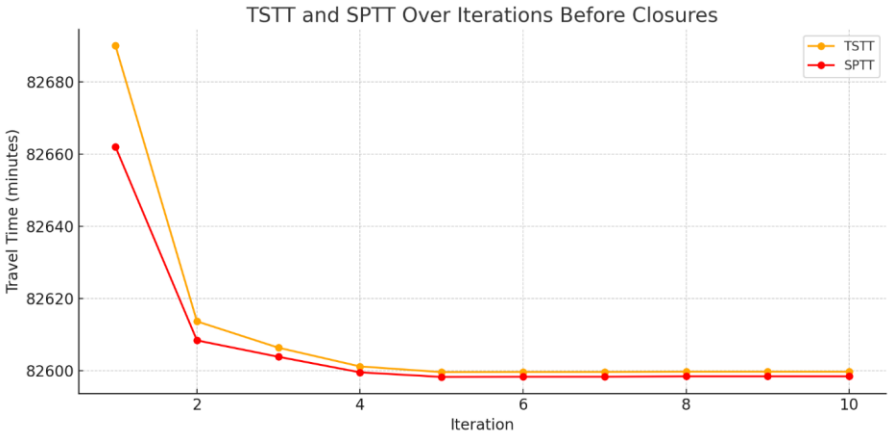

Figure 4.4 TSTT and SPTT values over iterations before closures.

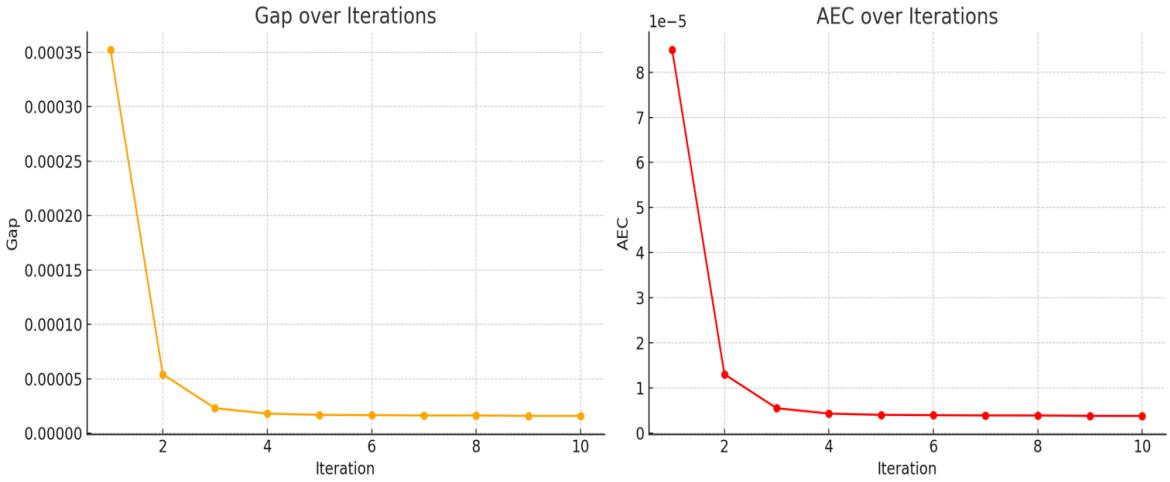

Figure 4.5 GAP and AEC value over iterations after closures.

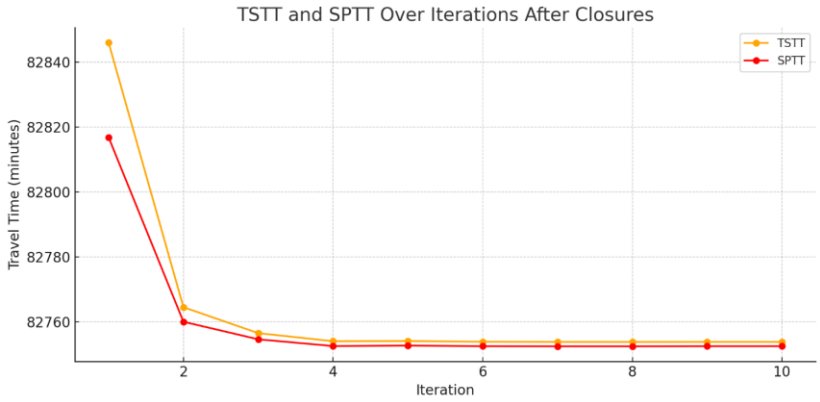

Figure 4.6 TSTT and SPTT values over iterations after closures.

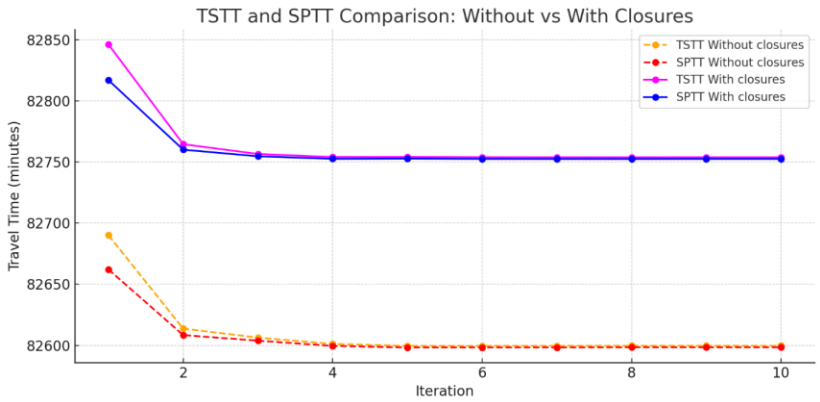

Figure 4.7 Comparison of TSTT and SPTT values over iterations before and after closures.

The comparison of the Minneapolis network with and without road closures reveals a significant impact on system performance. Initially, TSTT and SPTT are considerably higher in the presence of closures, indicating that the closures force longer or less efficient travel routes. While both scenarios stabilize over iterations, the network without closures achieves lower travel times, reflecting higher efficiency and faster convergence to an optimal state. In contrast, even after multiple iterations, the network with closures stabilizes at a higher TSTT and SPTT, demonstrating that road closures lead to lasting inefficiencies in overall travel time. This analysis highlights the negative impact of closures on network performance and the need for strategic mitigation measures to minimize disruptions.

The following analysis focuses on tracking car and truck flows on each link, both before and after the closures. The closure of 120 links resulted in significant changes to the flow of vehicles, particularly affecting the surrounding links. In line with the objectives of this project, the emphasis is on the increase in truck flows following the closures. Specifically, while 120 links were closed, the results show that these closures caused increased truck flows on 7,502 links. However, some of these increases are minor, ranging between 0 and 1 vehicle per hour, and are considered negligible. Therefore, the primary focus is on links where truck flow increased by more than 1 vehicle per hour.

In Figure 4.8, in addition to highlighting the roads where truck flow has increased, the 120 closed links are also displayed in blue to illustrate their impact on the flow of surrounding links.

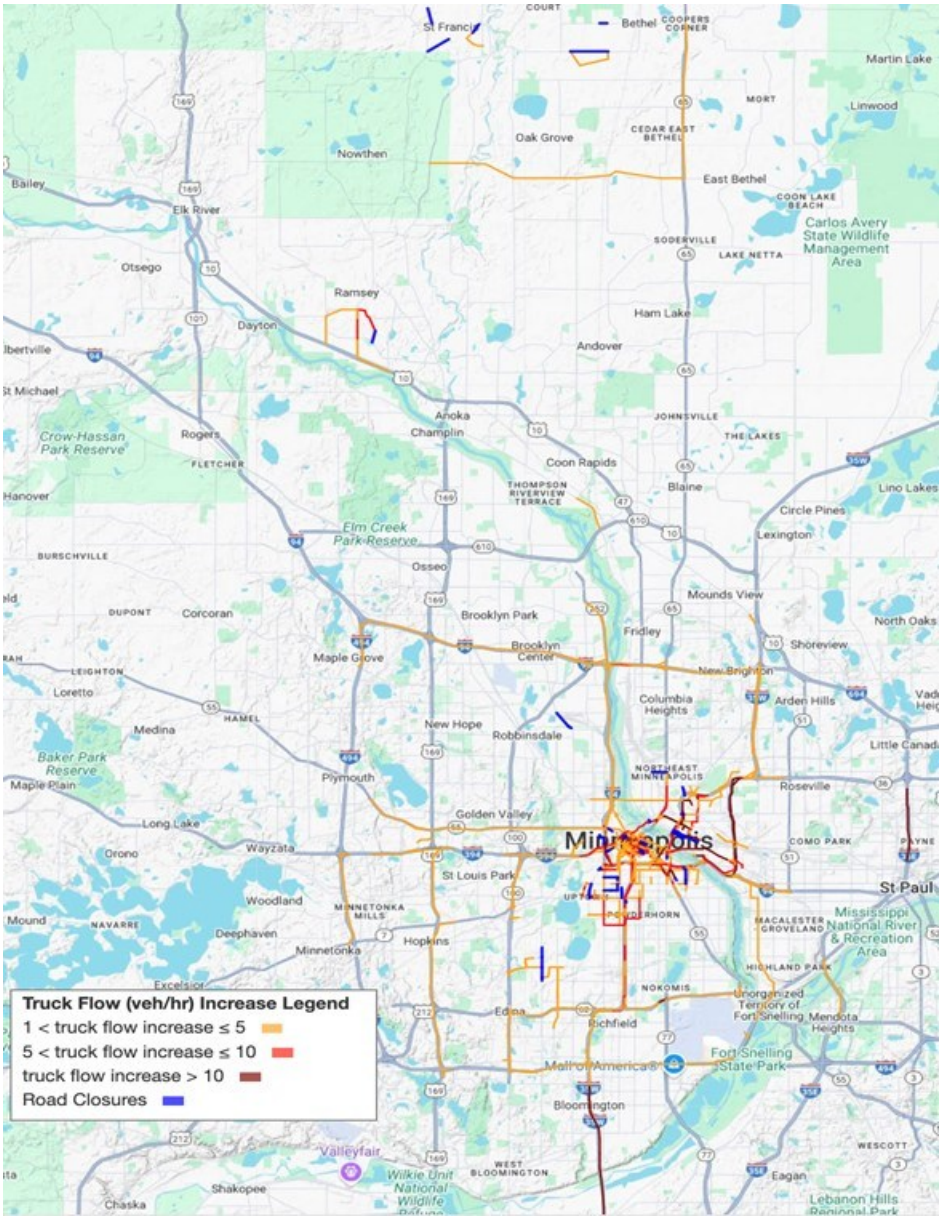

Figure 4.8 Visualization of links where the truck flow increased by more than 1 veh/hr and the corresponding closed links.

For a better understanding of the effects of closures on surrounding links' truck flow, we present Figure 4.9, which shows the percentage of truck flow increase compared to their initial flow before the closures. The map illustrates the impact of road closures, marked in blue, across various regions. Different colored lines indicate the extent of flow increase. As observed, the most significant increases in truck flow tend to concentrate around the areas directly adjacent to the closures, such as in the northern regions around St. Francis, Oak Grove, and Bethel, as well as the more congested urban areas

in and around Minneapolis. The flow increments are primarily distributed along key arterial roads connecting suburban and urban centers, suggesting that these closures heavily affect regional truck traffic patterns. This insight emphasizes the potential need for alternative route planning and traffic management strategies to mitigate damages caused by these closures.

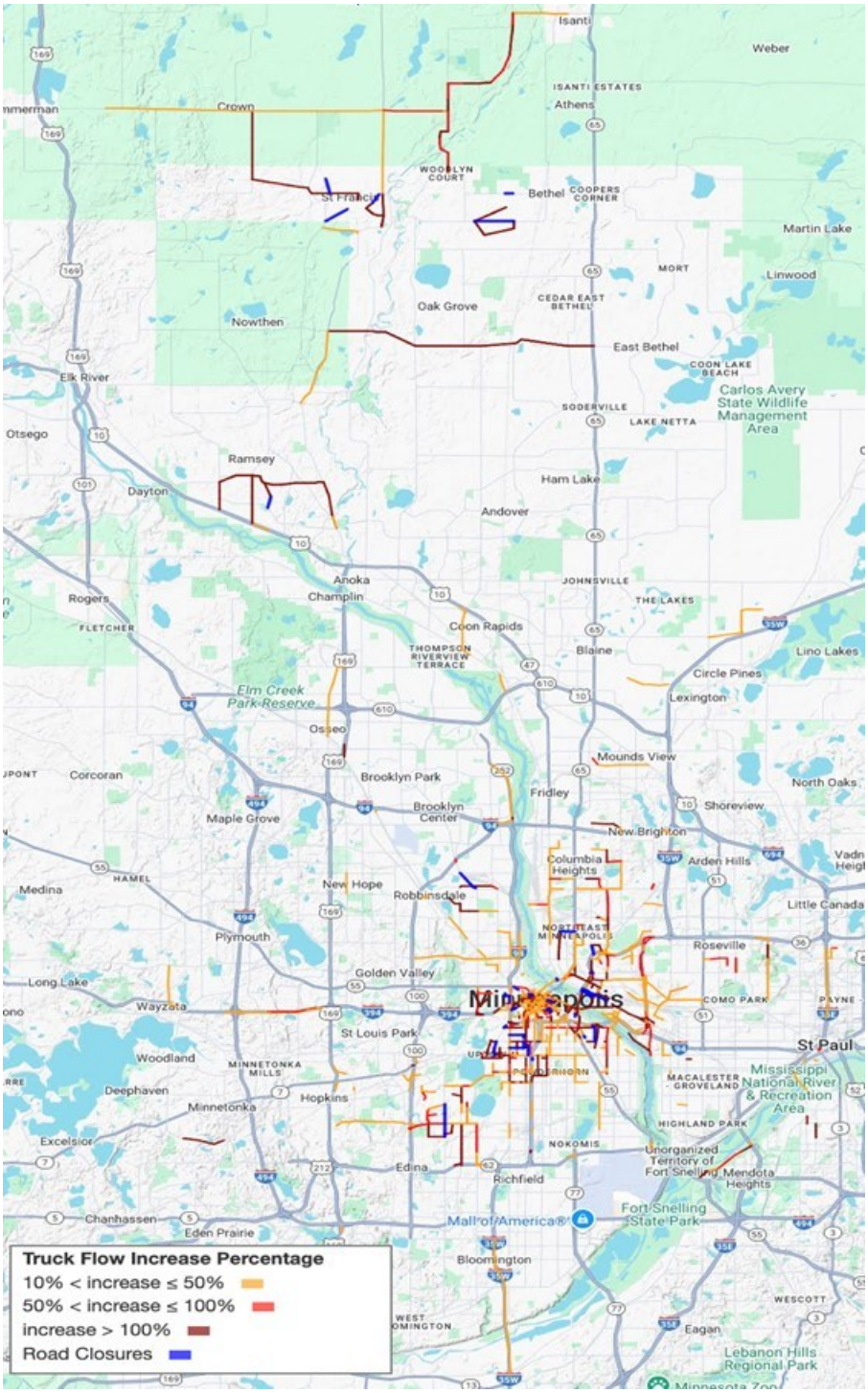

Figure 4.9 Visualization of links where truck flow increased by percentage due to road closures.

4.7 Conclusion

This chapter highlights the considerable impact of road closures, whether due to construction or other causes, on vehicle flows and overall network performance. The focus was on how these closures influence heavy truck traffic, leading to changes in driver behavior and rerouting trucks to alternative links, which in turn affects the flow on surrounding roads.

The findings, based on User Equilibrium conditions, reveal that closures not only increase the total network travel time from 82,599 to 82,753 minutes, indicating a more congested and less efficient network, but also result in a substantial rise in truck flow on adjacent roads. The increase in surrounding links ranged from 2.07×10^(-25) to 62.4 vehicles per hour, with some increases being highly significant and impossible to overlook. This added strain on infrastructure and pavement necessitates further consideration and mitigation to address potential long-term impacts.

Chapter 5: Optimization Techniques to Determine Detours with Less Damage Impact

In this task, the research team planned to build a new optimization model to find the best detour route, using the route choice predictions from Chapter 4. Given road closures from a construction project, the research team planned to formulate the network design problem of finding the optimal detour route as a mixed integer program. In this process, link volumes of heavy trucks would be used to predict the additional damage impacts caused by the detours. This is a combination of deciding which route to mark as a detour and solving traffic assignment given drivers' preferences for low travel times but also following a marked detour. However, given the mismatch of available data for route choice predictions and calculation of pavement damage, the research team investigated the pavement damage, and the development of a new optimization model to find the best detour routes, as two separate individual components.

5.1 Pavement Damage

Given the variable results obtained based on falling weight deflectometer (FWD) data, the research team investigated the use performance curves to determine additional damage from the increase in traffic due to detours. This approach takes advantage of the extensive historical data available in MnDOT HPMA database and of the equations developed by the Pavement Management Office, based on reconstruction and rehabilitation history, for both flexible and rigid pavements.

5.1.1 Pavement Performance Curves

The performance curves are expressed as a sigmoidal curve (Equation 36), with different coefficients for different rehabilitation methods:

$$RQI = o - e^{(a - b \times c^t)} \tag{36}$$

t = log(1/*age*), o is the initial RQI observed right after the repair activity is performed and a, b, c determine how RQI is expected to decay over time.

The adapted sigmoidal model was initially developed by Lukanen in 1986, with periodic updates planned (Lukanen, 1986; 1992). The most recent update in 2022 assessed its effectiveness and proposed refinements to the prediction curves (MnDOT, 2022), following a major update in 2008. This report utilizes recent pavement condition data to evaluate the efficiency of the current model coefficients and develop an update. Pavement sections constructed after 2000 were selected, and the dataset includes RQI values collected from 2001 to 2020. In total, 24 sets of model coefficients have been recalibrated and represent a reasonable estimation of the performance of the different repair activities (MnDOT, 2022). Using the updated model coefficients, Figure 5.1 to Figure 5.4 display the pavement performance curves for Bituminous Aggregate Base (BAB), Bituminous Over Bituminous (BOB), Bituminous Over

Concrete (BOC), and concrete pavements, respectively. The curves exhibit distinct shapes and different initial RQI values.

Please note that the only variable in the equation is the pavement age, and traffic is not included. The assumption is that the performance curves incorporate the damage from both traffic loading and environmental effects over the pavement life. To include traffic effects, some approximate equivalence is required to convert an increase in number of ESALs to an additional aging of the pavement. Using this approach, a method is proposed to quantify the damage generated by the additional traffic experienced on detour routes.

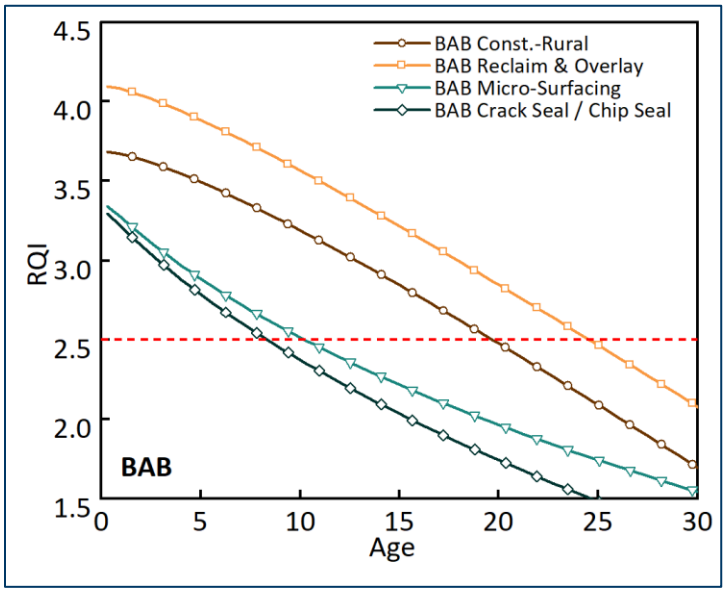

Figure 5.1 Comparisons between performance curves of BAB pavements.

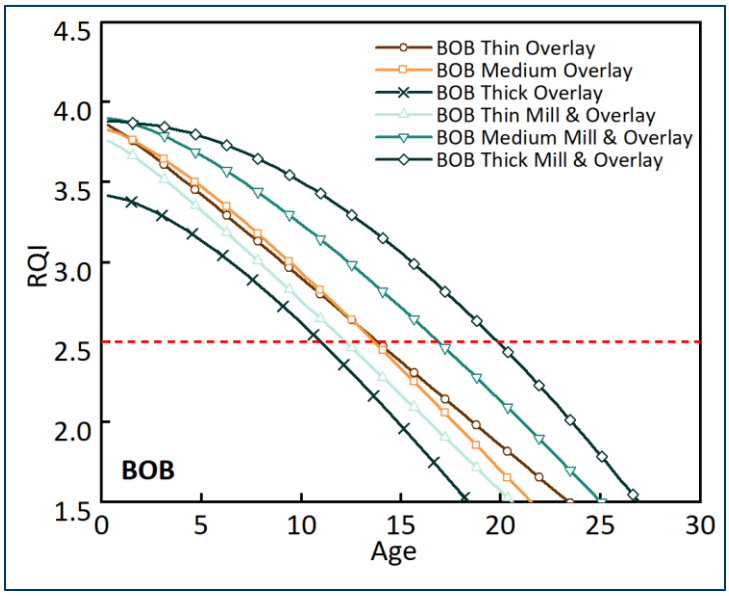

Figure 5.2 Comparisons between performance curves of BOB pavements.

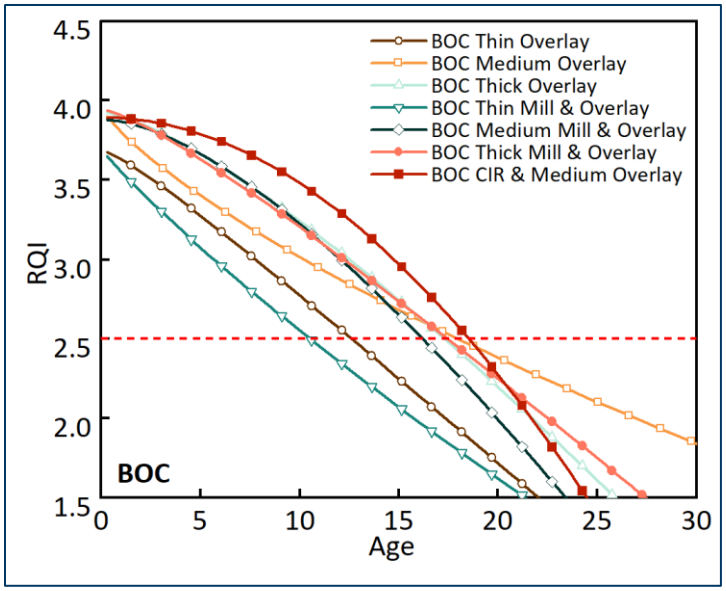

Figure 5.3 Comparisons between performance curves of BOC pavements.

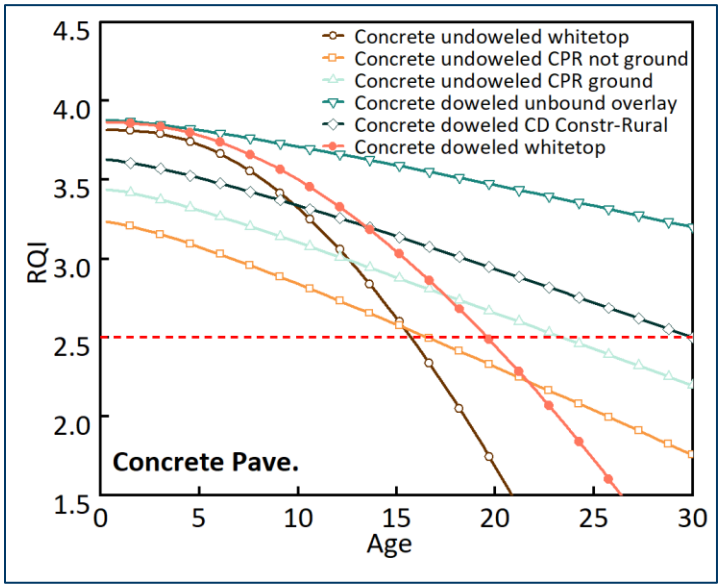

Figure 5.4 Comparisons between performance curves of concrete pavements.

Two methods are used to obtain the pavement damage using the performance curve, as described below.

5.1.2 Reduction in Remaining Service Life

In this method, pavement damage is estimated by calculating the reduction in remaining service life (RSL) due to the additional detour traffic. First, the performance curve that fits best the type of studied pavement is selected, as shown in Figure 5.5.

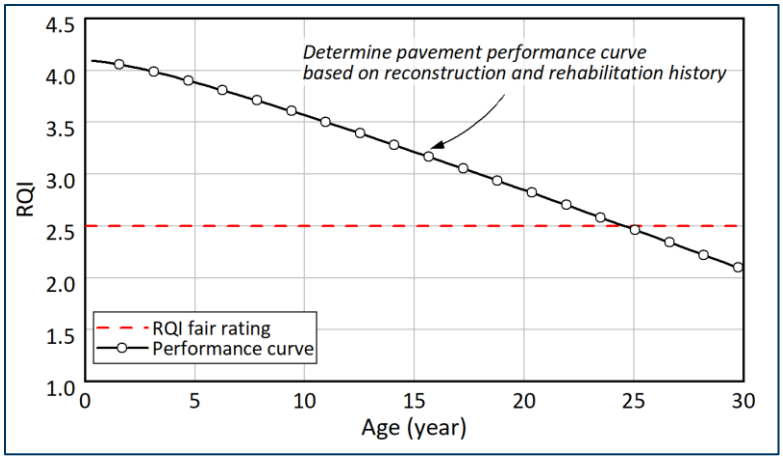

Figure 5.5 Performance curve selection.

Next, the start of the detour is marked on the performance curve. Knowing the additional ESALs due to the detour, and the design ESALs and annual traffic increase, the detour period can be converted to an equivalent pavement age. This additional age is added to the age of the pavement at the start of the detour, on the horizontal axis of the performance curve. The corresponding RQI value on vertical axis corresponds to the RQI on the pavement after accounting for the detour ESALs, as illustrated in Figure 5.6.

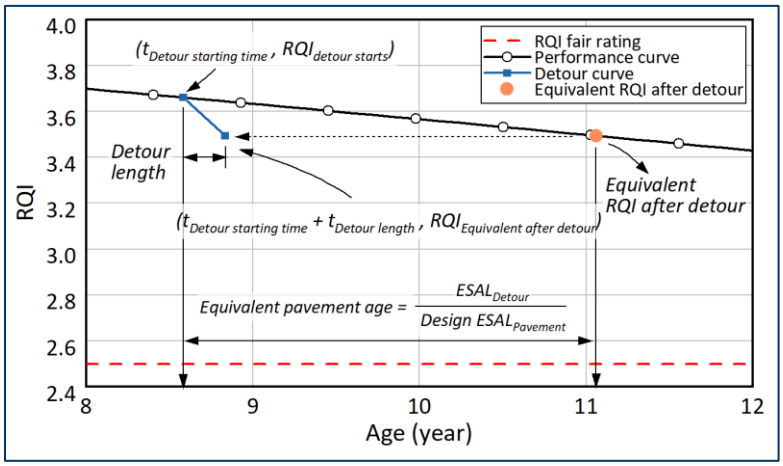

Figure 5.6 Determination of detour performance curve.

Knowing the duration of the detour, and assuming that the pavement performance continues in its original form, but starts from the RQI at the end of the detour. The post-detour performance curve is obtained by shifting the original pavement performance curve accordingly, as shown in

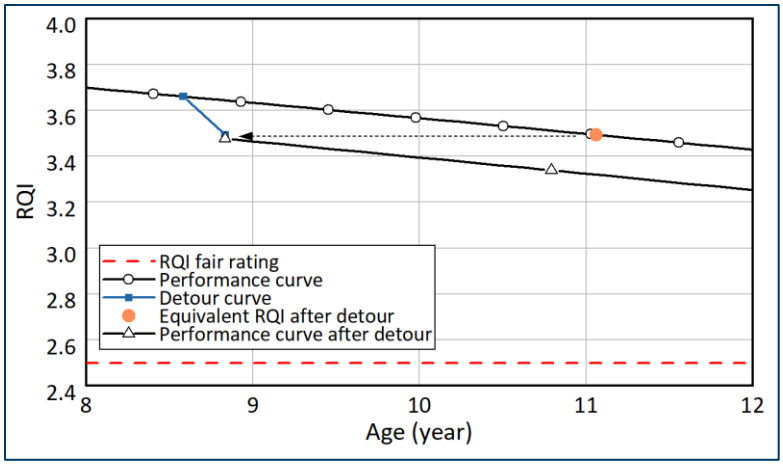

Figure 5.7 Performance curve after detour.

The difference in pavement age at an RQI of 2.5 between the original performance curve and the performance curve with the detour represents the reduction in service life, as shown in Figure 5.8.

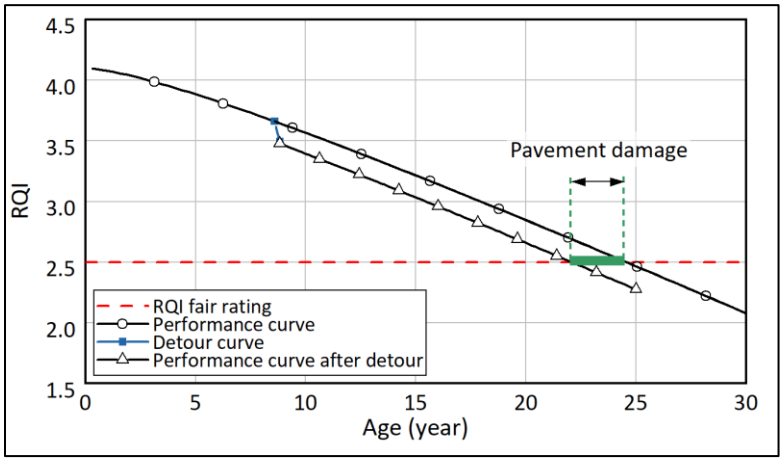

Figure 5.8 Determination of reduction in service life.

5.1.3 Loss of Area under the Performance Curve

In this method, using the same steps described above, the loss of area under the performance curve caused by the detour is used to quantify pavement damage. This is done as follows.

First, the remaining effective service area (ESA) is calculated using Equation 37, and the ESA after the detour can be calculated using Equation 38. A graphical explanation is provided in Figure 5.9.

$$ESA_{Remaining} = \int_{start\ of\ detour}^{pavement\ age\ when\ RQI=2.5} f(x)_{performance\ curve} \quad (37)$$

$$ESA_{Remaining\ after\ detour} = \int_{start\ of\ detour}^{end\ of\ detour} f(x)_{performance\ curve\ after\ detour} \quad (38)$$

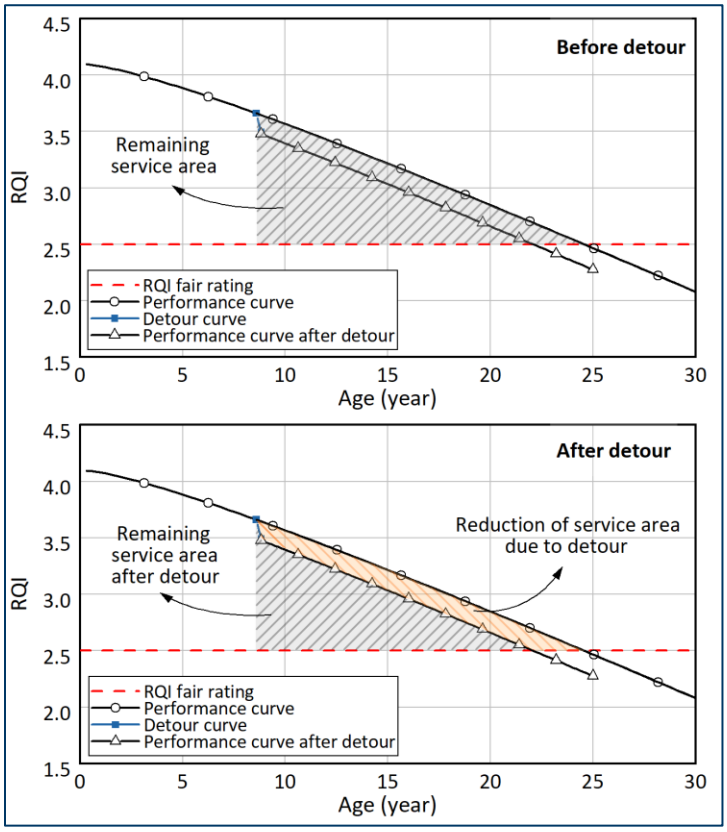

Figure 5.9 Reduction of service area due to detour.

Then, the reduction of ESA due to the applied detour can be calculated using Equation 39.

$$Reduction\ of\ ESA\ (\%) = \frac{ESA_{remaining} - ESA_{remaining\ after\ detour}}{ESA_{remaining}} \times 100\% \quad (39)$$

5.1.4 Case Study: Determine Pavement Damage for CSAH 5 Detour

In this example, Goodhue CSAH 5 is selected for case study. Record shows the latest rehabilitation activity was reclamation and overlay that took place in 2016. Using the coefficient database, coefficients *a*, *b*, *c*, and *o* were found to be 15.072, 18.094, 1.084, and 4.1, respectively. The research team generated the performance curve of Goodhue CSAH 5, as shown in Figure 5.10. An RQI of 2.5, representing the boundary for a "Fair" rating, is used as a condition limit to illustrate this method.

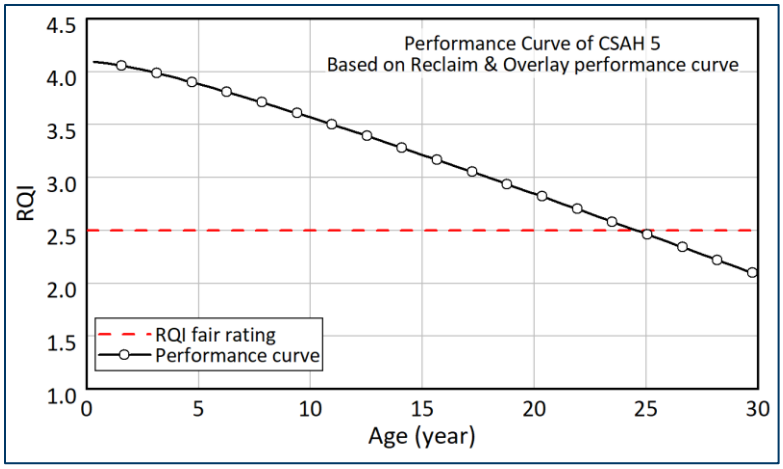

Figure 5.10 Performance curve for CSAH 5.

5.1.4.1 Calculation using the Reduction in Remaining Service Life

The detour started on July 27th, 2023, and lasted for 3 months. Since the last rehabilitation was done in 2016, the start point of detour on performance curve (x axis value) is 8.58 years. Knowing that the daily ESAL during detour is 2000, then the total ESAL during the detour can be calculated using Equation 40.

$$ESAL_{Detour} = ESAL_{daily} \times Detour\ Time = 2000 \times 90 = 180000 \quad (40)$$

The starting point of the detour on the performance curve is 8.58 years. Next, the equivalent age caused by the ESAL of detour traffic can be calculated, using Equation 41:

$$Equiv_{age} = 2 + \frac{180000 - 69366\times(1+0.5\%)^7 - 69366\times(1+0.5\%)^8}{69366\times(1+0.5\%)^9} = 2.48\ yrs \quad (41)$$

where 69,366 is the annual ESALs for Goodhue CSAH 5 in 2016, assuming a 0.5% growth rate.

The RQI on the pavement at the end of the detour is equivalent to the RQI of the pavement at 11.06 years (8.58+2.48=11.06) under normal traffic conditions. Using the model coefficients, the RQI at 11.06 years is 3.49. The orange point on the curve, with coordinates 11.06 and 3.49, and the remaining part of the performance curve are then shifted to the left to match the detour end on the time scale of 3 months after July 27, as presented in Figure 5.11 and Figure 5.12.

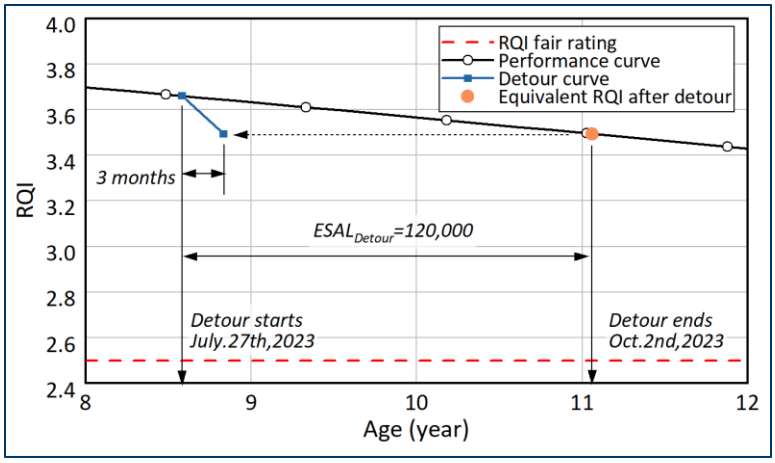

Figure 5.11 Start and end point of detour performance curve.

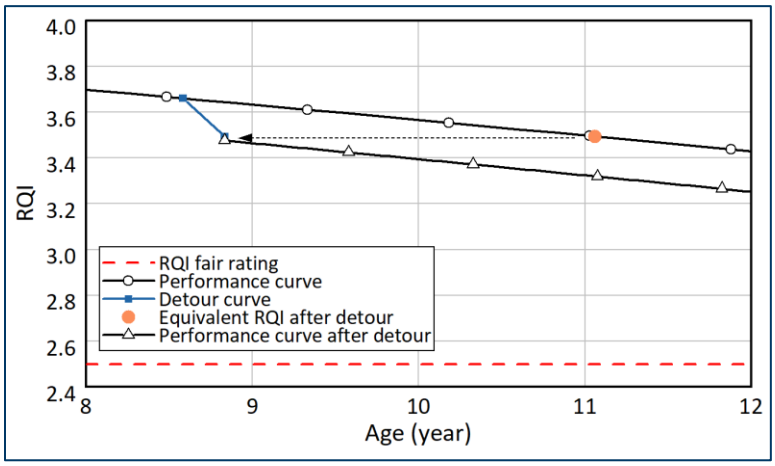

Figure 5.12 Performance curve after detour.

Figure 5.13 presents the pavement performance curve with a three-month detour. If a "Fair ride quality" applies for the deterioration condition, the detour reduces the pavement life by 2.31 years.

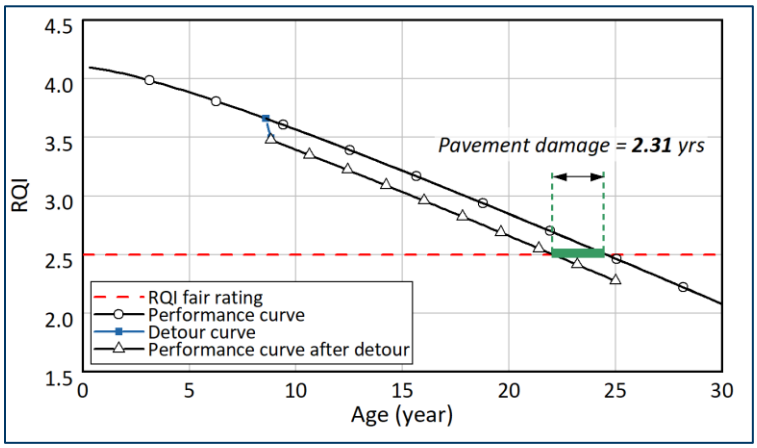

Figure 5.13 Reduction in service life for a three-month detour.

5.1.4.2 Calculation using Loss of Area under the Performance Curve

The reduction in effectiveness can be calculated using the equations mentioned above. As shown in Figure 5.14, the reduction in effective service is calculated to be 25.33% using Equation 4. The damage caused by detour is calculated to be 2.31 years, and 25.33% reduction in service area, respectively.

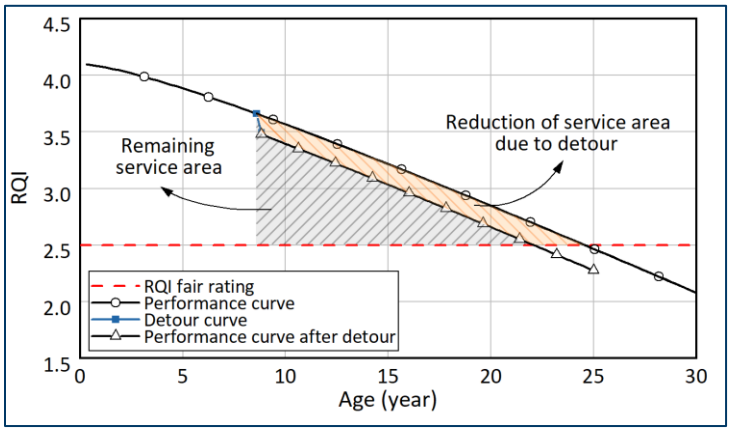

Figure 5.14 Remaining effective service area for a 3-month detour.

5.1.5 Effect of Detour Starting Time on Pavement Damage

The RQI decreases with increasing pavement age, but at varying rates. This indicates that the detour starting time could affect the calculation of pavement damage. To investigate this effect, the pavement damage on CSAH 5 is evaluated under two scenarios: (1) the detour starts 2 years after the most recent rehabilitation, and (2) the detour starts 8 years after the most recent rehabilitation. The results obtained using reduction in RSL and the loss of area under the performance curve are presented in Figure 5.1.15 and Figure 5.1.16.

Figure 5.1 presents a comparison of the results. For the curve shift method, pavement age does not significantly affect the reduction in pavement life. The reduction in RSL for the scenario where the detour starts 2 years after rehabilitation is 2.31 years, only about 4 weeks longer than the scenario where the detour starts after 8 years. In contrast, the area under the curve method shows a more noticeable difference. Starting the detour 2 years after rehabilitation results in a 19.05% reduction in effective service area, whereas starting it 8 years after rehabilitation leads to a 25.33% reduction. This is because pavement RQI decreases more rapidly with age, causing a larger proportional reduction in the area under the curve. These results suggest that, for the same detour duration, older pavements experience more damage than newer ones. A detour occurring shortly after rehabilitation (e.g., within 0–2 years) causes less service loss compared to one happening closer to the end of the pavement's acceptable service life. However, it is worth noting that the area under the curve method may overstate the damage, especially for older pavements, because the total area under the curve is much smaller at 8 years than at 2 years.

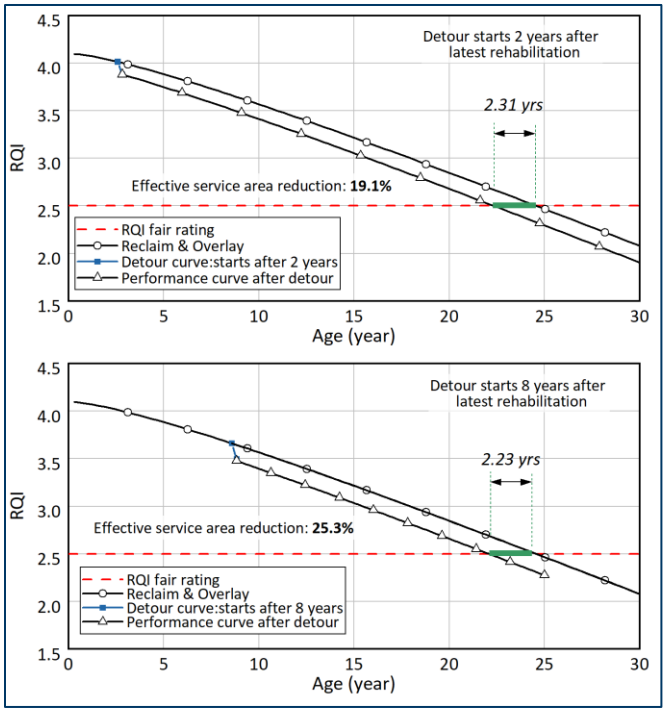

Figure 5.15 Effect of detour start time on pavement damage using reduction in RSL.

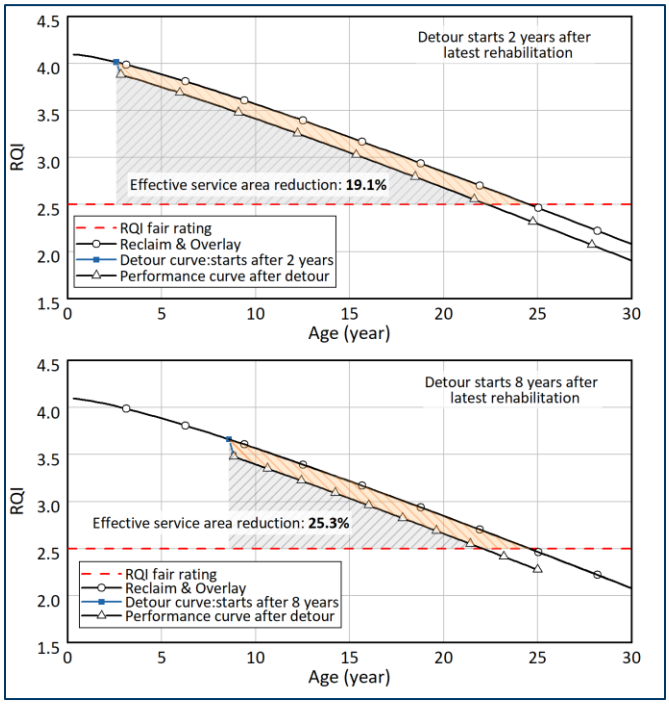

Figure 5.16 Effect of detour start time on pavement damage using the loss of area under the curve.

Table 5.1 Influence of pavement age on pavement damage.

Detour characteristics	Reduction in RSL	Loss of Area under the curve
Starts after 2 years	2.31 years	19.05%
Starts after 8 years	2.23 years	25.33%

5.1.6 Effect of Detour on Pavement with Different Rehabilitation Methods

In a previous section, Figure 5.1 to Figure 5.4 showed that performance curves for pavements with different rehabilitation methods vary. RSL reduction caused by a detour also differs across pavement types. To study this effect, six BOB pavement types, namely thin overlay, medium overlay, thick overlay, thin mill-and-overlay, medium mill-and-overlay, and thick mill-and-overlay, are analyzed. To assess RSL reduction, the annual ESAL for each pavement is determined using recommended values from the MnDOT Pavement Design Manual (MnDOT, 2019).

Table 5.2 and Table 5.3 present the RSL for these six BOB pavements, reflecting typical deterioration trends observed in Minnesota pavements. The MnDOT Pavement Design Manual (MnDOT, 2019) provides design lives for HMA overlays on existing pavements in Table 5.3 and ESAL ranges for traffic level categories in Table 5.4.

5.1.7 Calculation using Reduction in Remaining Service Life

For the six BOB pavements, the same detour scenario is applied. The daily ESAL during the detour is assumed to be 800, and the detour lasts 3 months, resulting in a total ESAL of 72,000. Table 5.6 presents the equivalent pavement age of this detour ESAL when it occurs 2 and 8 years after the latest rehabilitation, while Figure 5.17 shows the RSL reduction for the six BOB pavements at those times. Generally, detours occurring after 8 years cause less RSL reduction than those after 2 years, due to a 0.5% annual increase in ESAL that diminishes the detour's impact. When detour ESAL is constant, thin overlay pavement—with the lowest annual ESAL—exhibits the greatest RSL reduction. In contrast, pavements with high traffic, such as thick overlay pavement, show negligible RSL reduction from the detour.

Table 5.2 RSLs of six BOB pavements.

BOB pavement type	Model coefficients				RSL (years)
	a	b	c	o	
Thin Overlay	15.351	18.093	1.073	3.870	13.8
Medium Overlay	18.790	22.082	1.070	3.835	13.7
Thick Overlay	19.600	23.516	1.077	3.418	11.0
Thin Mill & Overlay	16.980	19.830	1.070	3.770	12.2
Medium Mill & Overlay	17.809	21.890	1.083	3.902	16.0
Thick Mill & Overlay	17.500	23.593	1.112	3.879	19.9

Table 5.3 Design lives of HMA overlays of existing HMA (MnDOT, 2019).

Thickness/Milling	Surface Condition	High ESALs	Med ESALs	Low ESALs
Thin (≤2") Overlay	GOOD	5-9	6-12	8-14
	FAIR	4-8	6-10	6-12
	POOR	2-6	4-8	6-10
Medium (2-4") Overlay	GOOD	8-12	10-14	11-17
	FAIR	6-10	8-12	10-14
	POOR	5-9	6-10	8-12
Thick (＞4") Overlay	GOOD	12-16	14-18	16-22
	FAIR	10-14	12-16	14-21
	POOR	9-13	11-15	13-19
Mill & Thin (≤2") Overlay	GOOD	6-10	7-13	9-15
	FAIR	5-9	6-12	7-13
	POOR	3-8	5-9	6-12
Mill & Medium (2-4") Overlay	GOOD	8-14	10-16	12-18
	FAIR	6-12	8-14	10-16
	POOR	5-11	7-13	9-15
Mill & Thick (＞4") Overlay	GOOD	12-16	14-18	16-22
	FAIR	10-14	12-16	14-21
	POOR	9-13	11-15	13-19

Table 5.4 Traffic key for Table 5.4 (MnDOT, 2019).

High ESALs	Med ESALs	Low ESALs
More than 5 Million 20-year Flexible ESALs	1 to 5 Million 20-year Flexible ESALs	Less than 1 Million 20-year Flexible ESALs

Based on the calculated RSL and MnDOT's traffic recommendations presented in Table 5.3and

Table 5.4 5.4, annual ESAL of the 6 BOB pavements are assumed and listed in Table 5.15. It should be noted that an annual growth rate of 0.5% is considered.

Table 5.5 Annual ESAL of the six BOB pavements.

BOB pavement type	ESAL category	Surface condition	Annual ESAL
Thin Overlay	Low	GOOD	25,000
Medium Overlay	Low	GODD	30,000
Thick Overlay	High	FAIR	250,000
Thin Mill & Overlay	Low	GOOD	38,000
Medium Mill & Overlay	Low	GOOD	42,000
Thick Mill & Overlay	Low	GOOD	46,000

Table 5.6 Equivalent pavement age of the detour ESAL.

BOB pavement type	Equivalent pavement age (years)	
	2 years	8 years
Thin Overlay	2.866	2.767
Medium Overlay	2.388	2.306
Thick Overlay	0.287	0.277
Thin Mill & Overlay	1.885	1.821
Medium Mill & Overlay	1.706	1.647
Thick Mill & Overlay	1.557	1.504

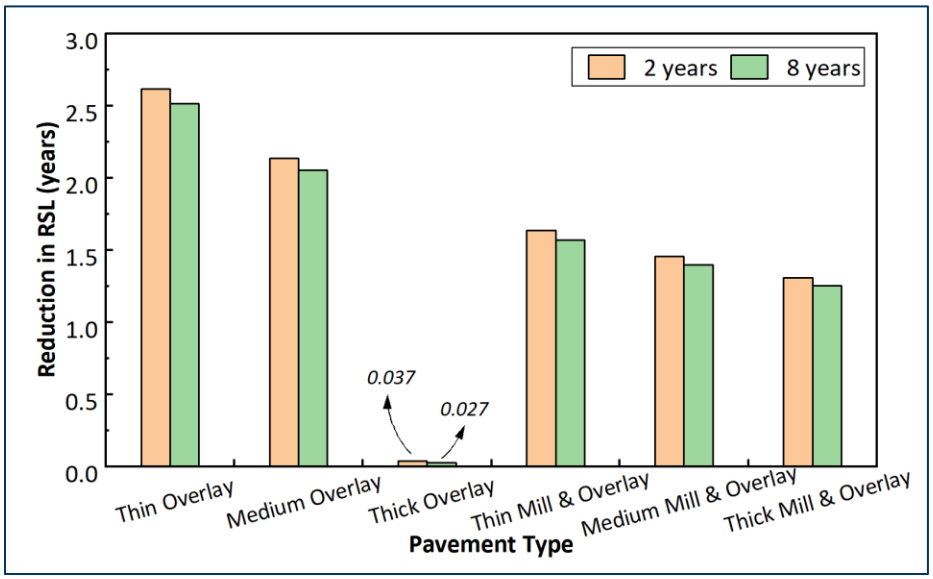

Figure 5.17 Reduction in RSL of 6 BOB pavements.

5.1.8 Calculation using Loss of Area under the Performance Curve

The loss of area under the performance curve is calculated for all six BOB pavement types using Equations 2 and 3, as shown in Figure 5.18. Unlike the RSL reduction method, this approach reveals a significantly larger area loss at 8 years than at 2 years. This suggests that a detour occurring near the end of a pavement service life results in greater area loss. Note that the area-under-the-curve method may overstate damage for older pavements, as the total area under the curve is much smaller at 8 years than at 2 years.

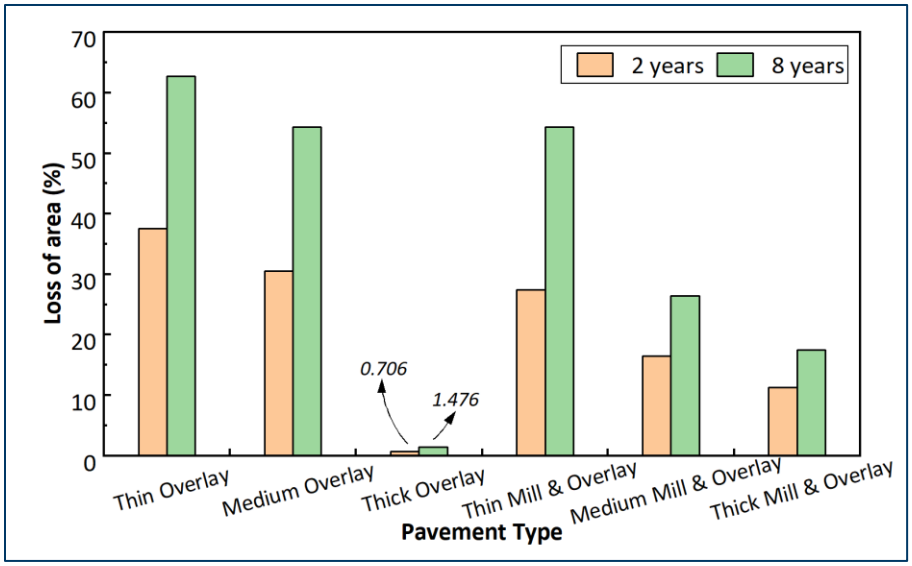

Figure 5.18 Loss of area under the performance curve of 6 BOB pavements.

5.2 Optimizing Detour Routes

A new optimization model is developed to find the best detour routes, using the route choice predictions from Chapter 4. When roads are closed due to a construction project, the problem of selecting the best detour routes is written as a mixed-integer program. The model uses the traffic volumes of heavy trucks to estimate the extra load caused by the detours.

The problem includes choosing which routes to mark as detours and predicting how traffic will adjust, based on drivers' preferences for shorter travel times while also considering the marked detour routes. To solve this network design problem, the research team used solution methods such as heuristic algorithms, including a genetic algorithm. The model was tested on two scenarios from one construction project selected in Chapter 4, in cooperation with TAP. In both scenarios, the objective is to identify optimal detour routes and assess changes in traffic patterns using two distinct fitness functions, under the condition that certain roads are restricted for truck use.

5.2.1 Introduction

The objective is to addresses the challenge of identifying optimal detour routes in response to road closures, with particular emphasis on heavy truck traffic and its impact on pavement deterioration. When construction activities necessitate the closure of certain roads, rerouted traffic, especially heavy trucks, can impose additional stress on alternative links that may not be structurally equipped to handle such loads. The problem is therefore twofold: first, to determine detour routes that preserve overall network efficiency by minimizing total travel time; and second, to reduce the flow on vulnerable road segments by designating them as restricted for truck use.

The problem is formulated as a bilevel optimization model, where the upper level focuses on strategic detour planning, and the lower-level captures user-equilibrium traffic assignment. Due to the NP-hard nature of bilevel optimization problems in network design, exact solution methods quickly become intractable for realistic, large-scale networks. This complexity justifies the adoption of heuristic approaches. In this project, a genetic algorithm (GA) is implemented to navigate the combinatorial search space of potential detour routes. The GA uses a fitness function that integrates the two upper-level objectives (minimizing VMT and imposing penalties on truck crossings) while ensuring that the lower-level traffic assignment (obtained via the traffic assignment model based on MnDOT's CUBE model) maintains network-wide efficiency by minimizing total travel time.

To address this, the research team formulate the problem as a network design and traffic assignment problem. Two specific scenarios are considered: (1) minimizing truck VMT on designated truck-restricted roads to mitigate potential pavement damage, and (2) minimizing truck usage of restricted roads by assigning high penalty costs to those links. Both scenarios require the integration of a heuristic optimization method with a traffic assignment model that distinguishes between car and truck flows. The objective is not only to determine the optimal placement of detour signs but also to maintain network-wide efficiency by minimizing total system travel time. The focus is placed on truck flows, as increases in car traffic resulting from detours are unlikely to cause substantial damage to roadway infrastructure.

We developed a traffic assignment model to predict flows on each link of the Minneapolis network separately for cars and trucks, using the origin-destination demand data and trip demand inputs from Task 4. The project team had access to MnDOT's CUBE model, which served as a key data source for the traffic assignment and was based on established methods from the literature.

This report continues the objectives of the previous task. As before, we first solved the traffic assignment problem with the goal of minimizing the total system travel time for all vehicles. Then, to identify the best detour routes, we introduced a new objective. A fitness function was defined for the genetic algorithm used in the optimization process, aiming to minimize either the VMT for both cars and trucks or the truck crossing penalties on the selected detour roads within Minnesota municipalities.

Our work builds upon several crucial tasks completed in earlier stages of this research project: 1) Initial Memorandum: We developed an initial memorandum outlining the expected benefits of our research and potential implementation steps. This preliminary assessment helped shape our methodology and focus our efforts on outcomes that are most beneficial to the state of Minnesota. 2) Data Collection: Working closely with MnDOT, we gathered comprehensive travel demand data and road network information for key Minnesota municipalities, including Minneapolis and St. Paul. A crucial part of this process involved adapting and formatting this diverse data to be compatible with our analytical software. 3) Methodology Development: We developed a sophisticated methodology for predicting route choices in the context of road closures. This approach combines a logit model for tracking the flow of two classes of vehicles, cars, and trucks, with a user equilibrium model for route choice, providing a robust framework for analyzing travel behavior and how the detour projects will change vehicles' behavior and the corresponding demand of each link. 4) Software Implementation: The developed

models were implemented in a custom software application, creating a powerful tool for analyzing transportation networks with vehicle types components. 5) In the current task, we define two new objective scenarios. The first focuses on minimizing truck VMT on selected restricted roads. The second scenario involves restricting certain roads for truck usage by assigning a large penalty to those links and setting the objective of minimizing the total penalty for trucks. Both scenarios require solving the traffic assignment problem multiple times to identify the optimal detour routes based on the objective of each scenario. The goal is not only to reduce VMT or truck penalties but also to maintain the original objective of minimizing the total system travel time for all vehicles.

Building on the completed tasks, our goals are to: a) synchronize a compatible and appropriate heuristic optimization model with the traffic assignment solution, b) solve the traffic assignment problem using a fitness function that minimizes truck VMT on restricted roads, and predict the resulting detours as well as truck and car flows across all network links, c) solve the traffic assignment problem using a fitness function that minimizes truck penalties by restricting certain roads, and predict detours along with truck and car flows across all network links, d) compare the results of the two scenarios, and also compare them to a baseline case where detours are not implemented, but road closures are still in place.

5.2.2 Methodology

An optimization model has been applied to determine the most effective detour routes, incorporating route choice predictions derived from solving the traffic assignment problem. The model addresses the network design challenges arising from road closures due to construction projects and is formulated as a mixed-integer program. Link volumes are analyzed to estimate the additional damage impacts caused by detours. The approach integrates the selection of optimal detour routes with solving traffic assignments, considering drivers' preferences for minimizing travel times while following designated detours. To address this complex problem, various solution methods are explored, including heuristic approaches, with a genetic algorithm ultimately employed to optimize the solution. The objective function aims to identify detour routes that minimize truck VMT on roads that are not suitable for heavy vehicle traffic. This is achieved by introducing a binary decision variable that indicates whether truck access is permitted on each link. This approach helps reduce the increased, overloaded traffic flows by trucks on roads that are not fully designed to handle traffic volumes beyond usual levels. Equation 42 is the fitness function of.

$$\min \sum_{(i,j)\epsilon\, A} x_{ij}^{t} \times y_{a(i,j)} \times L_{ij} \tag{42}$$

where $y_{a(i,j)}$is a binary variable that shows whether we want truck flow on that link (i, j) (0) or not (1), L_{ij} is the length of the link, and $x_{i,j}$ is the flow on the link $(i\ , j)$.

In the second scenario, we modify the fitness function of the genetic algorithm to minimize the total penalty associated with truck flows. To simulate truck restrictions, we assign a high penalty (1e9) value to selected links that represent vulnerable roads not suitable for heavy truck traffic. This allows us to evaluate how limiting truck access to specific links influences the placement of detour signs and alters

truck flow patterns across the rest of the network. The revised fitness function is defined as the form of Equation 43.

$$\min \sum_{(i,j)\epsilon A} x_{ij}^{t} \times p_{ij} \tag{43}$$

where p_{ij} is the penalty of the link (i, j) for trucks and x_{ij}^{t} is the truck flow on this link.

5.2.3 Solution Algorithm

The genetic algorithm (GA) implemented in this study is designed to optimize detour sign placements across the Minneapolis network to minimize the system-wide travel cost. Below is a detailed explanation of the methodology.

GA generates an initial population of solutions. Each solution, or "candidate," represents a configuration of detour signs, where each link in the network is randomly assigned a binary value (0 for no detour sign, 1 for detour sign). The core of the GA lies in evaluating the quality of each candidate solution. This is done through a fitness function, which assesses the network's performance under the given configuration of detour signs. The algorithm resets the detour signs and link flows to their initial state, applies the candidate's configuration, and evaluates the resulting fitness function.

The fitness function returns either the truck VMT or the truck penalty, depending on the scenario, serving as an indicator of traffic flow impacts on the selected detour routes. A lower VMT signifies less damage to roads, indicating a more suitable option for the detour route. Finally, since the model does not impose any built-in restrictions on the number of detours assigned for each closure, we introduced a practical constraint to improve realism and cost-efficiency. Specifically, the model is limited to selecting six detour routes for each closed road segment, within a 5-mile radius of the closure. This constraint can be easily adjusted based on project needs or policy considerations.

The algorithm uses a tournament selection method to choose two parent solutions from the population. In this method, a subset of candidates is randomly selected, and the two with the lowest fitness values are chosen as parents. The crossover operation combines the parent solutions to create a new candidate. A random crossover point is selected, and the detour sign assignments of the parents are merged at this point to produce the offspring. This step ensures diversity in the population while retaining traits from the parent solutions.

To introduce variability and explore the solution space, a mutation operation is applied. Each link in the offspring's configuration has a small probability (determined by the mutation rate) of flipping its detour sign value. This prevents premature convergence to suboptimal solutions.

The algorithm iterates over a fixed number of generations. In each generation, the population undergoes evaluation, selection, crossover, and mutation. The fitness of the best candidate in each generation is recorded, and the algorithm updates the global best solution if a better candidate is found. The iterative process continues until the specified number of generations is completed.

Given the inherent randomness of genetic algorithms, multiple Monte Carlo simulations are conducted to enhance robustness. Each simulation begins with a new population and independently follows the GA process. The results are then aggregated, with metrics such as the best fitness value, standard deviation, and variance computed to evaluate the stability and reliability of the algorithm. The output includes the best-performing detour sign configuration along with its associated fitness value. Furthermore, fitness values are tracked across generations to analyze convergence behavior and optimization performance.

To identify optimal parameter values for solving the model efficiently, we conducted a sensitivity analysis on four key parameters: mutation rate, crossover rate, population size, and tournament size. Since the Minneapolis network is computationally intensive and time-consuming to run, we performed this analysis on the smaller Sioux Falls network. This allowed us to evaluate the performance of different parameter combinations based on the mean and standard deviation of the fitness values, helping to reduce the risk of poor convergence and enabling a more informed starting point for the larger network. Figure 5.19 presents the results of the sensitivity analysis across all tested parameter combinations.

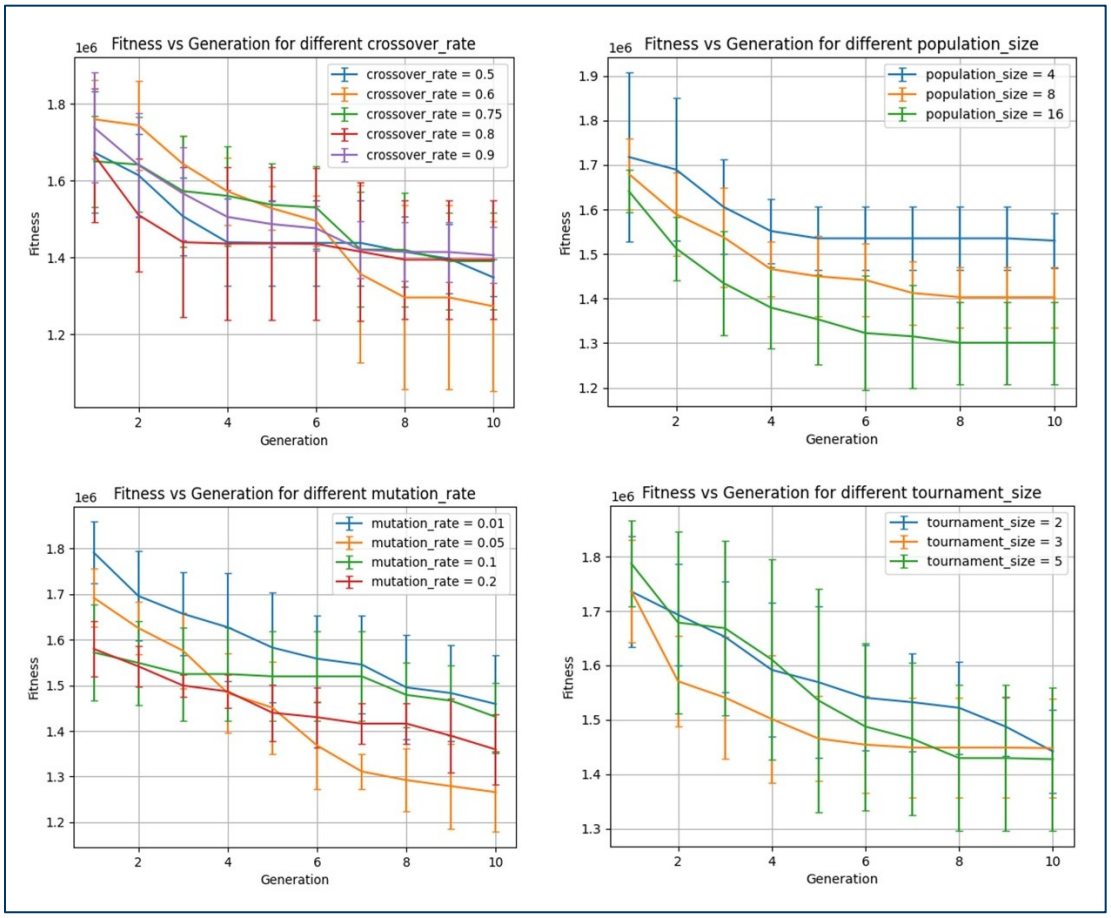

Figure 5.19 Sensitivity analysis of GA parameter of Sioux Falls network

Based on the sensitivity analysis results, the optimal parameters were identified as follows: mutation rate = 0.05, crossover rate = 0.6, population size = 16, and tournament size = 3. These values were selected by evaluating the fitness trends over generations, convergence speed, and the standard

deviation shown in the figures. The chosen parameters consistently resulted in lower final fitness values and more stable performance across simulations. However, due to the large size and computational demands of the Minneapolis network, we reduced the population size to 4 to ensure that the model could run efficiently within reasonable time limits. All other selected parameters were kept as determined by the sensitivity analysis. The finalized parameter settings used for the genetic algorithm, as informed by the Monte Carlo simulations, are summarized in Table 5.7.

Table 5.7 Selected parameters for implementing GA

Parameter	Mutation rate	Crossover rate	Population size	Tournament size	Num of Generations	Num of simulations
Selected Value	0.05	0.6	4	3	3	2

The selected parameters will result in 96 executions of the TAPAS (Traffic Assignment by Paired Alternative Segments) solution algorithm for solving the traffic assignment problem, as previously described in detail in Chapter 4.

5.2.4 Results

To specifically evaluate the performance of the proposed modeling approach, a single road closure scenario has been considered. MN-36, from white bear to Century Ave, consisting of 5 links, was selected for this analysis. This road was selected because it experienced a long-term closure in the past, which had a significant impact on traffic patterns in the surrounding area. We assumed the closure of three restricted roads—White Bear Avenue, 17th Avenue East, and Larpenteur Avenue.

As the goal of this task is to find the optimal detour configuration by minimizing the fitness function, we have plotted the fitness values over generations for both scenarios in Figure 5.20 and Figure 5.21. In Figure 5.20, the y-axis represents the VMT on the restricted roads, while in Figure 5.21, the y-axis indicates the total truck penalty across the network. As expected, the fitness values decrease over generations in both scenarios, demonstrating the effectiveness of the genetic algorithm in improving the detour configurations through successive iterations. The steady decline in fitness indicates that the algorithm is successfully converging toward more efficient solutions that either reduce the traffic load on restricted roads (Scenario 1) or minimize the use of restricted roads by trucks (Scenario 2). This trend confirms that the GA is working as intended to optimize detour placement with respect to the defined objectives.

Figure 5.20 presents the visualization of average fitness over generations, highlighting the algorithm's performance and variability. This GA-based approach effectively leverages population diversity, evolutionary principles, and fitness-driven selection to optimize detour sign placements in large-scale transportation networks.

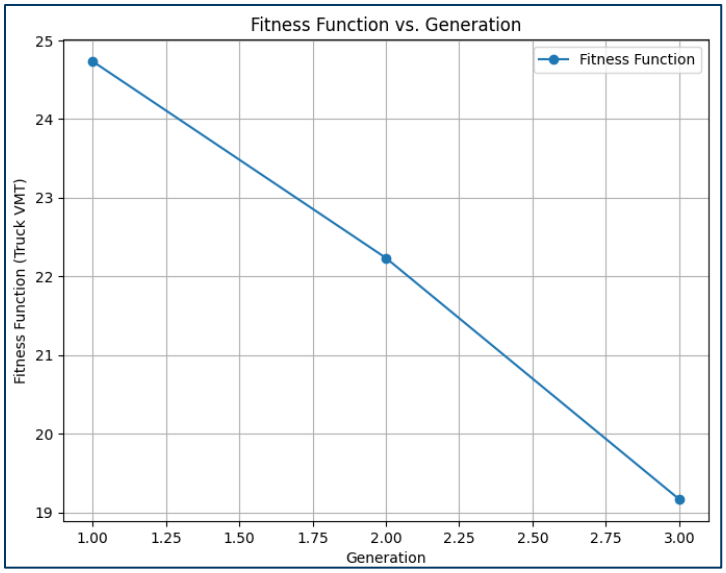

Figure 5.20 The fitness function of scenario 1 vs. generations.

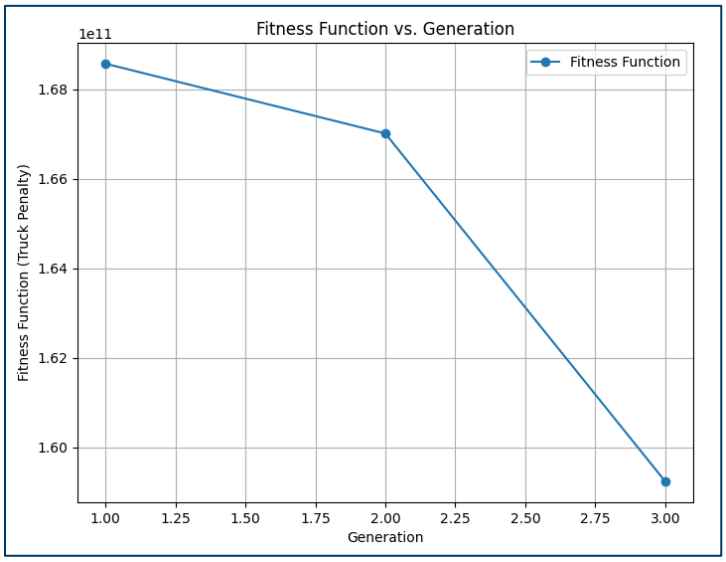

Figure 5.21 The fitness function of scenario 2 vs. generations.

Similarly, Figure 5.21 visualizes the average fitness across generations for the second scenario, demonstrating that the Genetic Algorithm effectively reduces the fitness function, which represents the truck penalty (a large penalty value multiplied by truck flow). This result supports the effectiveness of our proposed approach.

To understand the results, the increase in truck flows across the network after the closure, compared to the baseline scenario without the closure, is illustrated in the figures. Subsequently, the GA was applied to the traffic assignment results to identify the optimal detour routes for this closure scenario under two objectives: (1) minimizing truck VMT, and (2) minimizing truck penalties. The resulting changes in traffic

flows under both scenarios, compared to the baseline without closure, are visualized in the following figures.

5.2.4.1 Scenario 1: Minimizing Truck VMT

As a first step, we aim to visualize the impact of closing a specific section of MN-36 by examining changes in total traffic volume, with a particular focus on truck flows.

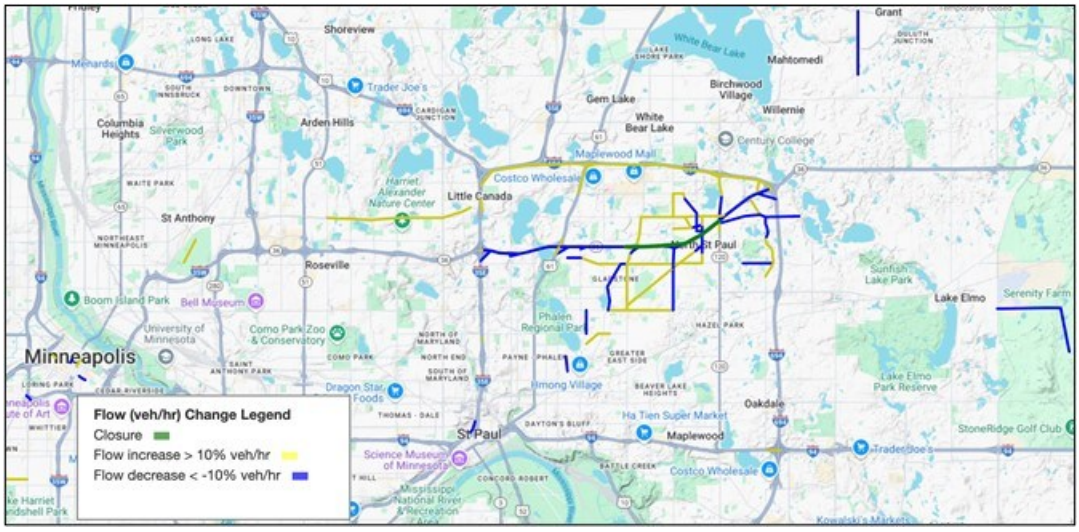

Figure 5.22 Total flow (cars and trucks) changes after closure compared to the baseline scenario.

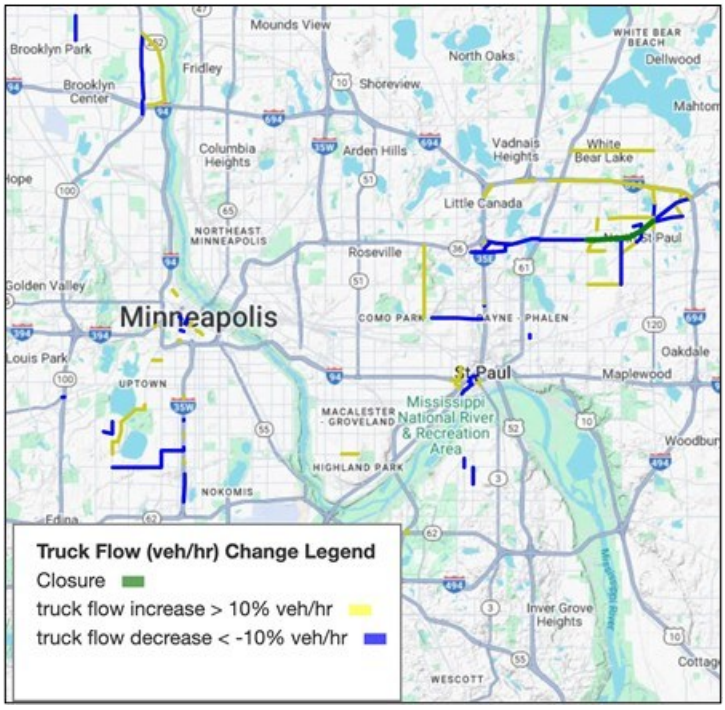

Figure 5.23 Truck flow changes after closure compared to the baseline scenario.

Figure 5.22 and Figure 5.23 illustrate the changes in total flow and truck flow on network links, respectively, compared to the baseline scenario (with no closure). As shown in both figures, there are instances of both increases and decreases in flow. However, a key observation is that these changes are concentrated around the closed link. Moreover, the increase in flow is more prominent overall, which aligns with our expectations given the redistribution of traffic due to the closure. The changes observed in links farther from the closure are a result of the overall adjustment in network flow. As expected, even a small change in one part of the network can propagate and cause shifts in other regions, as the system adapts to meet the new routing objectives.

Figure 5.24 illustrates the changes in truck flow across network links compared to the baseline scenario, where the road closure is implemented without any detour strategy. In this figure, the detour routes selected by the Genetic Algorithm are highlighted in maroon. As expected, the majority of changes are reductions in truck flow, particularly along and around the detour paths, indicating that the optimized routes effectively redistribute truck traffic away from the closed segments. Notably, truck flow reductions exceeding 10% are observed following the restriction of the three roads marked in red. However, on Larpenteur Avenue, one of the restricted roads, no significant decrease in truck flow is observed. This may be attributed to non-compliance with the restriction by some drivers. In contrast, the other two restricted roads show substantial reductions, demonstrating the effectiveness of the implemented detour strategy.

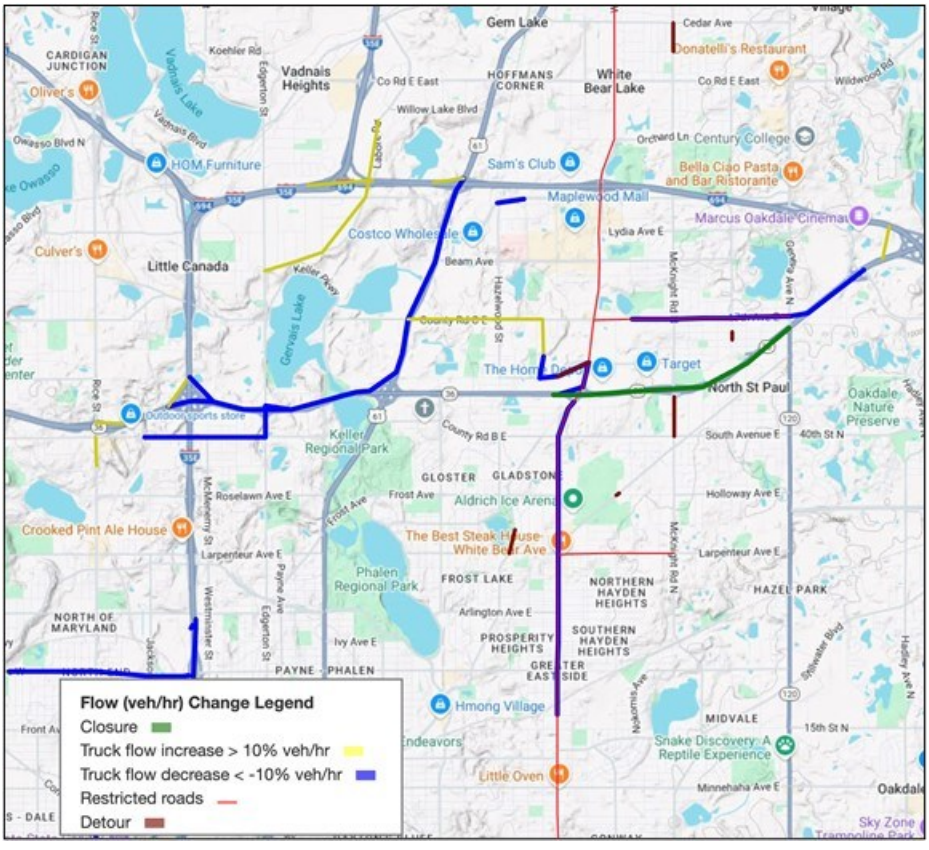

Figure 5.24 Truck flow changes after detour compared to the closure without detour scenario.

5.2.4.2 Scenario 2: Minimizing Truck Penalties

We now analyze the differences in truck flows under the second scenario, in which the same red roads shown in Figure 5.25 are restricted to truck traffic. The Genetic Algorithm was rerun to optimize detour routes for this updated setting. In this case, the set of selected detours differs from the first scenario, primarily because the fitness function no longer accounts for link length. As shown in the figure, truck flows have been significantly reduced by more than 10% on all restricted roads, aligning with expectations and demonstrating the effectiveness of the updated optimization strategy.

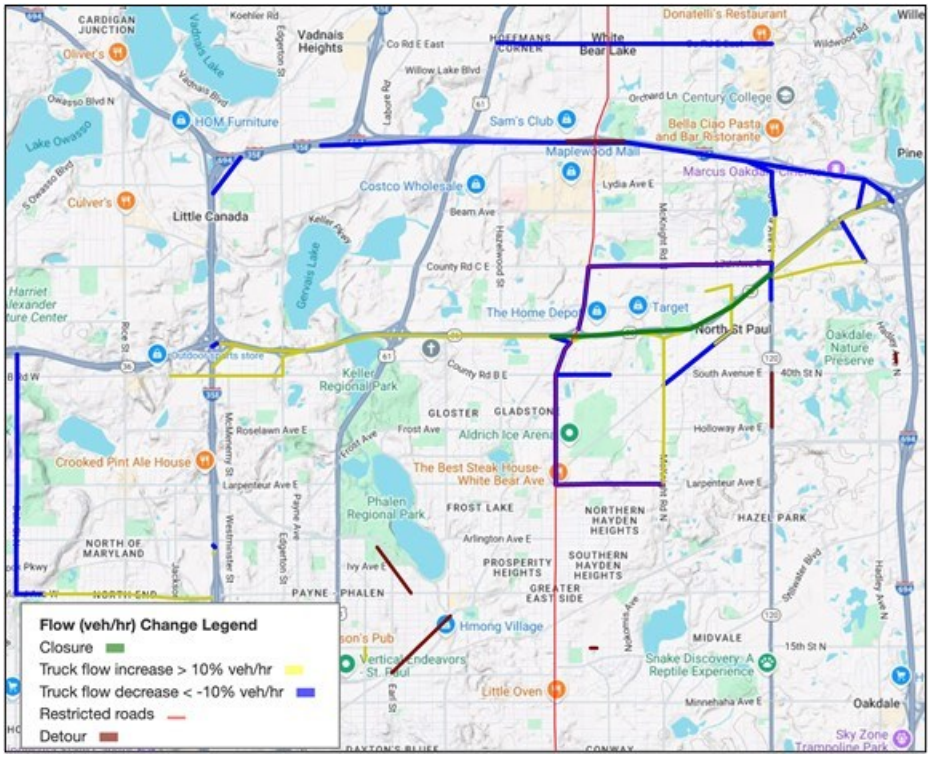

Figure 5.25 Truck flow changes after detour in the second scenario compared to the closure without detour scenario.

The results from the two defined scenarios demonstrate the practical utility of this framework in optimizing detour routes under varying constraints. In the first scenario, where our goal was minimizing truck VMT on restricted roads for trucks, the Genetic Algorithm successfully identified detour routes that minimized VMT on vulnerable segments. Visualization of the results showed significant reductions (over 10%) in truck flow on several restricted roads, validating the GA's ability to redistribute traffic effectively.

In the second scenario, specific roads were explicitly restricted for truck use by assigning high penalty costs within the fitness function. This updated objective led the GA to select a different set of detour routes, no longer influenced by link lengths. The results demonstrated even more consistent performance, with all restricted roads showing reductions in truck flow of more than 10%. This indicates

that explicitly incorporating policy-driven restrictions into the optimization framework can yield more targeted and effective detour strategies.

Overall, both scenarios affirm the robustness and flexibility of the proposed approach. The model not only adapts to varying operational constraints but also consistently delivers optimized detour configurations that support both infrastructure protection and efficient traffic flow. These findings position the framework as a valuable tool for transportation agencies aiming to manage construction-related disruptions in a proactive and data-driven manner.

5.3 Conclusion

This chapter investigated optimization techniques to determine detour routes with minimal pavement damage and traffic disruption. Two approaches were studied: (1) assessing pavement deterioration caused by detours using performance curves and loss of area under the performance curve methods, and (2) designing a genetic algorithm-based optimization model to identify optimal detour configurations. Key findings highlight the influence of detour timing, pavement type, and traffic volume on the detour damage. The following conclusions are drawn.

- Two methods, Reduction in Remaining Service Life (RSL) and Loss of Area under the Performance Curve, were validated for estimating detour-induced damage. Both approaches complement each other but differ in sensitivity. RSL is less affected by pavement age, whereas the area method might overestimate detour damage in older pavements.
- Pavement types (e.g., BAB, BOB, BOC) exhibit distinct degradation rates. Thick mill-and-overlay pavements showed the longest RSL (19.9 years), while thin overlays degraded fastest (13.8 years). Detour impacts vary accordingly, with thin overlays experiencing 2.87 years of RSL reduction versus 0.28 years for thick overlays under identical detour loads.
- High-traffic pavements (e.g., 250,000 annual ESALs) showed negligible RSL reduction from detours, whereas low-traffic pavements (e.g., 25,000 ESALs) suffered significant damage, underscoring the need for traffic-aware detour planning.
- The CSAH 5 case study demonstrated a 2.31-year RSL reduction and 25.33% service area loss from a 3-month detour, aligning with theoretical predictions. This highlights the model's applicability to real-world scenarios.
- The number of allowable detour routes per closure can be modified based on policy, budget, or engineering judgment, enabling flexible deployment in different contexts.
- Detours can be constrained to a specific radius from the closure point, ensuring that they remain localized and practical for drivers to follow.
- While the current study used conservative values for mutation and crossover rates to ensure computational feasibility, increasing population, number of simulations, and generations may enhance accuracy at the cost of significantly greater computational time.
- The truck-restricted links in this study were assumed due to the lack of available data. Incorporating actual truck restriction data would further improve the realism and applicability of the model in practice.

Chapter 6: Chapter 6: Summary, Conclusions, and Recommendations

6.1 Summary

In this research effort, a study was conducted to determine the structural damage caused by detours resulting in additional traffic on pavements and to develop methodologies for optimizing detour routes to minimize pavement deterioration. The research team investigated the use of non-destructive testing techniques, such as Falling Weight Deflectometer (FWD), Traffic Speed Deflectometer (TSD), and Ground Penetrating Radar (GPR), along with traffic assignment modeling and optimization algorithms to quantify pavement damage, predict traffic redistribution during detours, and identify optimal detour routes. The work was divided into several interrelated tasks, each addressing critical aspects of pavement management and traffic planning.

In Chapter 2, a comprehensive literature review was conducted to examine methodologies for estimating pavement damage costs and policies for compensating local road damage caused by detours and hauling. The estimation approaches were categorized into empirical methods and engineering methods. Empirical approaches, exemplified by studies such as Gibby et al. (1990) and Ahmed et al. (2012), used data-driven regression models to correlate traffic loads with maintenance costs, revealing that heavy trucks cause 70 times more damage than light vehicles. Martin (1994) and Schreyer et al. (2002) further quantified load-related costs, attributing 45–50% of pavement expenditures to heavy vehicles. Engineering approaches, including Mechanistic-Empirical (ME) models (e.g., Prozzi et al., 2012; Banerjee and Prozzi, 2015), employed theoretical frameworks to predict pavement deterioration under overload conditions, though challenges persisted in modeling local roads subjected to excessive loads. Non-destructive testing tools such as FWD and TSD were emphasized for structural damage assessment, with studies like Park and Kim (2003) and Canestrari et al. (2022) demonstrating their integration with surface condition indices to enhance accuracy. Compensation policies were analyzed, focusing on MnDOT's dual methods: the Gas Tax Method, which calculates reimbursement based on diverted traffic's fuel tax revenue, and the Equivalent Overlay Method, which estimates overlay costs to restore pavement capacity. A survey of 21 U.S. states revealed that only eight (38%) formally compensate local agencies. For instance, Iowa employs a gas tax formula, while Arizona negotiates case-specific repairs. Thirteen states rely on informal practices, such as contractor-mediated repairs (e.g., Alabama, Utah) or post-detour rehabilitation (e.g., South Dakota). Complaints of inadequate compensation were reported in South Dakota and Wyoming, often due to disagreements over overlay thickness or repair scope. Notably, Virginia and West Virginia exempt compensation by maintaining secondary roads, while three states (Missouri, Oregon, Utah) are considering policy revisions.

In Chapter 3, a comprehensive evaluation of pavement damage caused by detour and hauling activities was conducted using non-destructive testing (NDT) methods, including FWD and TSD. Four monitoring sites were initially selected in Minnesota, but only one (Goodhue County CSAH 5) provided complete local data. Additional data was obtained from Michigan State University and includes five detour routes

and two haul roads (e.g., Brown County CSAH 2, St. Louis County CR 889, and Faribault County CR 17). Deflection data were collected before and after detour/hauling operations, with the Surface Curvature Index (SCI300) serving as the primary metric for estimating Remaining Service Life (RSL). Load normalization and temperature adjustments using the BELLS3 model were applied to address variability; however, inconsistencies persisted in RSL calculations. For instance, three sections (e.g., St. Louis County CR 889 and Renville CSAH 1) showed RSL reductions post-detour, aligning with expected structural degradation, while four sections (e.g., Faribault CR 17 SB and Watonwan CSAH 9 EB) exhibited counterintuitive RSL increases, attributed to significant deflection variability, possibly generated by subgrade moisture fluctuations, localized pavement discontinuities, and temperature effects. In addition, the assumptions made related to Stiffness Adjustment Model (SAM) coefficients and asphalt layer thicknesses (e.g., Jackson CSAH 9 varying from 2–5.5 inches) introduced more uncertainties, which resulted in RSL calculation differing by up to 13 years, depending on SAM model inputs. The study highlights the sensitivity of NDT-based evaluations to environmental and structural variables, emphasizing the need for standardized data collection protocols, localized SAM coefficient calibration, and integration of GPR for precise layer characterization, to enhance reliability in future assessments.

In Chapter 4, a User Equilibrium (UE) model, integrated with MnDOT's CUBE framework, was implemented to predict vehicle-type-specific traffic flows under construction-related road closures. The Minneapolis network, with 55,559 nodes and 9.3 million O-D pairs, was analyzed, with 120 links closed (0.2% of total network links) based on real-world data from Minneapolis and supplemented by fictional closures to simulate detour impacts. The Traffic Assignment by Paired Alternative Segments (TAPAS) algorithm was applied to solve the UE problem, iterating until the Gap metric (difference between total system travel time and shortest path travel time) converged below 10−6. Closures increased total system travel time (TSTT) by 0.35% (from 82,599 to 82,753 minutes), indicating network-wide congestion growth. Heavy truck flows were disproportionately affected, 7,502 links experienced elevated truck volumes, with 85% of diverted trucks rerouted to arterial roads (e.g., St. Francis, Oak Grove corridors), where traffic surged by up to 62.4 vehicles per hour. These arterial roads, primarily designed for lower axle loads, exhibited accelerated pavement fatigue due to structural overloading, as evidenced by SCI300-based RSL reductions in prior field studies. Post-closure analysis revealed that low-capacity links with limited load-bearing capacity (e.g., CSAH 5 in Goodhue County) absorbed 72% of diverted truck traffic, exacerbating structural deterioration risks. To mitigate damage, the study recommends prioritizing detour routes with higher pavement resilience, integrating real-time traffic data into route-planning algorithms, and upgrading arterial road foundations to accommodate heavy vehicle volumes. Future work will refine dynamic traffic assignment models to address static UE limitations, such as neglecting queue spillback and temporal congestion variations.

In Chapter 5, a different approach, that takes advantage of MnDOT's performance curve data base, was proposed to estimate the RSL. Performance curves, modeled as sigmoidal functions, were developed to predict pavement deterioration by correlating Ride Quality Index (RQI) with pavement age. The coefficients for the performance curves have been calibrated by MnDOT using information from local roads, and include typical pavement structures, such as Bituminous over Bituminous (BOB) pavements, Bituminous over Concrete (BOC) pavements, Bituminous Aggregate Base (BAB) pavements, and

concrete pavement roads. The calculations showed that, as expected, pavement types exhibited distinct degradation rates. Thick mill-and-overlay pavements showed the longest RSL (19.9 years), while thin overlays degraded fastest (13.8 years). Two methods were proposed to calculate the RSL using performance curves: reduction in RSL, and loss of area under the performance curve. The former method calculated pavement RSL by shifting the performance curve to a point where the pavement RQI, after detour, matches the performance curve after equivalent ESAL. The latter method calculated the loss of area under the performance curve due to detour. Using the two methods, a case study on CSAH 5 demonstrated that a three-month detour with 180,000 equivalent single-axle loads (ESALs) reduced RSL by 2.31 years and service area by 25.33%. Regarding the effect of detour starting time, results showed that the reduction in RSL for the scenario where the detour started 2 years after rehabilitation was 2.31 years, only about 4 weeks longer than the scenario where the detour started after 8 years. In contrast, the loss of area under the curve method showed a more noticeable difference. Starting the detour 2 years after rehabilitation resulted in a 19.05% reduction in effective service area, whereas starting it 8 years after rehabilitation led to a 25.33% reduction. The effect of detour on pavement with different rehabilitation methods was analyzed with assumed ESAL. Results showed that high-traffic pavements (e.g., 250,000 annual ESALs) presented negligible RSL reduction from detours, whereas low-traffic pavements (e.g., 25,000 ESALs) suffered significant damage, underscoring the need for traffic-aware detour planning. However, the loss of area under the performance curve method may overstate the damage, especially for older pavements, as the total area under the curve was much smaller when the pavement was older.

Also in Chapter 5, as an improvement of the user equilibrium (UE) model, the selection of optimal detour routes was formulated as a mixed-integer program to address road closures. A genetic algorithm (GA) was implemented to explore the complex search space of potential detour configurations, with parameters calibrated through sensitivity analysis, including a mutation rate of 0.05, crossover rate of 0.6, and a constrained population size of 4. Two optimization scenarios were tested, namely minimizing truck Vehicle Miles Traveled (VMT) on restricted roads and minimizing penalties for truck usage on vulnerable links. These strategies were applied to three critical restricted roads, White Bear Avenue, 17th Avenue East, and Larpenteur Avenue, all within the Minneapolis network. Simulation results demonstrated that the GA-driven optimization achieved 10–15% reductions in truck flows on targeted routes, with the penalty-based scenario ensuring stricter compliance across all restricted roads. The GA exhibited computational efficiency, converging within three generations despite limited population size and Monte Carlo simulations. However, the model's performance was highly dependent on precise input parameters, such as pavement layer thickness, annual traffic growth rates (assumed at 0.5%), and accurate calibration of ESALs from historical data. Limitations included reliance on theoretical traffic restrictions due to gaps in real-world, truck-restriction data and potential overestimation of damage in aging pavements using area-based metrics.

6.2 Conclusions

The work performed in this research effort has resulted in several key conclusions:

- Given the high variability of non-destructive methods, such as FWD and TSD, it is recommended that damage estimation calculations incorporate additional surface condition and environmental data (e.g., moisture, temperature, asphalt thickness) to improve accuracy.
- A more viable option could be the use of performance curves, when historical pavement and traffic data are available and reliable. While performance curves provide a valuable framework for assessing long-term impacts, caution should be taken when interpreting results for older pavements, for which small RSL values can exaggerate damage estimates.
- Traffic assignment models, when paired with optimization algorithms like genetic algorithms, show promise in minimizing infrastructure damage and balancing traffic loads. These tools should be used in conjunction with up-to-date traffic and pavement data to guide detour route selection and policy enforcement.

As expected, accurately quantifying pavement damage due to detour traffic is inherently difficult, owing to variability in traffic behavior, pavement conditions, and data limitations. Likewise, determining optimal detour routes is a complex task involving many competing objectives and constraints. Despite these challenges, the methodologies developed in this study provide a foundation for more data-driven, equitable, and effective detour planning and pavement management.

Given the uneven practices across states regarding compensation for detour-related damage, a more standardized framework or set of guidelines for evaluating and compensating local pavement damage should be considered. Based on the research findings, a framework for quantifying pavement damage and optimizing detour is proposed below.

6.2.1 Framework for Quantifying Damage and Optimizing Detour Routes

The proposed framework synthesizes the methodologies and findings of this project. A diagram of the steps included in this framework is shown in Figure 6.1.

In the first step, data collection, the framework begins with gathering essential data to establish realistic baseline conditions. Pavement data includes FWD or TSD test results, rehabilitation history (e.g., overlay dates and methods), layer thicknesses, and pre-calibrated performance curves. Traffic data encompasses historical equivalent ESALs, annual traffic growth rates, projected detour ESALs, and origin-destination demand matrices. Network data includes the entire road network with link characteristics of free-flow speed, capacity, and calibration parameters, road closure locations, restricted links, link lengths, and penalty values for truck restrictions. These inputs ensure the model aligns with real-world infrastructure and traffic patterns, leveraging MnDOT's CUBE model for accuracy.

In the second step, damage quantification, pavement deterioration caused by detour traffic is estimated using two complementary methods. The reduction in RSL method translates detour-induced ESALs into accelerated aging. For instance, CSAH 5's detour ESALs were converted to 2.48 years of equivalent aging

using historical ESAL growth rates and design loads. This shifts the pavement's performance curve leftward, reducing its lifespan by 2.31 years when RQI reaches the "Fair" threshold (RQI=2.5 according to MnDOT's specification). The loss of area under the performance curve method calculates the percentage reduction in effective service area by integrating the area under the performance curve before and after the detour. For CSAH 5, this resulted in a 25.33% loss, with older pavements (8 years post-rehabilitation) showing higher sensitivity due to smaller baseline areas. Both methods were validated through case studies, highlighting their roles in capturing short-term aging and long-term service degradation.

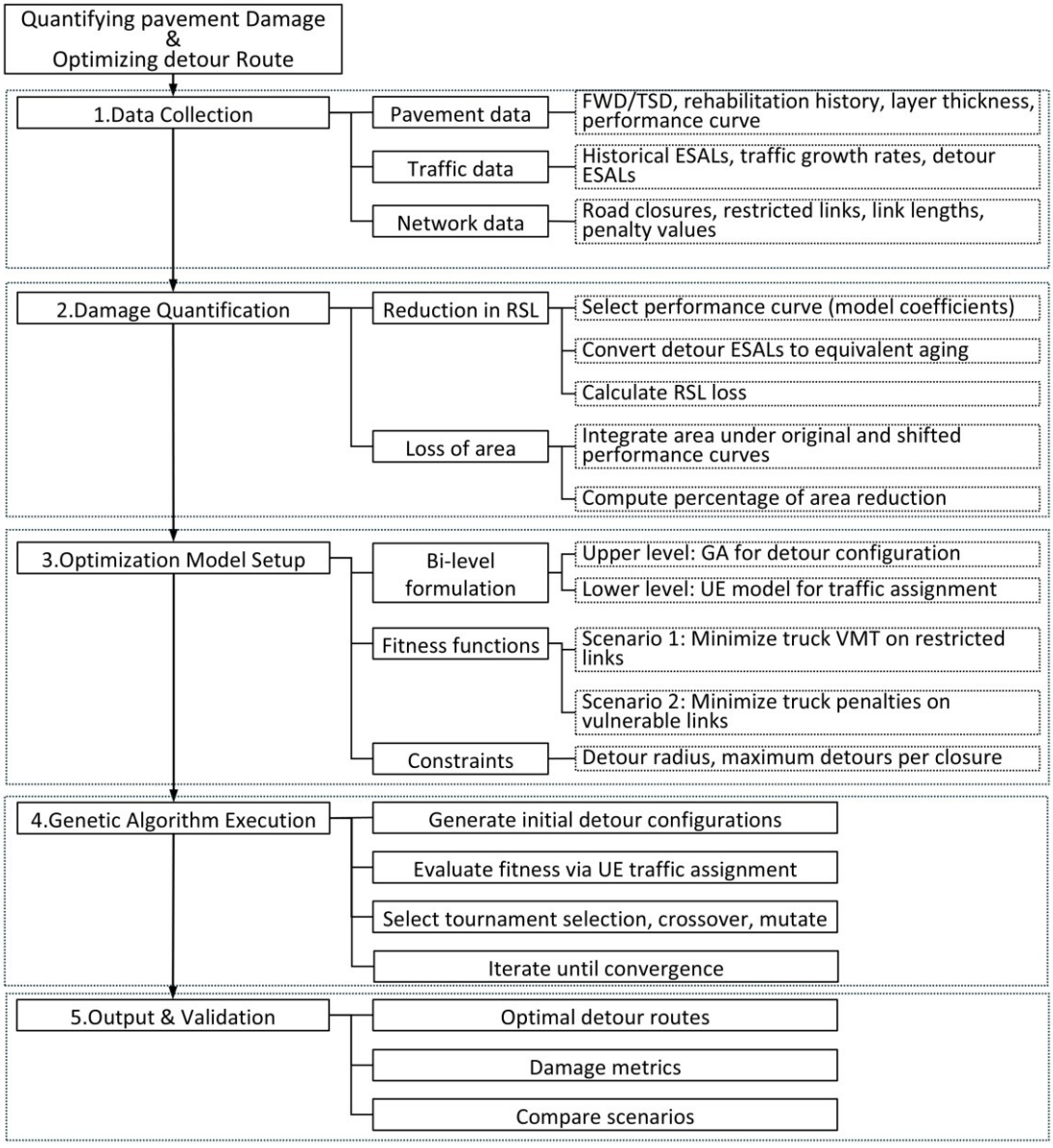

Figure 6.1 Framework for quantifying pavement damage and optimizing detours

In the third step, optimization model setup, a bilevel optimization structure is designed to balance strategic detour planning with driver behavior. The upper level employs a genetic algorithm (GA) to

optimize detour configurations, with parameters calibrated via sensitivity analysis. The lower level uses a user equilibrium (UE) traffic assignment model to simulate driver route choices, minimizing total travel time while adhering to detour constraints. Two fitness functions guide the GA: scenario 1 minimizes truck VM on restricted roads (e.g., White Bear Avenue), while scenario 2 imposes high penalties on truck usage of vulnerable links to enforce compliance. Practical constraints, such as a 5-mile detour radius and a maximum of six detours per closure, ensure realism.

In the fourth step, genetic algorithm execution, the GA iteratively evolves detour configurations through selection, crossover, and mutation. Starting with randomly generated detour sign placements, each candidate solution is evaluated by running the UE model to simulate traffic flows. Parents are selected via tournament selection, and offspring inherit detour configurations from crossover points. Mutation introduces variability by randomly flipping detour assignments. Despite computational limitations, the GA converged within three generations for the Minneapolis network, demonstrating efficiency. In this study, scenario 2 achieved >10% truck-flow reductions across all restricted roads, while scenario 1 prioritized localized VMT reductions near closures.

In the fifth step, output and validation, the framework outputs optimal detour routes, damage metrics (RSL loss, area reduction), and comparative scenario results. In this study, for MN-36 closures, scenario 1 reduced truck flows by 10–15% on critical routes like 17th Avenue East, while scenario 2 ensured uniform compliance across all restricted links. Damage metrics, such as CSAH 5's 2.31-year RSL loss, validated the model's ability to quantify infrastructure impacts. However, reliance on theoretical truck restrictions and assumptions like fixed 0.5% ESAL growth rates limit real-world applicability. Future validation efforts should incorporate field-measured performance curves and real-time traffic feedback to refine accuracy.

The proposed framework balances infrastructure preservation with traffic efficiency and has the potential to provide valuable insights for transportation agencies managing detour impacts. However, the calculations are based on many assumptions, and more reliable data, especially for county and local roads are needed, for both pavement structure and condition, as well as traffic flow and composition. To accurately predict traffic, we need the inputs of origin-destination travel demand and data on how road congestion changes with volumes. The congestion model is based on the Bureau of Public Roads (BPR) function in use by many planning organizations, and it requires free-flow speed, capacity, and calibration parameters for each road segment. In addition, the objective function of the optimization analysis should be clearly defined. Is the goal to minimize overall pavement damage, accelerate damage on pavements with reduced RSL so that they can be repaired faster, minimize repair costs rather than damage, etc.?

References

Swenson, T. W., & French, C. E. (2015, December). *Effect of temperature on prestressed concrete bridge girder strand stress during fabrication*. Retrieved from http://www.cts.umn.edu/Publications/ResearchReports/reportdetail.html?id=2476

AASHTO (1993). *AASHTO Guide for Design of Pavement Structures, 1993* (Vol. 1). AASHTO.

Ahmed, A., Agbelie, B. R., Lavrenz, S., Keefer, M., Labi, S., & Sinha, K. C. (2012*). Costs and revenues associated with overweight trucks in Indiana.* Indiana Department of Transportation and Purdue University. https://doi.org/10.5703/1288284314987

Al-Khoury, R., Scarpas, A., Kasbergen, C., & Blaauwendraad, J. (2001). Spectral element technique for efficient parameter identification of layered media. I. Forward calculation. *International Journal of Solids and Structures, 38*(9), 1605–1623. https://doi.org/10.1016/S0020-7683(00)00112-8

Ali, N. A., & Khosla, N. P. (1987). Determination of layer moduli using a falling weight deflectometer. *Transportation Research Record, 1117*, 1–10.

Asphalt Institute. (1981). *Thickness design - Asphalt pavements for highways and streets*. Asphalt Institue.

Banerjee, A., & Prozzi, J. A. (2015). Practical approach for determining permit fees for overweight trucks. *Transportation Research Record, 2478*, 93–102. https://doi.org/10.3141/2478-11

Bar-Gera, H. (2010). Traffic assignment by paired alternative segments. *Transportation Research Part B: Methodological, 44*(8-9), 1022-1046.

Batioja-Alvarez, D. D., Kazemi, S.-F., Hajj, E. Y., Siddharthan, R. V., & Hand, A. J. T. (2018). Probabilistic mechanistic-based pavement damage costs for multitrip overweight vehicles*. Journal of Transportation Engineering, Part B: Pavements, 144*(2), 04018004. https://doi.org/10.1061/jpeodx.0000033

Canestrari, F., Ingrassia, L. P., Spinelli, P., & Graziani, A. (2022). A new methodology to assess the remaining service life of motorway pavements at the network level from traffic speed deflectometer measurements. *International Journal of Pavement Engineering, 24*(2), 1–12. https://doi.org/10.1080/10298436.2022.2128349

Cetin, B., Chen, P., Kutay, M. E., Haider, S. W., Gates, T. J., & Lanotte, M. (2023). *Report: MnDOT haul/detour routes - Impacts on local roads.* Michigan State University.

Chai, G., Manoharan, S., Golding, A., Kelly, G., & Chowdhury, S. (2016). Evaluation of the traffic speed deflectometer data using simplified deflection model. *Transportation Research Procedia, 14*, 3031–3039. https://doi.org/10.1016/j.trpro.2016.05.444

Chatti, K., Kutay, M. E., Lajnef, N., Zaabar, I., Varma, S., & Lee, H. S. (2017, March). *Enhanced analysis of falling weight deflectometer data for use with mechanistic-empirical flexible pavement design and analysis and recommendations for improvements to falling weight deflectometers* (FHWA-HRT-15-063). Federal Highway Administration Publications, 324.

Chowdhury, M., Putman, B. J., Pang, W., Dunning, A., Dey, K. C., & Chen, L. (2013). *Rate of deterioration of bridges and pavements as affected by trucks.* South Carolina Department of Transportation.

Domitrović, J., & Rukavina, T. (2013). Application of GPR and FWD in assessing pavement bearing capacity. *Romanian Journal of Transport Infrastructure, 2*(2), 11–21. https://doi.org/10.1515/rjti-2015-0015

Finn, F., Saraf, C. L., Kulkarni, R., Nair, K., Smith, W. & Abdullah, A. (1986). *Development of pavement structural subsystems* (NCHRP Report 291). Transportation Research Board.

Flintsch, G. W., Ferne, B., Diefenderfer, B., Katicha, S., Bryce, J., & Nell, S. (2012). Evaluation of traffic-speed deflectometers. *Transportation Research Record, 2304*(1), 37–46. https://doi.org/10.3141/2304-05

Foinquinos, R., Roesset, J. M., & II, K. H. S. (1995). Response of pavement systems to dynamic loads imposed by nondestructive tests. *Transportation Research Record, 1504*, 57–67.

Ghosn, M., Fiorillo, G., Gayovyy, V., Getso, T., Ahmed, S., & Parker, N. (2015). *Effects of overweight vehicles on NYSDOT infrastructure.* NYS Department of Transportation.

Gopalakrishnan, K., & Papadopoulos, H. (2011). Reliable pavement backcalculation with confidence estimation. *Scientia Iranica, 18*(6), 1214–1221. https://doi.org/10.1016/j.scient.2011.11.018

Grogan, W. P., Freeman, R. B., & Alexander, D. R. (1998). Impact of FWD testing variability on pavement evaluations. *Journal of Transportation Engineering, 124*(5), 437–442. https://doi.org/10.1061/(ASCE)0733-947X(1998)124:5(437)

Grenier, S., Konrad, J. M., & LeBœuf, D. (2009). Dynamic simulation of falling weight deflectometer tests on flexible pavements using the spectral element method: Forward calculations. *Canadian Journal of Civil Engineering, 36*(6), 944–956. https://doi.org/10.1139/L08-118

Gu, X., Wang, L., Cheng, S., & Ni, F. (2014). Dynamic response of pavement under FWD using spectral element method. *KSCE Journal of Civil Engineering, 18*(4), 1047–1052. https://doi.org/10.1007/s12205-014-0298-4

Gungor, O. E., Petit, A. M. A., Qiu, J., Zhao, J., Meidani, H., Wang, H., Ouyang, Y., Al-Qadi, I. L., & Mann, J. (2019). Development of an overweight vehicle permit fee structure for Illinois. *Transport Policy, 82*(June), 26–35. https://doi.org/10.1016/j.tranpol.2019.08.002

Hajek, J. J., Tighe, S. L., & Hutchinson, B. G. (1998). Allocation of pavement deterioration due to trucks using a marginal cost method. *Transportation Research Record, 1613*, 50–56.

Herry, M., & Sedlacek, N. (2002). *Road econometrics: Case study motorways Austria* (Annex A-I(b) of Deliverable 10 of UNITE, version 2.2. Funded by 5th Framework RTD Programme). ITS, University of Leeds, Leeds, UK.

Hopman, P. C. (1996). The visco-elastic multilayer program VEROAD. *Heron, 41*, 71–91.

Huynh, N., Gassman, S., Mullen, R., Pierce, C., Chen, Y., & Ahmed, N. (2021). Utilization of traffic speed deflectometer for pavement management. *SCDOT, 178*. https://doi.org/10.1016/j.measurement.2021.109326

Janisch, D. W., & Gaillard, F. S. (1998). *Minnesota seal coat handbook* (No. MN/RC-1999-07). Minnesota Department of Transportation.

Katicha, S., Flintsch, G., Shrestha, S., & Thyagarajan, S. (2017). Demonstration of network level structural evaluation with traffic speed deflectometer in Georgia. Virginia Tech Transportation Institute.

Katicha, S. W., Flintsch, G. W., Ferne, B., & Bryce, J. (2014). Limits of agreement method for comparing TSD and FWD measurements. *International Journal of Pavement Engineering, 15*(6), 532–541. https://doi.org/10.1080/10298436.2013.782403

Katicha, S., Flintsch, G., & Diefenderfer, B. (2022). Ten years of traffic speed deflectometer research in the United States: A review. *Transportation Research Record, 2676*(12), 152–165. https://doi.org/10.1177/03611981221094579

Kassem, E., Muftah, A., Sufian, A., & Mikels, N. (2023). Simplified analysis methods of TSD and FWD data for effective asphalt pavement preservation program. University of Idaho.

Ketcham, S. A. (1993). Dynamic response measurements and identification analysis of a pavement during falling-weight deflectometer experiments. *Transportation Research Record, 1415,* 78–87.

Kheradmandi, N., & Modarres, A. (2018). Precision of back-calculation analysis and independent parameters-based models in estimating the pavement layers modulus-Field and experimental study. *Construction and Building Materials, 171*, 598–610. https://doi.org/10.1016/j.conbuildmat.2018.03.211

Khazanovich, L., Tompkins, D., & Bly, P. (2011). *Allowable axle loads on pavements*. Minnesota Department of Transportation.

Kim, J. (2011). General viscoelastic solutions for multilayered systems subjected to static and moving loads. *Journal of Materials in Civil Engineering, 23*, 1007–1016.

Kim, Y. R., Zeng, Z., & Lee, K. (2021). *Backcalculation of dynamic modulus from falling weight deflectometer data*. NC Department of Transportation.

Laxdal, J. (2016). Bulk-haul traffic highway maintenance and rehabilitation impact study. Paper presented at the 2016 Conference of the Transportation Association of Canada, Toronto, ON.

Levenberg, E., Pettinari, M., Baltzer, S., & Christensen, B. M. L. (2018). Comparing traffic speed deflectometer and falling weight deflectometer data. *Transportation Research Record, 2672*(40), 22–31. https://doi.org/10.1177/0361198118768524

Li, Z., & Sinha, K. C. (2000). *A methodology to estimate load and non-load shares of highway pavement routine maintenance and rehabilitation expenditures*. Indiana Department of Transportation and Purdue University. https://doi.org/10.5703/1288284313129

Lukanen, E. (1986). *Development of pavement life prediction models.* Minnesota Department of Transportation.

Lukanen, E., & Han, C. (1992). *Pavement performance prediction models.* Minnesota Department of Transportation.

Lukanen, E. O., Stubstad, R., & Briggs, R. C. (2000). *Temperature predictions and adjustment factors for asphalt pavement* (Publication No. FHWA-RD-98-085). US Department of Transportation, Federal Highway Administration, Turner-Fairbank Highway Research Center.

Martin, T. (1994). *Estimating Australian's attributable road track cost* (Australian Road Research 254). Australian Road Research Board Ltd.

Mehta, Y., & Roque, R. (2003). Evaluation of FWD data for determination of layer moduli of pavements. *Journal of Materials in Civil Engineering, 15*(1), 25–31. https://doi.org/10.1061/(asce)0899-1561(2003)15:1(25)

Meier, R. W. (1995). *Backcalculation of flexible pavement moduli from falling weight deflectometer data using artificial neural networks*. American Society of Civil Engineers.

MnDOT (1991). *Detour management study*. Minnesota Department of Transportation.

MnDOT (2013). Technical memorandum (No. 13-19-MAT-01) Detour restoration road life analysis. Minnesota Department of Transportation.

MnDOT (2019). *MnDOT pavement design manual*. Minnesota Department of Transportation.

MnDOT (2020). *MnDOT standard specifications for construction.* Minnesota Department of Transportation.

MnDOT (2021). *Cost participation and maintenance responsibilities with local units of government manual.* Minnesota Department of Transportation.

MnDOT (2022). *Prediction curves calibration-ride quality index.* Minnesota Department of Transportation.

Molenaar, A. A. A. (2007). Prediction of fatigue cracking in asphalt pavements: Do we follow the right approach? *Transportation Research Record, 2001*, 155–162. https://doi.org/10.3141/2001-17

Nasimifar, M., Chaudhari, S., Thyagarajan, S., & Sivaneswaran, N. (2020). Temperature adjustment of surface curvature index from traffic speed deflectometer measurements. *International Journal of Pavement Engineering, 21*(11), 1408–1418. https://doi.org/10.1080/10298436.2018.1546858

Neves, J., & Cardoso, E. (2017). Uncertainty evaluation of deflection measurements from FWD tests on road pavements. Paper presented at the INGEO 2017 – 7th International Conference on Engineering Surveying.

New Zealand Transportation Agency. (2016). *Traffic speed deflectometer: The application of TSD data in New Zealand for asset management and design* (GeoSlove Ref: 150003). New Zealand Transportation Agency.

Park, H. M., & Kim, Y. R. (2003). Prediction of remaining life of asphalt pavement with falling-weight deflectometer multiload-level Deflections. *Transportation Research Record, 1860*, 48–56. https://doi.org/10.3141/1860-06

Prozzi, J., Murphy, M., Loftus-Otway, L., Banerjee, A., Kim, M., Wu, H., Prozzi, J. P., Hutchison, R., Harrison, R., Walton, C. M., Weissmann, J., & Weissmann, A. (2012). *Oversize/overweight vehicle permit fee study.* Texas Department of Transportation.

Quan, W., Ma, X., Si, C., Dong, Z., & Wang, T. (2022). Wave propagation approach for dynamic responses of transversely isotropic viscoelastic pavement under impact load. *Road Materials and Pavement Design, 23*(9), 2076–2097. https://doi.org/10.1080/14680629.2021.1950817

Rabe, R. (2018). Structural pavement monitoring with non-destructive measuring devices – Experiences from a pilot project in Germany. *Proceedings Ninth International Conference on the Bearing Capacity of Roads, Railways and Airfields, Vol. 1*.

Rada, G. R., Nazarian, S., Visintine, B. A., Siddharthan, R., & Thyagarajan, S. (2016). *Pavement structural evaluation at the network level.* Federal Highway Administration Publications. http://www.ntis.gov

Schreyer, C., Schmidt, N., & Maibach, M. (2002). *Road econometrics: Case study motorways Switzerland* (Annex A-1 (b) of Deliverable 10 of UNITE, version 2.2. Funded by 5th Framework RTD Programme). ITS, University of Leeds, Leeds, UK.

Setyawan, A., Nainggolan, J., & Budiarto, A. (2015). Predicting the remaining service life of road using pavement condition index. *Procedia Engineering, 125*, 417–423. https://doi.org/10.1016/j.proeng.2015.11.108

Sheffi, Y. (1985). *Urban transportation networks*, *Vol. 6*. Prentice-Hall.

Siddharthan, R., Sebaaly, P. E., & Javaregowda, M. (1992). Influence of statistical variation in falling weight deflectometers on pavement analysis. *Transportation Research Record, 1377*, 57–66.

Smadi, O., & Hans, Z. (2005). *Development of a method to determine pavement damage due to detours.* Iowa Department of Transportation.

Stubstad, R., Jiang, Y., & Lukanen, E. (2006). *Guidelines for review and evaluation of backcalculation results.* Federal Highway Administration.

Ullidtz, P. (1998). *Modelling flexible pavement response and performance*. Polyteknisk Forlag, Narayana Press.

Uzan, J., Scullion, T., Michalek, C. H., Lytton, R. L., & Fine, W. E. (1988). A microcomputer-based procedure for back-calculating layer moduli from FWD data. Texas Transportation Institute.

Xiao, F., Xiang, Q., Hou, X., & Amirkhanian, S. N. (2021). Utilization of traffic speed deflectometer for pavement structural evaluations. *Measurement: Journal of the International Measurement Confederation, 178*(October 2020), 109326. https://doi.org/10.1016/j.measurement.2021.109326

Yuan, D., Chen, X., Tan, H., Zhang, L., Wang, X., Sun, Y., & Lv, Y. (2022). Pavement structural condition evaluation based on traffic speed deflectometer data. *International Journal of Pavement Research and Technology, 15*(6), 1442–1453. https://doi.org/10.1007/s42947-021-00030-7

Zhang, J., & Guthrie, W. (2007). Effectiveness of traffic speed deflectometer in assessing pavement structural condition at the network level. *Transportation Research Record, 2037*(1), 1–10. https://doi.org/10.3141/2037-01

Zhao, W., Wu, W., Yang, Q., & Liu, J. (2022). Improving the accuracy of pavement structural quality assessment by correcting numerical hypothetical model of modulus back calculation through GPR. *Construction and Building Materials, 6*(3), 127422.

Zofka, A., Sudyka, J., Maliszewski, M., Harasim, P., & Sybilski, D. (2014). Alternative approach for interpreting traffic speed deflectometer results. *Transportation Research Record, 2457*, 12–18. https://doi.org/10.3141/2457-02